(Bio-) stratigraphic correlation of geothermal aquifers in the West Netherlands Basin

July 2016

(Bio-) stratigraphic correlation of geothermal aquifers in the West Netherlands Basin

Author
A.G. Vondrak

Reviewed by
C.T.A.M. Leo
D. Vlad
A. van de Weerd
C.J.L. Willems

Prepared for
Dr. M.E. Donselaar
Dept. of Geoscience and Engineering
Delft University of Technology
Stevinweg 1
2628 CN Delft
The Netherlands

Prepared by
PanTerra Geoconsultants B.V.
Weversbaan 1-3
2352 BZ Leiderdorp
The Netherlands
T +31 (0)71 581 35 05
F +31 (0)71 301 08 02
info@panterra.nl

Executive summary

This report describes a study on Lower Cretaceous reservoir architecture for geothermal energy exploitation in the West Netherlands Basin. In this study two conflicting geological models are compared that describe the regional distribution of the Delft Sandstone Member which is currently the main geothermal aquifer target in this basin. The coexistence of these models increases uncertainty in the prediction of thickness and continuity of the aquifer. Because these factors can influence doublet life time, net-energy production and possible interference, it is crucial to identify which of the geological models is more realistic. So far, with only a few active doublets, both geological models complied. As more doublets are deployed, however, a better understanding of the regional fluvial architecture is required. In this study, biostratigraphic analyses are carried out on drill cuttings of three geothermal wells in different fault blocks. These analyses make it possible to (1) identify the age of different intervals, (2) identify depositional environment and (3) identify regional correlation markers. Therefore this approach circumvents subjective log correlation based on visual interpretation of well logs.

With this approach we were able to identify a difference in age of the production interval in different geothermal doublets. They do not only differ in age but also occur at different stratigraphic depth. Our well log correlations imply that the individual sandstone rich layers are restricted in width and are not laterally continuous throughout the entire basin. Overlap of different sandstone layers can locally account for large thickness variations that were recognised in current West Netherlands Basin doublets and hydrocarbon wells.

This reports presents an overview of the biostratigraphic analysis and two new geological models that describe sandstone distribution in the top of the Nieuwerkerk Formation. These models describe the possible extent and occurrence of individual sandstone rich layers. Therefore, our report could be used for reservoir property extrapolation, thickness prediction and depth prediction that relate to drilling costs.

This study was carried out by Delft University of Technology in cooperation with Panterra Geoconsultants and TNO, in the context of the Research Agenda Geothermal Energy of the ministry of Economic Affairs and LTO Glaskracht Nederland en the innovation program 'Kas als Energiebron'.

.

Contents

1 Introduction

Technical University Delft initiated a study of the reservoir architecture of the units targeted for geothermal energy in the West Netherlands Basin.

The first deep geothermal doublet in the Netherlands was realised in 2007 in the West Netherlands Basin (WNB), since then six more doublets have been drilled (Figure 1-1). The rapid increase of the number of license applications for geothermal doublets in the WNB has led to a growing demand for detailed geological models of the targeted stratigraphic intervals for geothermal energy production.

Prerequisite for the optimal placement of a geothermal doublet is the availability of a detailed reservoir model in which size, shape, spatial distribution and connectivity of the geothermal aquifers are captured. Our current knowledge of the aquifers in the WNB is from hydrocarbon exploration carried out during 1950's until the 1990's. Exploration for hydrocarbons was aimed for a large part at the same reservoir units as those utilized for geothermal exploitation.

All wells drilled for oil and gas are located on structural highs, in contrast geothermal wells target the deeper areas in between the highs. Syn-sedimentary tectonism and inversion tectonics are mainly affecting the high areas. As a result, lithostratigraphical well-to-well correlations therefore have a limited spatial resolution, and are not necessarily valid for the low areas and thus have an inherent geological uncertainty. This study includes data from geothermal wells in the low areas of the basin, ensuring a widespread distribution of the data points.

This report aims to describe and integrate the results of the seismic interpretation, the well log correlation of formation tops and the biostratigraphy studies. The scope of this study is to reduce uncertainties regarding the distribution and reservoir properties of the Delft Sandstone, the main targeted geothermal reservoir in the West Netherlands Basin.

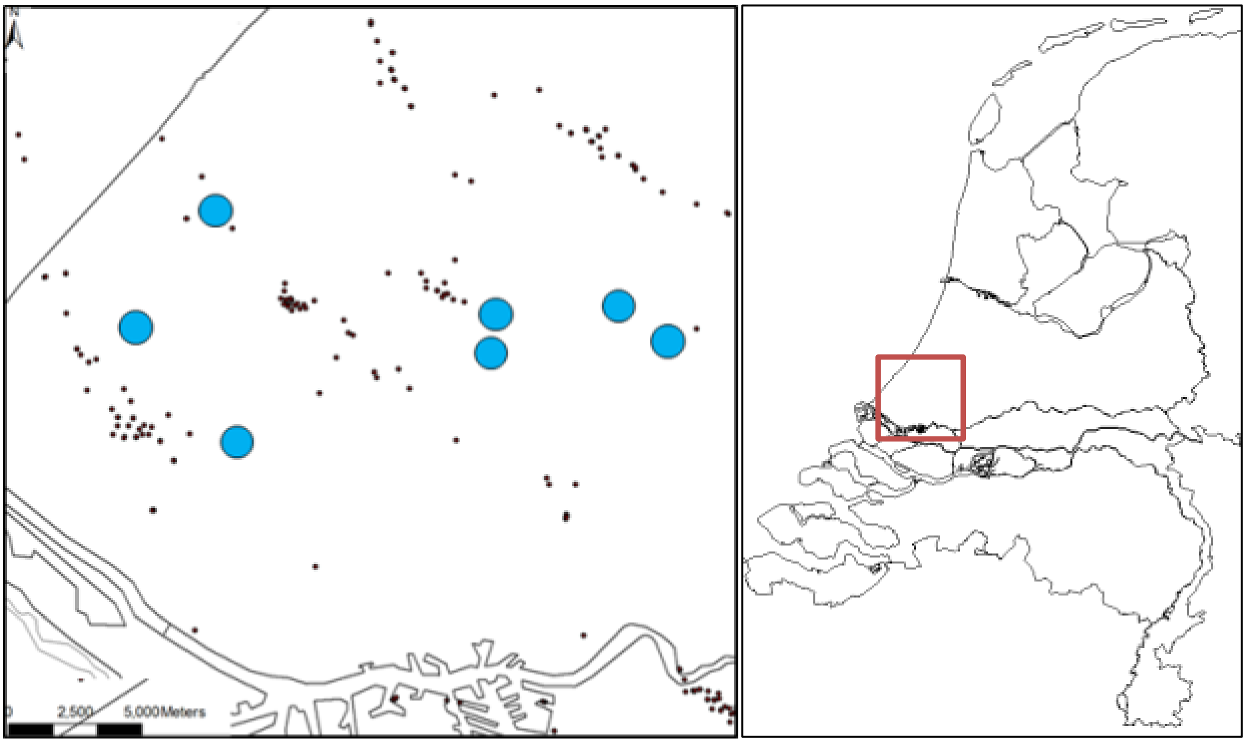

Figure 1-1 Map of the West Netherlands Basin (see red box on the right for the location), with all drilled wells and the geothermal doublets (blue dots).

2 Geology

2.1 West Netherlands Basin

The study area is located in the West Netherlands Basin; in particular the Early Cretaceous is of interest for geothermal applications. Because of the presence of hydrocarbons in the West Netherlands Basin, this basin has been the focus of many studies. For the general geological setting and structure of the basin reference is made to: Racero-Baena & Drake (1996). The hydrocarbon habitat has been described by De Jager et al. (1996). Den Hartog Jager (1996) described the stratigraphy and seismic expression of the interval of interest. The lithostratigraphy was established by Van Adrichem Boogaert & Kouwe (1993-1997). De Vault and Jerimiah (2002) and Jeremiah et al. (2010) describe the sequence stratigraphy and paleogeographic reconstructions.

The West Netherlands Basin is located between the London-Brabant Massif to the South and the Central Netherlands basin to the North (Figure 2-1).

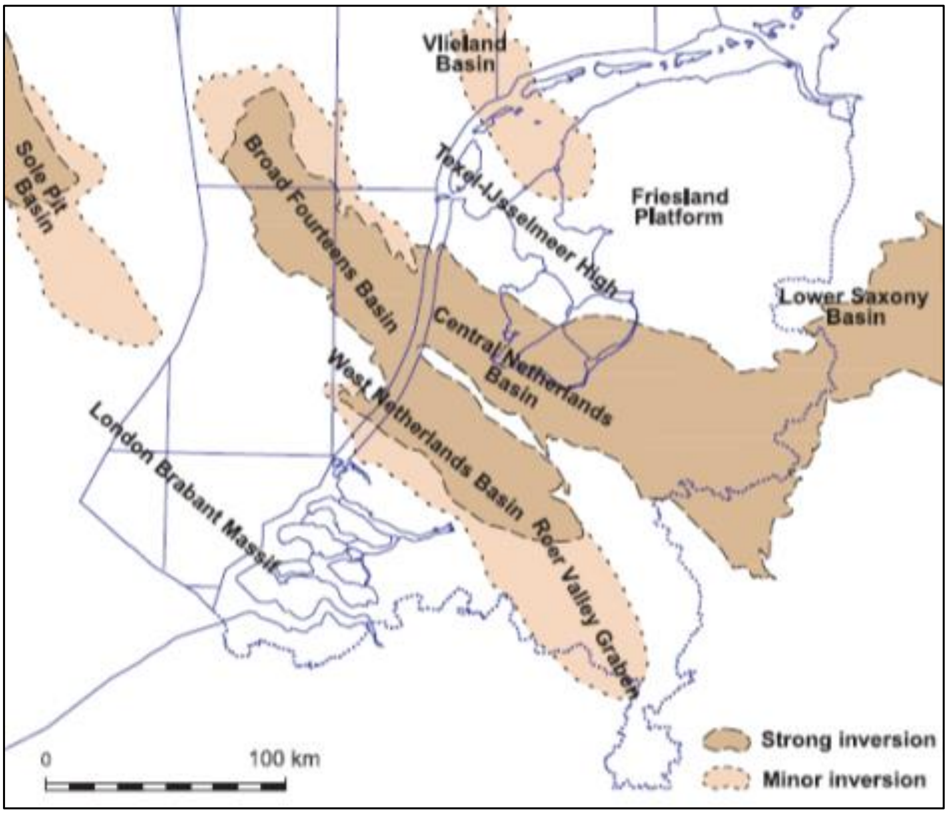

Figure 2-1 Map of the inverted basins in the Netherlands (from De Jager, 2007)

The West Netherlands Basin is an inverted rift basin. Rifting took place during Late Jurassic to Early Cretaceous, during a transtensional regime. The rifting was followed by inversion in the Late Cretaceous to Early Tertiary in a transpressional regime. Some of the rifting faults have been reactivated in the inversion stage. These tectonics resulted in NW-SE trending fault blocks in the West Netherlands Basin. In the West Netherlands Basin a number of anticlinal structures occur (e.g. Pijnacker, Rijswijk and Wassenaar structures; see Racero-Baena & Drake, 1996).

The target area and stratigraphy is dominated by two tectonic phases. The first is the syn-rift phase (Late Jurassic – Early Cretaceous) and the second is the post-rift phase (Early Cretaceous – Late Cretaceous, see Figure 2-2, Racero-Baena & Drake, 1996 and DeVault & Jeremiah, 2002).

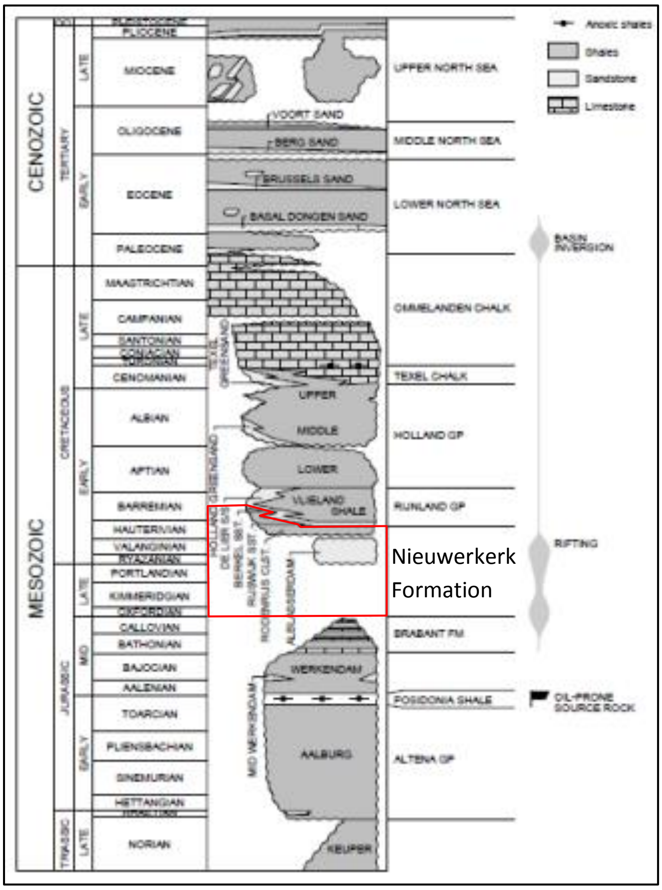

Figure 2-2 Stratigraphic column from DeVault & Jeremiah (2002) showing that the main part of the Nieuwerkerk Formation (red) is deposited during the rifting phase and the younger Cretaceous units are deposited in a tectonically quiet time.

In the study area the following sand bodies may be targeted for geothermal exploitation, in stratigraphic top to base order these are:

- IJsselmonde Sandstone Member
- Berkel Sandstone Member (including the Berkel-Sand-Shale Member)
- Rijswijk Sandstone Member
- Delft Sandstone Member
- Alblasserdam Member

The current geothermal wells are completed in the Berkel-, The Rijswijk- and the Delft Members. Full description of these sand bodies can be found in Racero-Baena & Drake (1996). The IJsselmonde and Berkel Sandstone members are interpreted as coastal barrier sands, the Rijswijk Member is interpreted as a marine transgressive sheet sand. The Alblasserdam and the Delft Sandstone Members were interpreted as being deposited by fluvial systems (Van Adrichem Boogaert & Kouwe, 1993-1997). The Delft Sandstone is the main target for five of the six existing doublets.

2.2 Nieuwerkerk Formation

Regarding the subdivision of the Nieuwerkerk Formation there are two hypotheses. The first hypothesis is suggesting that the Delft Sandstone is a continuous stacked channel deposit, occurring throughout most of the West Netherlands Basin. Underlying the Delft Sandstone is the Alblasserdam Member containing various sand bodies with little continuity (Van Adrichem Boogaert & Kouwe, 1993-1997and TNO-NITG, 2002). The second hypothesis does not acknowledge the Delft Sandstone as a separate member. In contrast its states that, stacked channel complexes occur throughout (DeVault & Jeremiah, 2002).

The thickness of the Nieuwerkerk Formation varies from a few meters to more than 1500 meters. This is a result of synsedimentary tectonics, subsidence and (partial) erosion during inversion (Den Hartog Jager, 1996 and TNO-NITG, 2002).

The Delft Sandstone is an important reservoir for geothermal exploitation, because it can be present as a thick reservoir (150m) and it is the deepest (thus warmest) reservoir at the 2-3km depth interval in the West Netherlands Basin. A better understanding of the deposition and distribution of the Delft Sandstone is needed for geothermal exploration.

3 Methods

3.1 Data Selection, Loading and Quality Control

3.1.1 Seismic data

The study area is covered by ten 3D seismic surveys (Figure 3-1) shot in the eighties and nineties of the last century. The original processing of these surveys is in the public domain and available for study

The surveys are merged for ease of manipulation and seismic interpretation. Vertical shifts are applied to a number of the surveys, ranging from 15 to 48 ms (see Table 9-1 in Appendix 9.1). The surveys overlap in many areas, the overlap is used to identify vertical differences.

The seismic surveys are loaded in the seismic software OpendTect in the RD-new coordinate system. A cube is constructed that fits all the required data. The inlines and crosslines for the three surveys belong to the same counting system. After the seismic data was loaded into OpendTect, it was visually inspected. In areas of overlap, the seismic survey with the best quality was used, and seismic edge effects were eliminated by choosing the right cutting line (see Appendix 9.1 for the selected areas).

Before the surveys were merged, the amplitude values were given the same order of magnitude. The amplitude values from the other surveys were matched to the best quality survey, by using the RMS amplitude attribute. To compensate for the differences in amplitude values, a scaling factor was used when merging the seismic data. All amplitude values in the seismic survey were multiplied by this scaling factor so that the amplitudes of all seismic surveys are equal (Janssen, 2015).

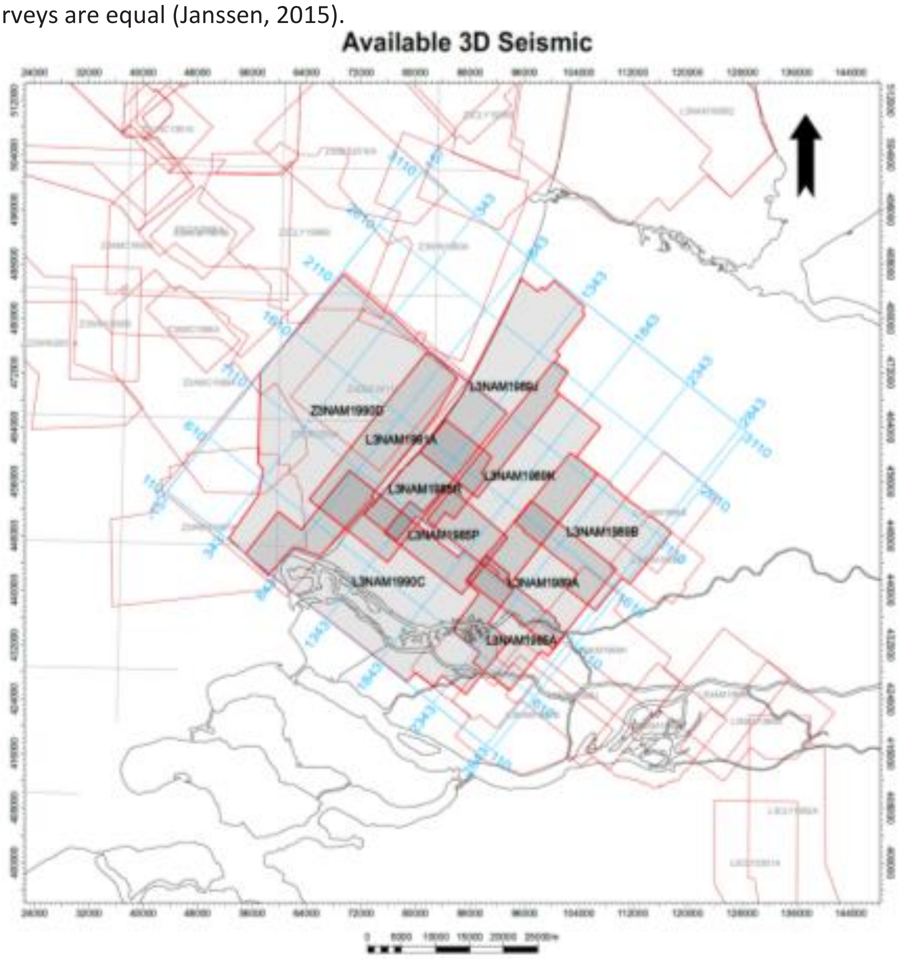

Figure 3-1 The ten seismic surveys used for this study indicated in grey.

3.1.2 Polarity

The onshore seismic lacks a seabed, therefore another event was chosen to delineate the polarity. The synthetics show that the top Texel Chalk (CKTX) is a hard kick (Figure 9-6 in Appendix 9.6 of Q13-08), indicated by a sudden decrease of the sonic, thus an increase in velocity. This signal results in a negative seismic response giving aSEG normal display. All seismic figures in this report are displayed conform SEG-normal (i.e. negative = a trough = red = velocity increase).

3.1.3 Well and area selection

All the wells in the WNB are selected based on a number of criteria:

- Stratigraphic level reached,
- Availability of velocity data,
- Availability of biostratigraphical data,
- Presence of cores,
- Purpose, geothermal or hydrocarbon well,
- Used in previous publications (DeVault & Jeremiah,2002; Jeremiah, et al. 2010).

A well ranking was made based on the above criteria. For the final well selection also the geographical spread of the wells is taken into account to ensure data availability in the complete study area. Since the focus of this study is on geothermal exploration, all the geothermal wells with data are selected. Table 3-1 shows the wells and the selection criteria they meet. Figure 3-2 shows the selected wells and the study area, whit the The Moerkappelle-Zoetermeer high as the northern boundary and the southwestern boundary located close to the Gaag structure.

The main interpretation focus is on the GR log, because this is the only log acquired in geothermal wells.

Table 3-1 Wells used in this study, with the criteria.

Well	Velocity data	Biostratigraphical data	DeVault, Jeremiah 2002	Jeremiah, Duxbury, Rawson 2010	Cores	Geothermal
BRK-02			x	x	x	
EEM-01			x	x	x	
GAG-02-S1	x			x	x	
HAG-GT-01						x
HAG-GT-02						x
HON-GT-01		x				x
HON-GT-02						x
IJS-64-S2	x		x		x	
LIR-45	x		x	x	x	
LIR-GT-01						x
LIR-GT-02						x
MKP-10	x				x	
PNA-13	x		x			
PNA-GT-01		x				x
PNA-GT-02		x				x
PNA-GT-03						x
PNA-GT-04						x
Q13-08	x			x		
Q13-09	x					
VDB-GT-01						x
VDB-GT-04		x				x
VLN-01-S1	x		x	x		

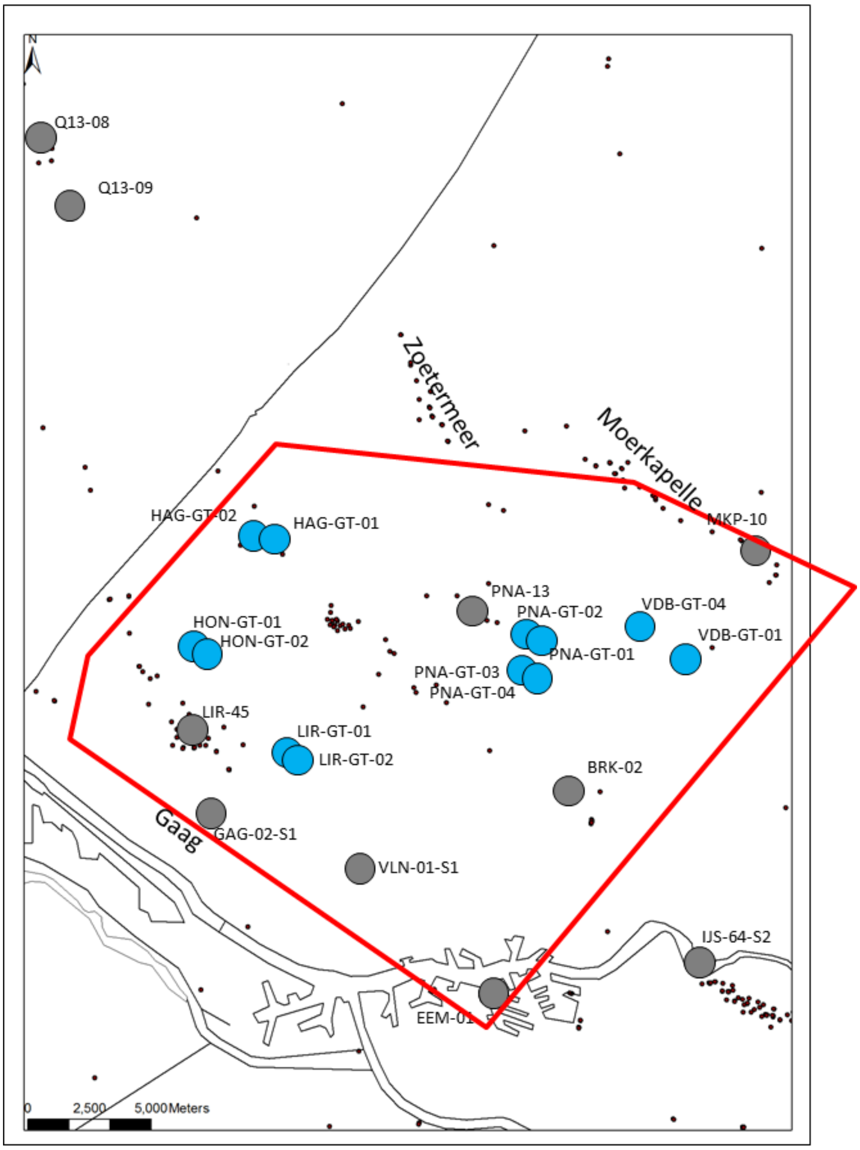

Figure 3-2 Map showing the location of the wells used for this study (blue- geothermal wells, grey - hydrocarbon wells)

3.2 Seismic interpretation

As a starting point for the seismic interpretation the seismic (maximum flooding) horizons of DeVault & Jeremiah (2002) have been selected (Figure 3-3).

The following horizons were selected:

- Top De Lier
- Denckmanni
- Elegans
- Speetonensis
- Regale

The level of interest is located below the Speetonensis (brown in Figure 3-3), the five horizons were interpreted to have an indication for the tectonic history. Three seismic lines were selected for interpretation (Figure 3-4). Two of them are oriented perpendicular to the strike of the faults to show tectonic grain (showing the fault architecture and activity). One is oriented parallel this strike in the HON-GT-01 fault block to indicate seismic trends. The last section intersects the wells to relate seismic interpretation to well log correlation.

Next to the interpretation of the indicated reflectors the interpretation of the base Rijnlad Group and the top Schieland Group from TNO are used as a guideline for thickness of the Nieuwerkerk Formation (RGD, 2014).

To have a better understanding of the fault movements, three cross-sections were analysed. All sections are shown flattened on the top De Lier and without flattening (Appendix 9.2). Flattening helps to identify thickness variations. On the sections without flattening, intervals of fault activity are marked by yellow bars on the active fault.

A basic fault interpretation was carried out on a larger data set than the initially selected lines to have a better understanding of which of the wells are in the same fault block.

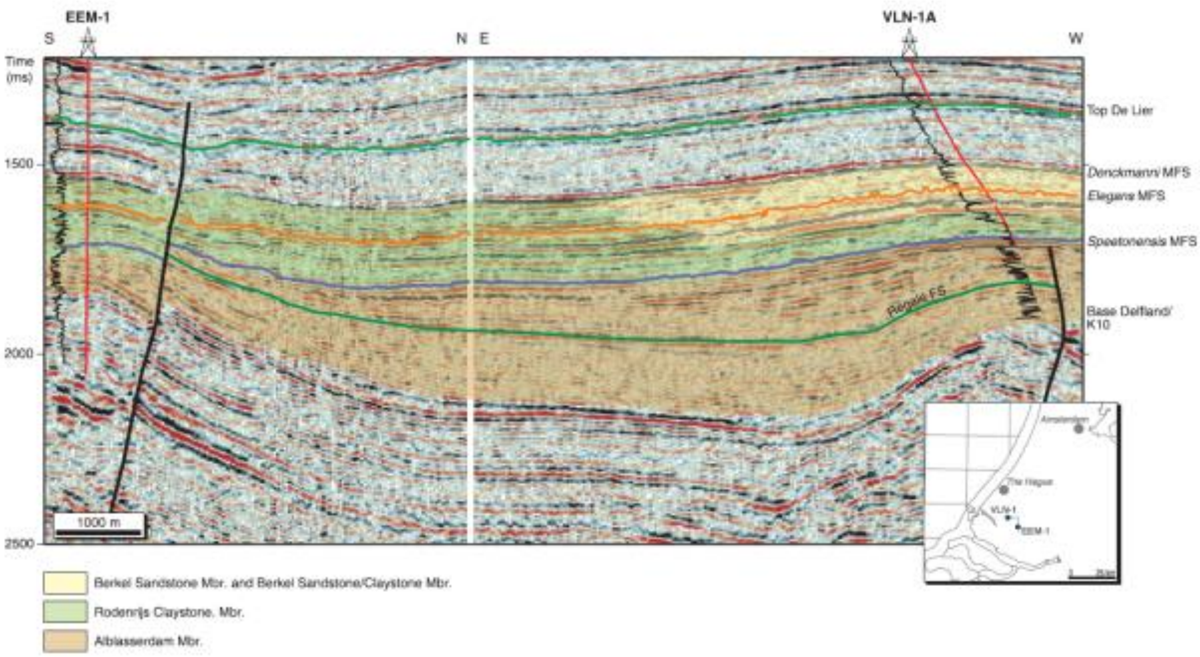

Figure 3-3 Cross-section from EEM-01 to VLN-1A from Devault and Jeremiah (2002), used as a starting point for this study.

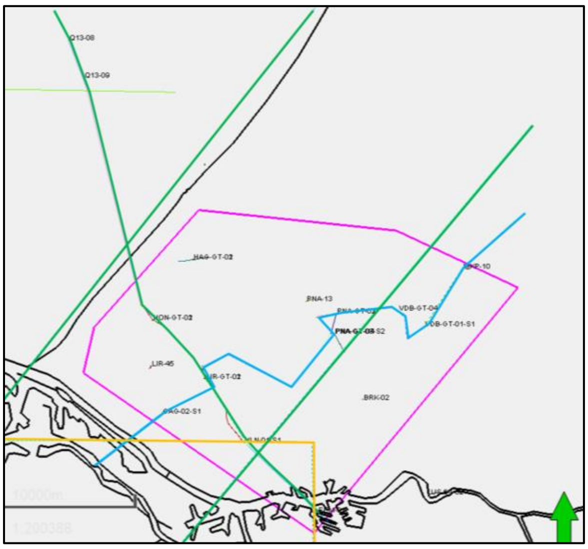

Figure 3-4 Interpreted seismic lines: in green the three main lines, in blue one line going through many wells of the study (SSW-NNE), and in orange the line by Devault and Jeremiah (2002) (see Figure 3-3).

3.2.1 **Wells in the seismic**

A number of seismic lines are shown in Appendix 9.7 these lines show the relation between the wells within the sub-basins and also between the sub-basins. These figures indicate that the resolution of the seismic is too low for the sands to be visible in the seismic.

On most of the lines the wells are projected, therefore the fit seems poor. However, for some wells the fit is indeed poor, this is caused by the lack of data in these wells to help the tie to the seismic (e.g. VDB-GT-01 and VDB-GT-04, see appendix 9.7). For these wells it was chosen to only apply the Velmod2 velocity model.

3.3 Biostratigraphy

For this project two new biostratigraphic studies on cuttings from geothermal wells have been performed on HON-GT-01, PNA-GT-02 and VDB-GT-04. Previously, cuttings of three geothermal wells were analysed by TNO on VDB-GT-04, PNA-GT-01 and PNA-GT-02 (Munsterman, 2012 and Musterman, 2013).

In the previous analyses of well VDB-GT-04 a very large interval was analysed (925-2006m MD, sampled every 25 to 10m) providing a good overview regarding age, facies and facies transitions. In wells PNA-GT-01 and PNA-GT-02 eight samples were taken at various depths. The analyses from PNA-GT-01 are quite accurate whereas the analyses from PNA-GT-02 contained more uncertainties. After correlating PNA-GT-02 with other wells, discrepancies in the biostratigraphic analyses become clear. Therefore, it was decided to expand the biostratigraphic analyses of well PNA-GT-02. The biostratigraphic analyses were carried out by D. Munsterman (TNO), thus providing consistency as well as more insight in the correlation possibilities to earlier analysed wells.

For the additional biostratigraphic study HON-GT-01, PNA-GT-02 and VDB-GT-04 were selected.
The GR logs of PNA-GT-01 and PNA-GT-02 have rather different signatures, leaving uncertainty in log correlation. In PNA-GT-02 the position of the Elegans marker was unclear, therefore the interval of 2120 – 2275 m MD is chosen to determine where the Elegans marker is located was considered useful. The second interval is a deeper interval in well PNA-GT-02 (from the top Delft Sandstone to TD) to gain a better understanding of the relation between the three wells in the Nieuwerkerk Formation.

Being located in a different sub-basin, HON-GT-01 was selected for biostratigraphic analysis in order to provide a cross correlation through the study area. For well HON-GT-01 two intervals were selected:
1) to locate the Elegans marker (2320 - 2420 m MD)
2) to investigate if correlation is possible of the fluvial Delft Sandstone between the wells HON-GT-01 and VDB-GT-04 (2560 – 2810 m MD).

From the original VDB-GT-04 data, the age of the deeper section was not clear (either Ryazanian or Valanginian), therefore the two marine sections at that interval are sampled again to better define the interval (at 1890 and 1910 m MD).

3.4 INPEFA

INPEFA, integrated prediction error filter analysis, is an analytical tool developed by ENRES and available in the Cyclolog software. The input data for INPEFA are wireline logs, usually GR logs. The basis of this tool is the possibility of detecting Milankovitch cycles in wireline logs. However, within the geological rock record discontinuities are commonly present, even within small units e.g. a formation, therefore cyclic patterns can be difficult to distinguish. INPEFA uses prediction coefficients by applying a prediction error filter analysis (PEFA) to a wireline log. The PEFA compares the wire line data with the filter, within a specified window, the output being the positive or negative error. The resulting PEFA curve is a serrated curve around a vertical line. Integration of the PEFA curve generates the INPEFA curve. The PEFA curve shows discontinuities and the INPEFA shows trends, which can be correlated to adjacent wells. The trends are indicated by turning points in the INPEFA curve, a negative trend implies a regression trend where as a positive trend implies a transgressive trend (Nio, et al., 2005). In this study INPEFA was applied to the gamma ray logs and for well BRK-02 to the SP log (no available GR log in this well).

4 Results

4.1 Seismic interpretation

The seimic interpretation indicated thickness variations throughout the West Netherlands Basin. Focussing on these variations in thickness and depth of the base an area of interest map is created. The map shows the structural setting which is related to the deposition of the Nieuwerkerk Fm. (Figure 4-1A). The axis of this part of the basin is represented by the Pijnacker structure, towards which the stratigraphic layers are dipping from the NE and SW directions.

The map shows a symmetrical rift basin where the current Pijnacker high was a depression during deposition of the Nieuwerkerk Formation.

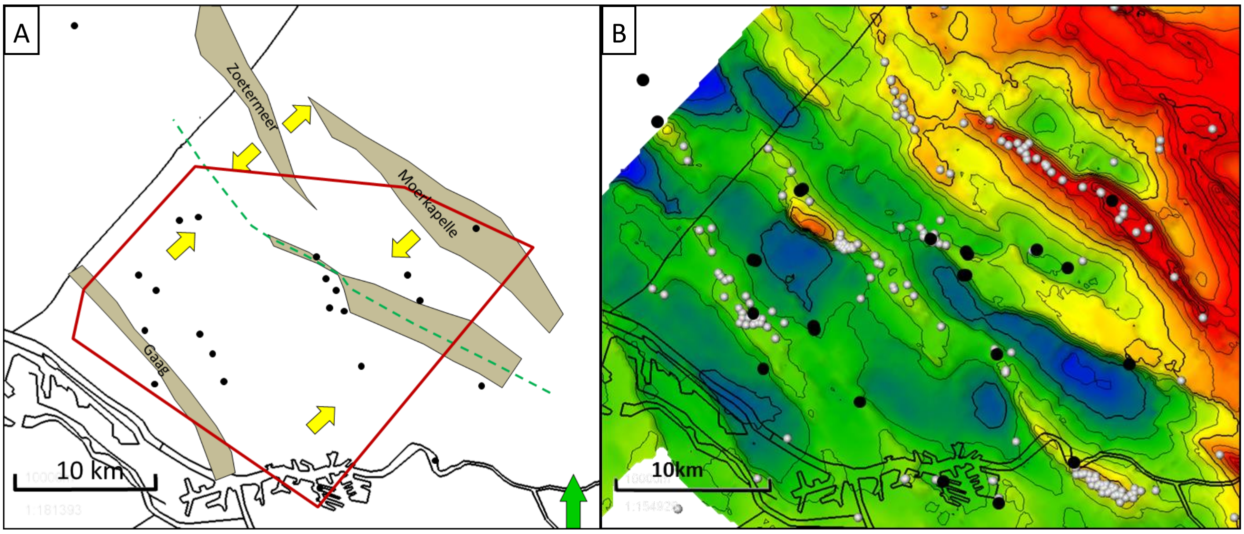

Figure 4-1 A: rough indication of the structure of the Nieuwerkerk Formation in the study area (red). The map was generated after flattening on the top of the Nieuwerkerk Formation. The (paleo-)highs are indicated in brown and the dips in the sub-basins indicated with the yellow arrows. The green line shows the axis of this part of the basin. B: Depth map of the base Nieuwerkerk Formation (RGD, 2014), showing the drilled wells in white and in black the wells used in this study.

4.1.1 Study area

From the middle part of the basin to its southern border, the thickness of the interval between Regale and De Lier is decreasing (Figure 4-2).

In the middle part of the basin, below the PNA structure there is a high around the Posidonia Shale Formation (Figure 4-2). The part from the Posidonia Shale to De Lier is much thinner in the middle of the cross section than in other parts of the basin displayed in this section. This implies that in this interval much of the sediments deposited in the time interval Posidonia Shale - Speetonensis have been eroded. It is likely that this area was already a high in the Cretaceous dividing the basin as is also suggested in Figure 4-1. This division could be a possible barrier for fluvial deposits in this basin.

The sections show that not all of the faults have been active all the time. The palinspastic reconstruction indicates that not all of the faults have been active simultaneously. In addition fault activity has continued throughout the whole Cretaceous. This is derived from the wedging seen between De Lier and Regale. The main faults that were active during the deposition of the Nieuwerkerk Formation are shown in Figure 4-3.

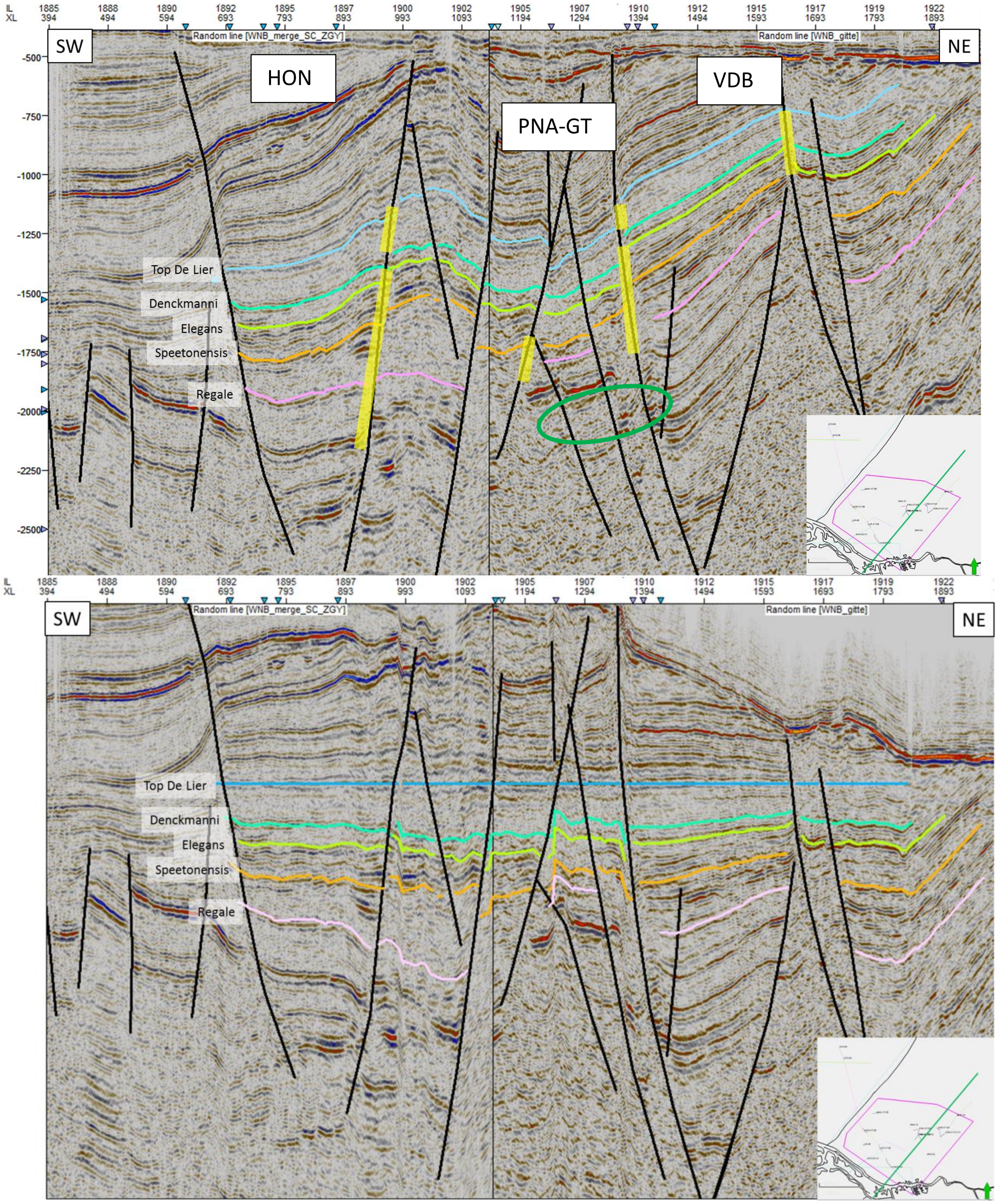

Figure 4-2 Top: SW-NE cross section through the West Netherlands Basin, perpendicular to the faults. The yellow bars indicate active fault intervals. The green circle indicates the position of the Posidonia Shale Formation and the presence of a paleo high. Bottom: same section flattened on top De Lier, showing the wedge shapes, indicating fault activity.

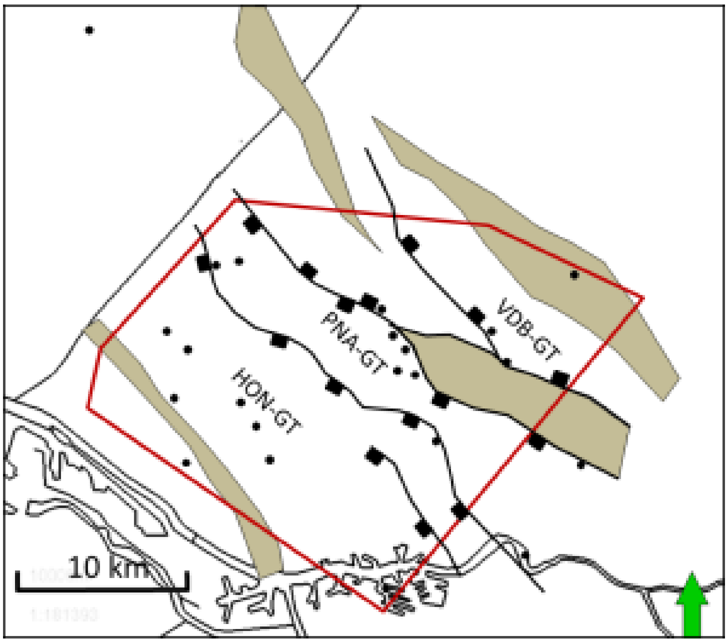

Figure 4-3 Map indicating the faults that were active during the deposition of the Nieuwerkerk Formation, derived from syntectonic sedimentation (wedging). Also indicated the names of the sub-basins.

4.1.2 Sub-basins

This sub-basin, where the two VDB doublets are located (Figure 4-3), is deep in the south and shallow in the north and may be interpreted as an inverted half graben.

Two tectonically active intervals seem to be present, as indicated by thickness differences: between Regale and Elegans horizons and between Denkmanni and De Lier horizons. The thickness of the Denkmanni-Elegans interval is more or less consistent in this basin, suggesting a time period without active faulting.
During both tectonically active intervals normal fault movements took place along the southern fault (Figure 4-2).

The seismic line oriented parallel to the tectonic strike shows that the thickness in HON-GT sub-basin is constant (Figure 4-4).

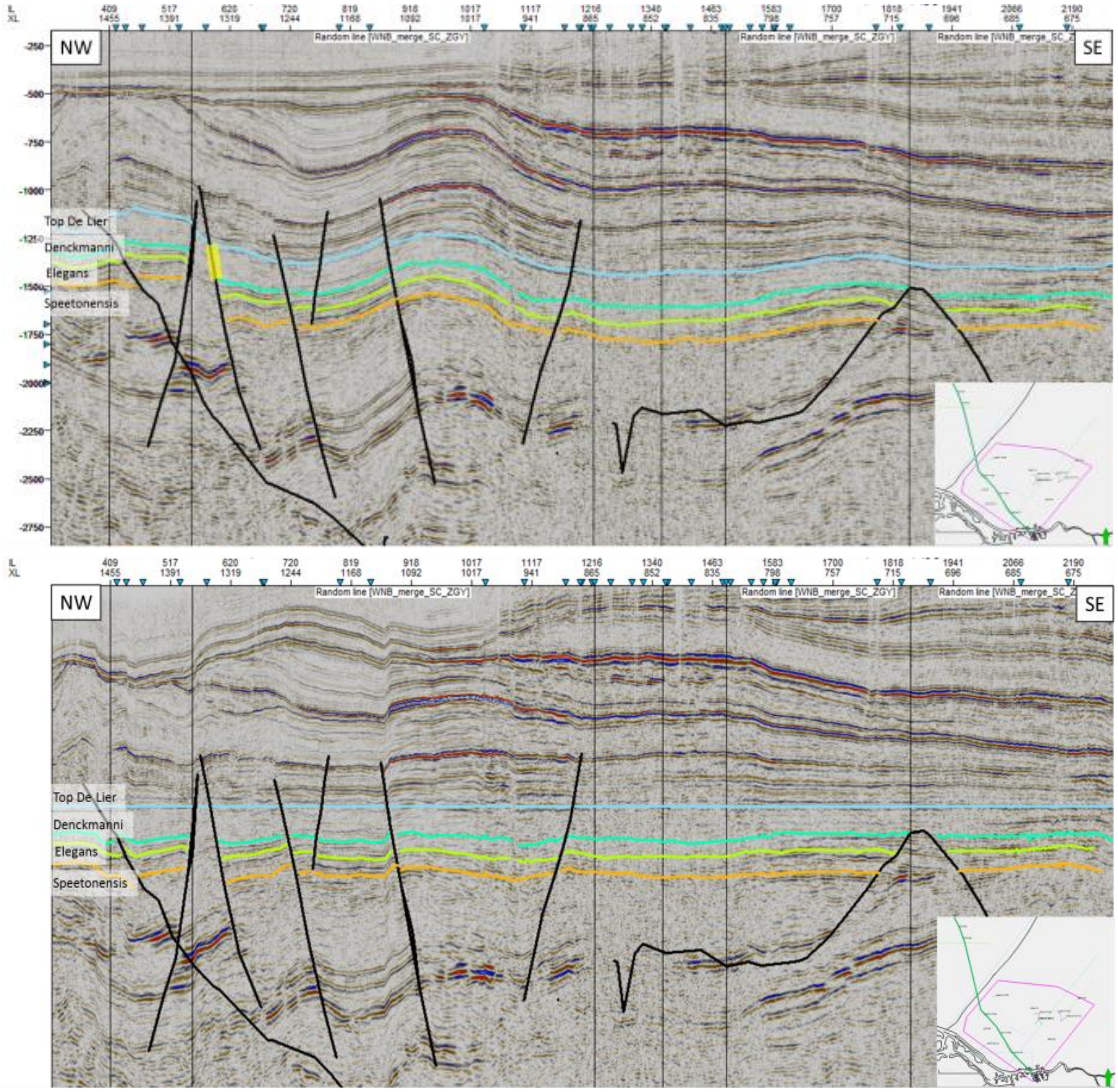

Figure 4-4 Top: NW-SE cross section through the HON sub basin, showing very little fault movement in the interpreted interval. Bottom: same section flattened on top De Lier, showing continuous thickness in the HON-GT basin.

4.2 Biostratigraphy

The two biostratigraphic reports can be found in Appendix 9.3, the main results are listed below.

4.2.1 HON-GT-01 and PNA-GT-02

Both wells show less marine influence in all the analysed sections when compared to VDB-GT-04. This could indicate that in the marine intervals the shoreline was closer to HON-GT-01 and PNA-GT-02 than to VDB-GT-04

The bulk of the terrestrial section of the PNA-GT-02 well shows no signs of marine incursions, like those observed in well HON-GT-01 and well VDB-GT-04, suggesting indeed a closer shoreline to HON-GT, as opposed to PNA.

The Ryazanian/Valanginian boundary can be defined in HON-GT-01. By using the SEG method (Abbink, 1998) two MFS's can be defined which correlate to the Gradstein, et al. (2005) MFS's, indicative for the Ryazanian. The MFS at 2728 m MD is interpreted to be the Paratollia MFS (within the Paratollia ammonite zonation) most likely the Lower Paratollia MFS from Jeremiah et al. (2010).

PNA-GT-02		
Interval (m MD)	Age	Facies
2120-2175	Late Barremian	Marine
2195-2215	late Early Barremian, Elegans Ammonite Zone or older	Lagoonal
2235-2275	earliest Early Barremian variabilis Ammonite Zone or older	

HON-GT-01		
Interval (m MD)	Age	Facies
2320	Late Barremian	Marine
2340-2360	early Late Barremian	Marine
2380-2420	late Early Barremian, Elegans Ammonite Zone or older	Marine
2560-2730	Valanginian	Fluvial/swamp
2740	early/earliest Valanginian	Fluvial/swamp
2750-2810	Late Ryazanian, post-kochi Ammonite Zone	Fluvial/swamp

4.2.2 **PNA-GT-02 and VDB-GT-04**

The results of both studies are shown in Figure 4-5, including the original interpretation of top Delft Sandstone. In well VDB-GT-04 no marker from the Ryazanian was encountered, the age of the sampled interval remains dated at Late Ryazanian – Early Valanginian. However, in both wells strong indications have been found for the Paratollia MFS, as was encountered in HON-GT-01. Both wells show a MFS and similar markers as were found in well HON-GT-01 around the Paratollia MFS.

PNA-GT-02	
Interval (m MD)	Age
2440-2590	Valanginian
2600-2850	Late Ryazanian (post-kochi Ammonite Zone) - Early Valanginian

VDB-GT-04	
Interval (m MD)	Age
1890-1910	Late Ryazanian - Early Valanginian

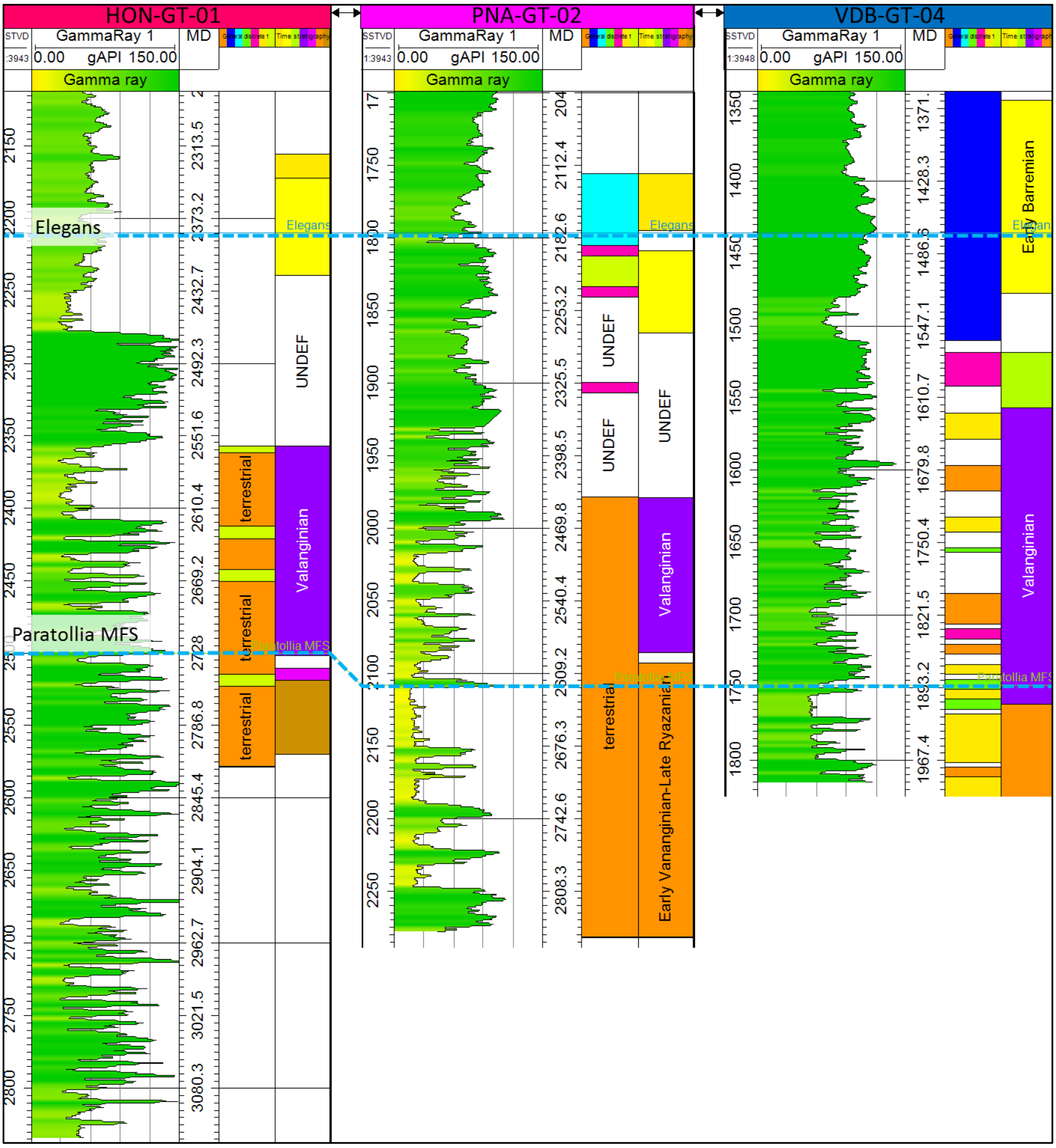

Figure 4-5 Well panel with the results of biostratigraphic analyses, flattened on the Elegans marker. In blue time lines, in orange lithology lines, in the fourth column the depositional environment and in the last column time zonations. (Colour coding for fourth column: orange – terrestrial, yellow – coastal plain, light green – marine influences, pink – restricted marine, bright green – marginal marine, light blue – shallow marine, dark blue – open marine. Colour coding for fifth column: dark yellow – Late Barremian, light yellow – Early Barremian, green – Hauterivian, dark purple – undefined Valanginian, light purple – Early Valanginian, orange – Early Valanginian – Late Ryazanian, brown – Late Ryazanian.)

4.3 Well log correlation

Often in fluvial settings it is difficult to find and correlate trends based on GR logs.; However, by using INPEFA curves, subtle trends can become visible. In this study combines the data from the biostratigraphy with INPEFA curves. The INPEFA curve is applied to correlate the big trends and visualise which units are deposited in the same time interval. In the deeper wells the lower Paratolia MFS marker was picked using the INPEFA curves (see Appendix 9.4 for correlation panels).

Figure 4-6 show the INPEFA curves and the Paratollia MFS from the biostratigraphy. PNA-GT-02 and VDB-GT-04 have a similar INPEFA character for the Paratollia MFS whereas HON-GT-01 is very different. The INPEFA character of HON-GT-01 is different over the whole well, not only in this section. Therefore the character from the other two wells is used for correlation (Appendix 9.4). Not all wells are suitable to locate the Paratolia MFS; the presence of faults breaks up the signal (e.g. IJS-64, CAP-01), or the well TD was too shallow to result in a clear signal over the deeper part (e.g. HAG-GT-01, PNA-GT-01).

The INPEFA analysis is used as a trend indicator in this study. It could be used for more detailed sequence stratigraphic interpretations if a better understanding of the shortcomings is obtained.

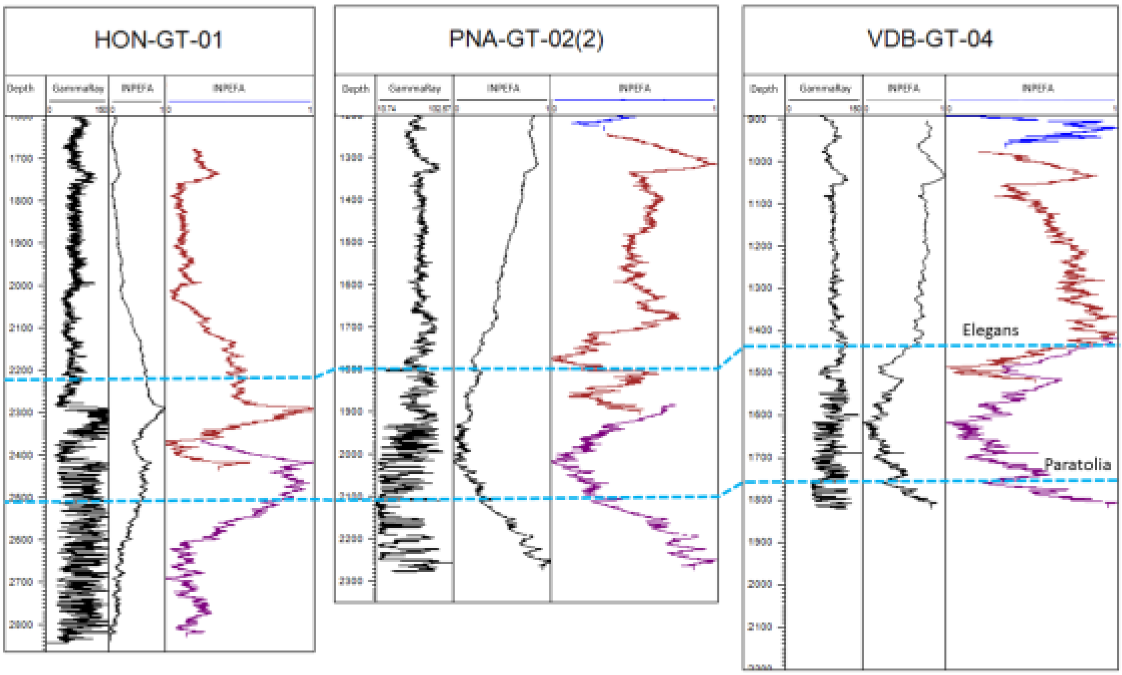

Figure 4-6 Three geothermal wells with biostratigraphy combined with the INPEFA signatures. The Paratollia MFS signature in PNA-GT-02 and VDB-GT-04 is quite similar and used as a reference point for correlation of this marker to the other wells.

The main goal of the well correlations is to determine the locations of the thick clean sand bodies. The correlations are mainly based on the GR logs. In the section below the marine Rijswijk Sandstone they are supported by INPEFA curves.

Based on well correlation and zonation, two dominant sand packages are identified in the upper part of the Nieuwerkerk Formation. Both sands have a high N/G and a blocky gamma ray signature. The sands are named Sand 1 and Sand 2, Sand 1 being the older of the two (Figure 4-7). The Paratolia MFS is used to indicate the top of Sand 1. None of the selected wells reached the base of the Nieuwerkerk Formation, thus there is a possibility of encountering similar clean and thick sand bodies in deeper sections of the Nieuwerkerk Formation.

The well correlation scheme (Figure 4-8) in the HON sub-basin indicates similar GR trends in all wells, similar to what is seen in the seismic section (Figure 4-4). However, in HON-GT-01 the thickness of the sandstone rich interval is significantly lower compared to the other wells.
The selected wells are displayed in a number of well panels (Appendix 9.5). The panels show the wells parallel and perpendicular to the fault structure, showing correlations within one sub-basin or between sub-basins.

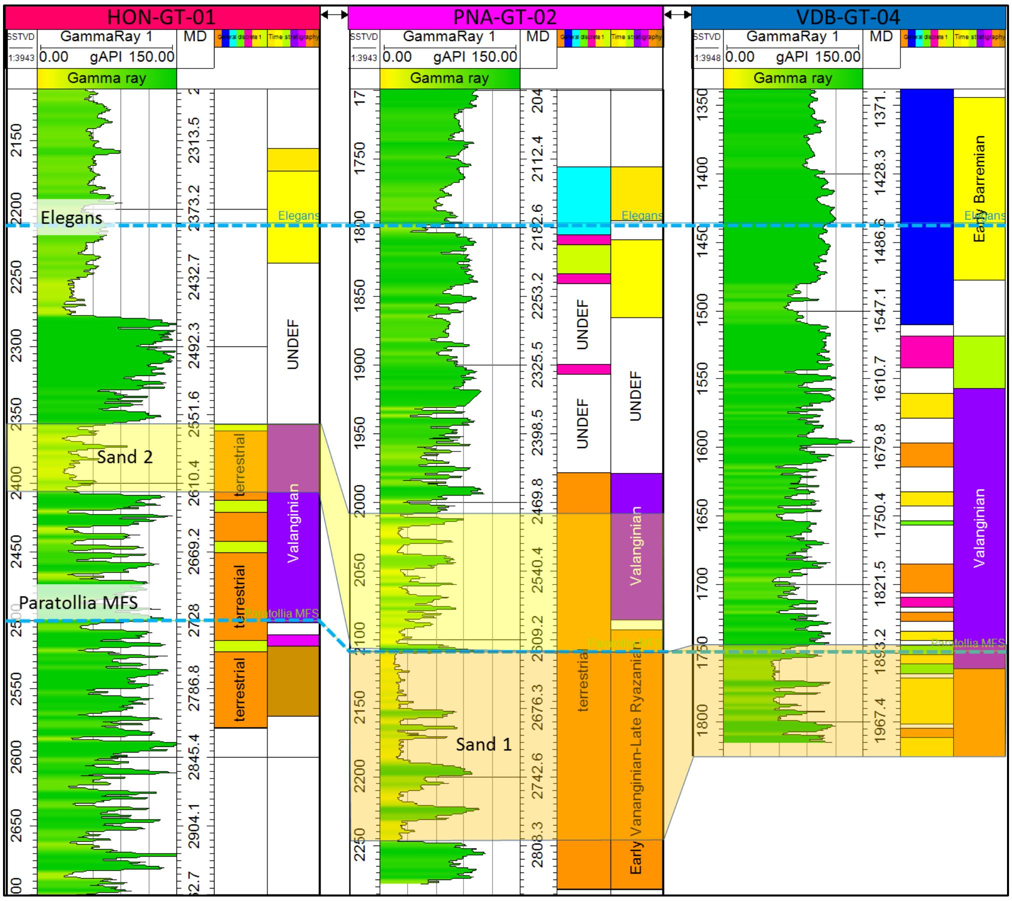

Figure 4-7 Section through the geothermal wells with biostratigraphical data, flattened on the Elegans MFS marker (green). Orange – Sand 1 and yellow – Sand 2, fourth column in the wells indicates age; yellow – Barremian, green – Hauterivian, blue – Valanginian, orange – Ryazanian.

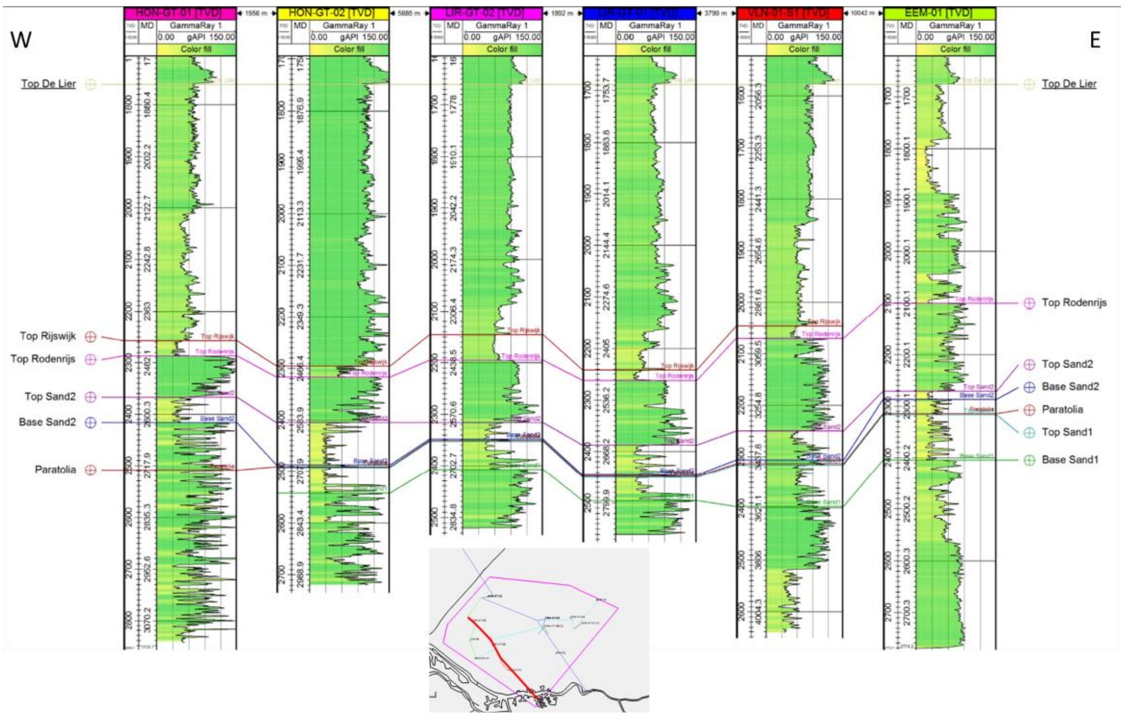

Figure 4-8 Well correlation panel from west to east through the HON-GT fault block.

4.4 Combined results of seismic, well correlation and biostratigraphy

All the biostratigraphical data is combined in Figure 4-9, where the sand bodies are shown in time. This time display shows that the Rijn Member (Q13 wells) and the Rijswijk Member are different sand bodies deposited at different time intervals. It is likely that the two sands are not the same and not necessarily connected. The Rijn member is interpreted as offshore shoal-bar complex and transgressive sheet-sands and the Rijswijk Member is interpreted as a transgressive (reworked) sand (Van Adrichem Boogaert & Kouwe, 1993-1997).

Simultaneously with the deposition of the Rijn Member, the Rodenrijs Member is deposited in three geothermal wells (PNA-GT-01, PNA-GT-02 and VDB-GT-04). The Rodenrijs Member is interpreted as a lower-coastal-plain to lagoonal deposit (Van Adrichem Boogaert & Kouwe, 1993-1997). The presence of the lagoonal Rodenrijs Member facies implies presence of a Rijn Member sand bar in the Q13 wells, protecting the lagoonal area of the Rodenrijs Member.

Figure 4-9 shows that the originally interpreted Delft Sandstone is deposited in the three geothermal wells, however, the biostratigraphical data shows that the sandstone was not deposited simultaneously in all three wells. Clearly the sand in VDB-GT-04 is older than the sand in HON-GT-01, this indicates non-synchronous deposition of the unit in these two different sub-basins.

Sand 2 is located directly underneath the Rodenrijs Member (see well HON-GT-01 in Figure 4-9), where Sand 1 is located substantially lower.

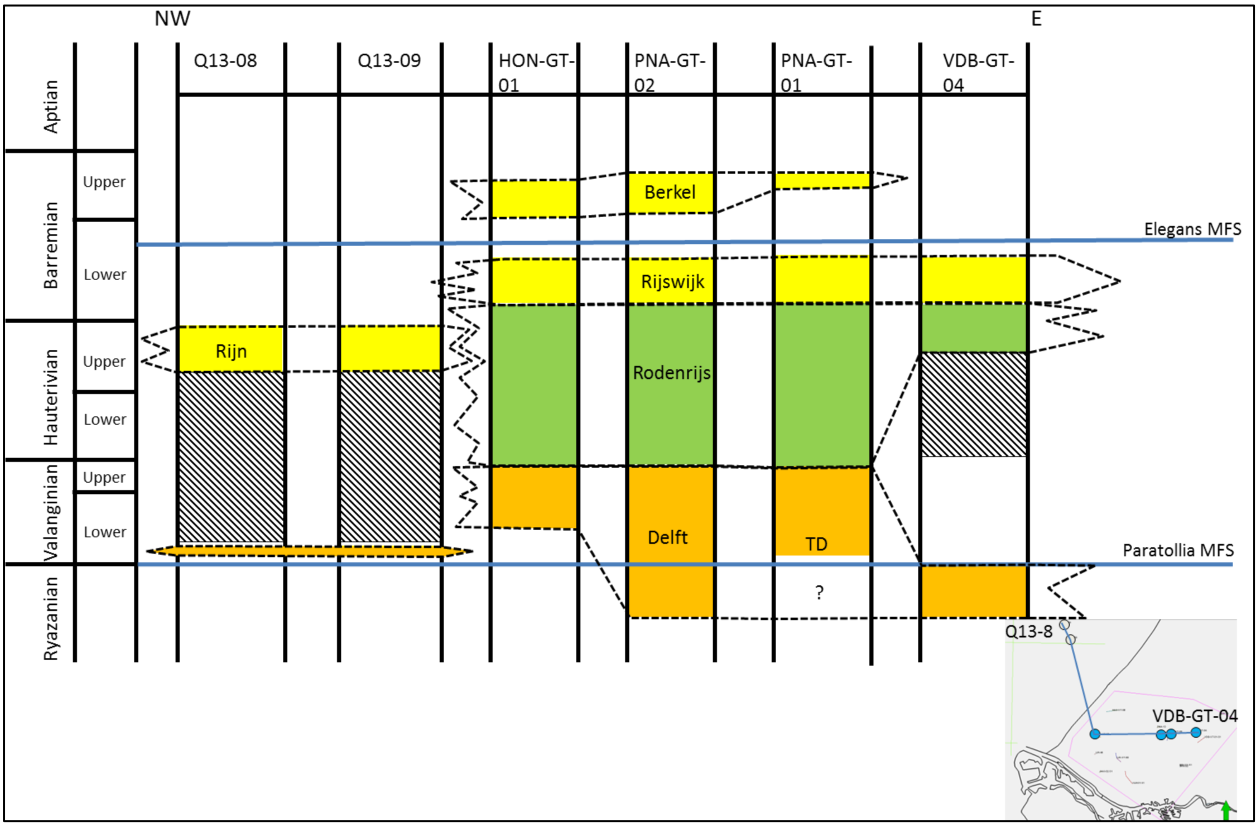

Figure 4-9 A cross section through the wells containing biostratigraphical data (from NLOG and TNO reports). There is a clear distinction between Q13 and the geothermal wells. Yellow = marine sands, green = lagoon, orange = fluvial sands and hatched = unconformity.

4.5 Thickness Sand 1 and Sand 2

Two conceptual gross thickness maps were created to illustrate the distribution and the gross thickness of Sand 1 and Sand 2 throughout the area (Figure 4-10). The maps are based on seismic observations as well as previous interpretations of the Nieuwerkerk Formation (RGD, 2014, Janssen, 2015 and A'Campo, 2014).

The following observations are taken into account from the seismic data:

- the axis of the basin in the study area (the axis of the basin is running NW-SE including the Pijnacker structure. All strata in the Nieuwerkerk Formation are dipping toward this part of the basin (Figure 4-1).
- faults active during deposition of the Nieuwerkerk Formation (identified by syn-sedimentary structures, e.g. wedging, Figure 4-3).
- identification of areas within the sub-basins where the Nieuwerkerk Formation is thickest.

The gross thickness maps show a high level view based on a conceptual model of a fluvial system guided by active faults. The figures are mainly based on the gross thickness resulting from the well correlations. Therefore, the maps are the most accurate around the wells, further away showing an unproven potential. The Sand 2 map is based on more data points than Sand 1; this is the reason for the difference in accuracy of the two maps.

Since Sand 1 is stratigraphically located close to Sand 2 in the Nieuwerkerk Formation and also has a fluvial character, it is expected to have similar influences as Sand 2. Therefore, in the distribution map the same major active faults in the Nieuwerkerk Formation are present and also the axis of the sub-basins are the same. The two sands overlap except in the VDB-GT sub-basin, where only Sand 1 was proven.

In appendix 9.8 the conceptual gross thickness maps are shown with the TVD of the top of the sand listed next to the wells as well as these maps with the N/G and gross thickness. The WNB underwent extensive inversion, therefore the present depth of the sands cannot help in indicating how the sands have been deposited.

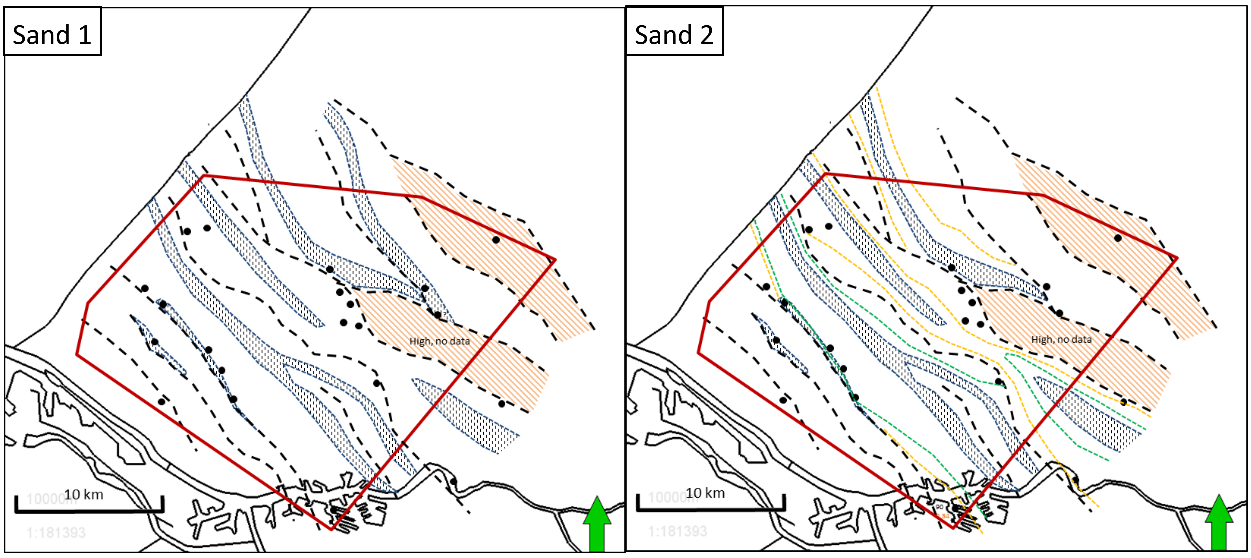

Figure 4-10 Conceptual thickness maps of Sand 1 and Sand 2. The maps show the deepest areas in blue (where the Nieuwerkerk Formation is the thickest), and the highs in orange. There is too little data for Sand 1 to create conceptual contour lines. The map of Sand 2 shows the proposed thickness variations throughout the study area, in blue the depocenters (where the Nieuwerkerk Formation is the thickest), in green intermediate thickness and in yellow the thinnest contour.

4.6 Geological model Nieuwerkerk Formation

Two models are proposed, the foundation of the two models is the same, the difference is the presence of lateral continuity. The sands are assumed to be a result of stacked channels. This occurred at least in two time intervals in the Nieuwerkerk Formation, however, there might be more stacked channels in older levels (Figure 4-11).

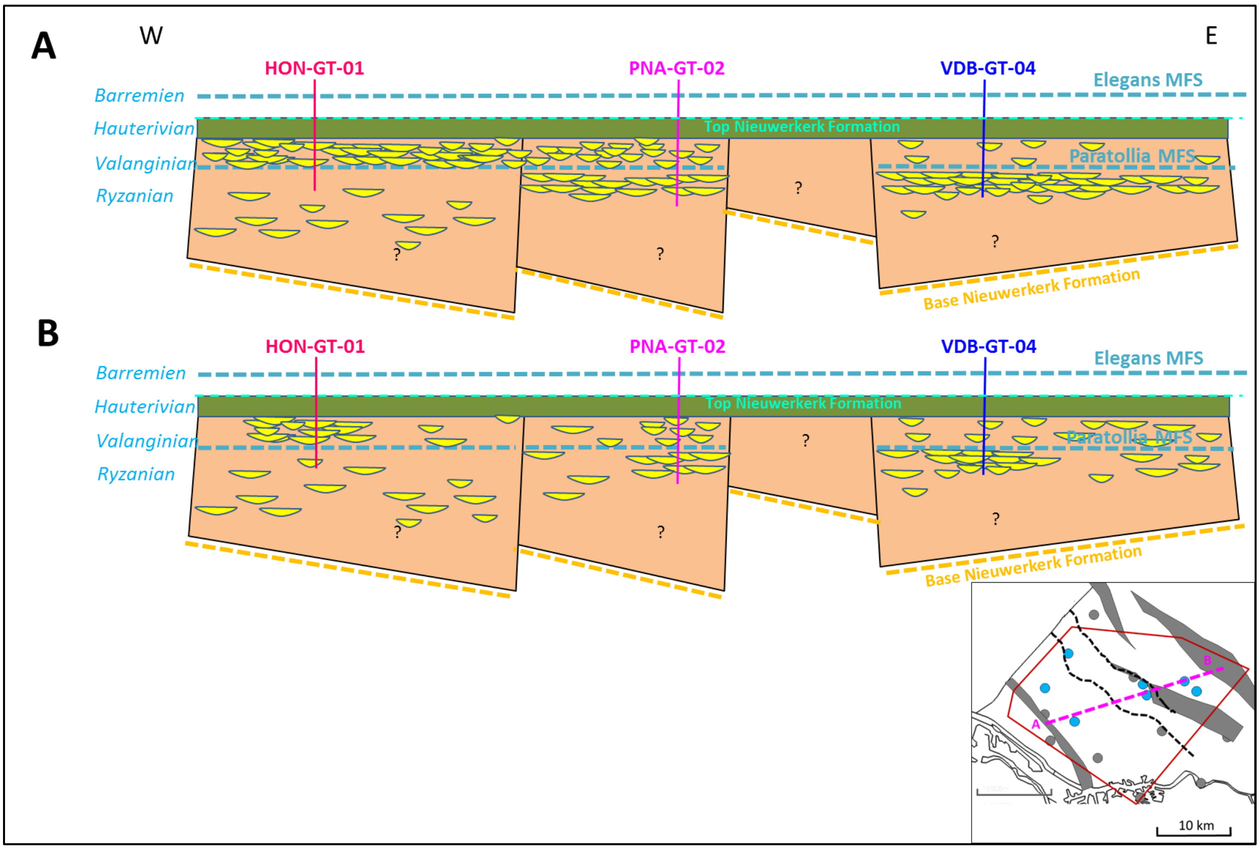

Figure 4-11 W-E section depicting the two geological models for the sands in the Nieuwerkerk Formation in time.

4.6.1 Depositional models

The sands in the Nieuwerkerk Formation are assumed to be fluvial deposits, close to the marine realm (DeVault & Jeremiah, 2002, Den Hartog Jager, 1996, Van Adrichem Boogaert & Kouwe, 1993-1997). The direction of the fluvial system is deemed to be guided by the fault structure (roughly NW-SE). This is supported by seismic, in which the Nieuwerkerk Formation varies in thickness towards faults making it improbable for fluvial systems crossing the active faults.

In this model the sediment influx is from the SW - SSW (Den Hartog Jager, 1996). The sequence of deposition is seen as follows: the older fluvial sediments of the Nieuwerkerk Formation were deposited first, then Sand 1 was deposited. Sand 1 was deposited in the sub-basin of VDB-GT-04 as well as in the HON sub-basin (VLN-01) and PNA sub-basin. In this model the chance to encounter sands increases towards the SW, towards the hinterland.

At the next stage Sand 2 is deposited, this sand not being present in VDB-GT-04. The absence of Sand 2 is extrapolated to the rest of the VDB sub-basin, for the well is located near the beginning of this sub-basin in the study area. The system moved to the SW to the HON and PNA sub-basins and the sub-basin NW of the PNA sub-basin. This shift can be induced by fault movement, or by changes in sediment influx in the hinterland.

From the available data there is no certainty if the sand bodies are continuous stacked channel deposits in the whole basin or that there are specific depocenters in each sub-basin ().

These models indicate that the highest chance to encounter both sands with one well is in the southeastern part of the HON sub-basin and in the southeastern part of the PNA sub-basin (seeFigure 4-12).

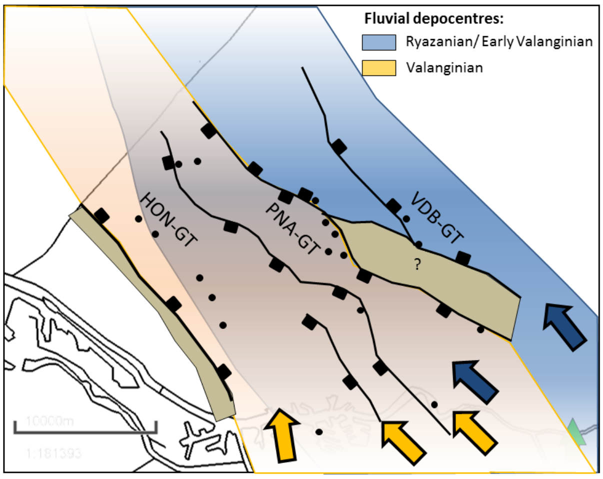

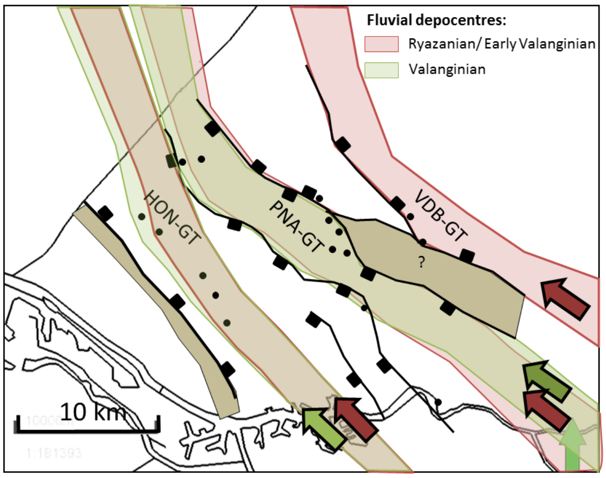

Figure 4-12 Top view of the two proposed depositional models, the arrows indicate sediment influx.

5 Discussion

5.1 PNA-GT wells

From the Ryazanian to Aptian conditions of rising relative sea level prevailed and the sea covered the West Netherlands Basin starting from the north moving southwards (Jeremiah, et al., 2010). The orientation of the wells from north to south is VDB-GT-04, PNA-GT-02 and HON-GT-01; for this reason it is striking that PNA-GT-02 has the least marine influences. The limited marine influence character of PNA-GT-02 is possibly related to its location close to the Pijnacker structure. This structure has been described in some detail by Racero-Baena & Drake (1996). It was a small pull-apart basin in the Early Cretaceous, converted to a pop-up structure during inversion in the latest Cretaceous. It may be speculated that PNA-GT-02 was located on the shoulder of this pull-apart basin, resulting in its slightly less marine character. This might also explain the reason for the Rijswijk Sandstone to be much thinner in the PNA-GT-02 well than in the other wells.

A detailed seismic interpretation in the PNA-GT area is another possible future research objective to be performed, considered the complexity of processes affecting the area. The log signatures of the Rodenrijs Member is different between the wells, and the Rijswijk Member displays a variable thickness as well.

5.2 Thickness difference between HON-GT-01 and -02

A striking thickness difference at reservoir level was observed in the Honselersdijk geothermal wells. These two wells are almost two km apart, and within this distance the clean sand in well 01 is almost three times thicker in well 02. No faults which might explain this rapid increase in thickness are identified between the two wells. A possible explanation is the change of direction of the channel in time, with a favoured location near well HON-GT-02 in early stage of deposition, followed by an expansion of the accommodation space at a later stage, when the fluvial system prefers both well locations. Another possibility is the presence of a paleo low, in the map of the base Nieuwerkerk Formation a low is visible close to HON-GT-02 (Figure 4-1). This depression might have provided the accommodation space for Sand 2.

5.3 Angular unconformity at the base of the Delft Sandstone

In earlier studies (Janssen, 2015, A'Campo, 2014) and also for geothermal license applications great importance was ascribed to angular unconformities. These unconformities are present throughout the Nieuwerkerk Formation and usually locally visible in the seismic. There is no evidence for the presence of one basin wide angular unconformity.

The base of the Delft Sandstone was interpreted as an angular unconformity. This unconformity can be regarded as the equivalent of the base of the newly identified Sand 2 package, but in the present study the focus was not on the identification and interpretation of stratigraphic discontinuities. For both the proposed depositional models, it was just assumed that the base of the sand packages is the base of fluvial channels cutting into the existing deposits. The presence or absence of bounding discontinuities, and their relationship with the base of different sand packages of the Nieuwerkerk Formation should be the object of further research studies.

5.4 Seismic

Since the seismic data has been acquired and processed, many reprocessing efforts have occurred improving the seismic data. Unfortunately, these data sets are not available in the public domain and could not be used. The the quality of the seismic data is poor and in parts hard to interpret. A higher quality and resolution seismic data set is necessary in order to better investigate whether the sands in the fluvial domain of the Nieuwerkerk Formation are suitable to be mapped by using seismic facies attributes.

A few of the synthetic seismograms show that in a number of wells the sands are thick enough and have sufficient different acoustic response to have a clear seismic character, this suggests that a reprocessing of the seismic might help with identifying the sand bodies in the seismic.

To have a better well tie and have a proper velocity model for the lows in the basin it is recommended to gather velocity data in the wells (e.g. sonic logs).

5.5 Paleo-flow

To have a better understanding of paleo-flow directions, investigation of sedimentary dips in the sands might be indicative for the flow direction. For this study a quick look was performed on old dip meter data. This data was present in only five wells, and the most dominant direction was NE. This data does not fit with any of the proposed models and might therefore provide new insights if more wells are included. The NE direction might also be the structural dip.

5.6 INPEFA

For this study the INPEFA tool was used to correlate the larger trends, however, for smaller trends this tool might prove to be valuable as well, in order to have a better idea of the various cycles and potential hiatuses in the fluvial section.

6 Conclusion

In the upper levels of the Nieuwerkerk Formation two sand packages have been identified, which are suitable for geothermal application; Sand 1 and Sand 2. Both sands have a blocky gamma ray signature, have a high N/G and a fluvial character.

6.1 Sand 2

Sand 2 is equivalent of the Delft Sandstone as was posed by Van Adrichem Boogaert & Kouwe (1993-1997). However, it is not charaterised by a sheetlike deposition that Van Adrichem Boogaert & Kouwe (1993-1997) suggested. It is a wide spread fluvial sand, and thickness varies per sub-basin as well as within a sub-basin (e.g. the HON doublet). It is not necessarilly present in every sub-basin, as well VDB-GT-04 illustrates.

When drilling this sand as a target it is important to know that this target is located directly underneath the fine-grained Rodenrijs Member, with regards to setting the casing.

With respect to well placement for a geothermal doublet, it is recommended to place the wells parallel to the fault structure to ensure connectivity. There are two reasons for this recommendation: the first is the smaller risk of encountering major faults between the two wells, the second reason is that the fluvial system is expected to have evolved parallel to the faults, thus the sands are mostlikely to be continuous in that direction (NW-SE, see also Figure 4-12).

6.2 Sand 1

The distribution and thickness distribution of Sand 1 in the study area is uncertain, because of limited well control, and because most of the wells did not reach the base of Sand 1 (TD-ed in it or faulted out). Since Sand 1 is stratigraphically located close to Sand 2 in the Nieuwerkerk Formation and also has a fluvial character, it is expected to have similar geometries as Sand 2).

Sand 1 is located deeper than Sand 2 and not directly underneath the Rodenrijs Member even if Sand 2 is not expected to be present (see well VDB-GT-04).

When targeting Sand 1 the same considerations for well placement apply as for Sand 2, i.e. parallel to the strike of the faults.

6.3 Reservoir characteristics

To determine the reservoir characteristics for a new well targeting Sand 1 and/or Sand 2 it is recommended to use the reservoir characteristics of all the wells that target the specific sand. The depositional system of the Sand 1 as well as Sand 2 is expected to be the same system throughout the study area. Local differences may occur so a weighted average is preferred (with the highest weight assigned to the nearest wells).

6.4 Depositional model

The maps of the two models indicate where the sands are expected to be present, in the blank parts higher uncertainty remains about the continuity of the sandstone rich layers.

7 Acknowledgements

We thank Kennisagenda Aardwarmte for funding this research as well as the Ministry of Economic Affairs, LTO Nederland and Kas als Energiebron. Biostratigraphic analyses as well as their interpretation are carried out by Dirk Munsterman (TNO Geological Survey of the Netherlands). In addition we would like to thank current WNB operators for kindly providing subsurface data. Harmen Mijnlieff (TNO Geological Survey of the Netherlands) and Dirk Munsterman are thanked for the discussions and support. Schlumberger is acknowledged for the academic Petrel license.

8 Bibliography

Abbink, O., 1998. Palynological investigations in the Jurassic of the North Sea region. *LPP Contribution Series,* Volume 8, p. 192.

A'Campo, Y., 2014. The Tectonic and Depositional History of the Onshore Southern Margin of the West Netherlands Basin (The Westland Area): The Geothermal Exploration Perspective, PanTerra G1058.

De Jager, J., 2007. Geological development. In: T. Wong, D. Batjes & J. De Jager, eds. *Geology of the Netherlands.* Herent: Royal Netherlands Academy of Arts and Sciences, pp. 5-27.

De Jager, J., Doyle, M., Grantham, P. & Mabillard, J., 1996. Hydrocarbon habitat of the West Netherlands Basin. In: H. Rondeel, D. Batjes & W. Nieuwenhuijs, eds. *Geology of Gas and Oil under the Netherlands.* Dordrecht: Kluwer Academic Publishers, pp. 191-211.

Den Hartog Jager, D., 1996. Fluviomarine sequences in the Lower Cretaceous of the West Netherlands Basin: correlation and seismic expression. In: H. Rondeel, D. Batjes & W. Nieuwenhuijs, eds. *Geology of Gas and Oil under the Netherlands.* Dordrecht: Kluwer Academic Publishers, pp. 229-243.

DeVault, B. & Jeremiah, J., 2002. Tectonostratigraphy of the Niewerkerk Formation (Delfland subgroup), West Netherlands Basin. *AAPG Bulletin,* October, 86(10), pp. 1679-1707.

Gradstein, F., Ogg, J. & Smith, A., 2005. *A Geologic Time Scale 2004.* Cambridge: Cambridge University Press.

Herngreen, G. & Wong, T., 2007. Cretaceous. In: T. Wong, D. Batjes & J. De Jager, eds. *Geology of the Netherlands.* Herent: Royal Netherlands Academy of Arts and Sciences, pp. 127-151.

Janssen, G., 2015. The tectonic and depositional history of the northern part of the West Netherlands Basin; consequences for the geothermal potential of Upper Jurassic and Lower Cretaceous sandstones, PanTerra P047. May.

Jeremiah, J., Duxbury, S. & Rawson, P., 2010. Lower Cretaceous of the southern North Sea Basins: reservoir distribution within a sequence stratigraphic framework. *NJG,* December, 89(3/4), pp. 187-203.

Munsterman, D., 2012. *De resultaten van het palynologische onderzoek naar de ouderdom van de Onder Krijt succesie in boring Van den Bosch-04 (VDB-04), interval 925-2006 m,* Utrecht: TNO.

Musterman, D., 2013. *De resultaten van het palynologische onderzoek naar de ouderdom van de Vlieland zanden in boringen Pijnacker-GT-01 (PNA-GT-01) en Pijnacker-GT-02 (PNA-GT-02),* Utrecht: TNO.

Nio, S., Smith, D., De Jong, M. & Böhm, A., 2005. Spectral trend attribute analysis: applications in the stratigraphic analysis of wireline logs. *First break,* Volume 23, pp. 71-75.

Racero-Baena, A. & Drake, S., 1996. Structural style and reservoir development in the West Netherlands oil province. In: H. Rondeel, D. Batjes & W. Nieuwenhuijs, eds. *Geology of Gas and Oil under the Netherlands.* Dordrecht: Kluwer Academic Publishers, pp. 211-229.

RGD, 2014. *NLOG.* [Online]
Available at: http://www.nlog.nl/nl/pubs/maps/geologic_maps/DGM_deep_onshore.html
[Accessed 08 August 2016].

TNO, 2015. *NL Olie- en Gasportaal.* [Online]
Available at: www.nlog.nl

TNO-NITG, 2002. *Geological Atlas of the Subsurface of the Netherlands, Explanation to map sheets VII and VIII: Noordwijk-Rotterdam and Amsterdam-Gorinchem.* Utrecht: s.n.

Van Adrichem Boogaert, H. & Kouwe, W., 1993-1997. *Stratigraphic nomenclature of the Netherlands; revision and update by RDG and NOGEPA.* 50 ed. Haarlem: Boom-Planeta.

Van Dalfsen, W., Van Gessel, S. & Doornenbal, J., 2007. Velmod-2. *Joint Industry Project, TNO report 2007-U-R1272C.*

9 Appendices

9.1 Merging

Table 9-1 Seismic cubes used in this study. The table indicates the extent of the surveys in the final merged cube, indicated by the minimum and maximum inlines and crosslines, the vertical shift and the scaling factor applied to each of the surveys.

Survey	Inline minimum	Inline maximum	Crossline minimum	Crossline maximum	Vertical shift (ms)	Median RMS	Scaling factor
L3NAM1985A	2270	2790	534	990	48	0.10	65000.00
L3NAM1985A_cut1	2270	2790	820	990	48	0.10	65000.00
L3NAM1985A_cut2	2500	2790	534	819	48	0.10	65000.00
L3NAM1985P	1290	1844	1030	1150	25	6630.00	1.00
L3NAM1985P_cut1	1450	1844	1030	1150	25	6630.00	1.00
L3NAM1985P_cut2	1290	1449	1030	1127	25	6630.00	1.00
L3NAM1985R	1108	1500	1030	1800	20	189.43	35.00
L3NAM1985R_cut1	1108	1289	1030	1127	20	189.43	35.00
L3NAM1985R_cut2	1108	1449	1128	1340	20	189.43	35.00
L3NAM1985R_cut3	1125	1500	1151	1800	20	189.43	35.00
L3NAM1989A	2000	2780	982	1549	15	1.10E+09	6.05E-06
L3NAM1989B	2000	2900	1550	2185	15	2451.00	2.71
L3NAM1989J	908	1500	1505	3110	20	1894.29	3.50
L3NAM1989K	1463	2230	1140	2640	15	6630.00	1.00
L3NAM1990C	590	2500	110	1140	0	6102.00	1.09
Z3NAM1990D	-157	880	110	2178	0	1823.00	3.64
L3NAM1991A	881	1107	720	2125	0	1038.00	6.39
WNB_MERGE	57	2900	110	3110	0	6630.00	1.00

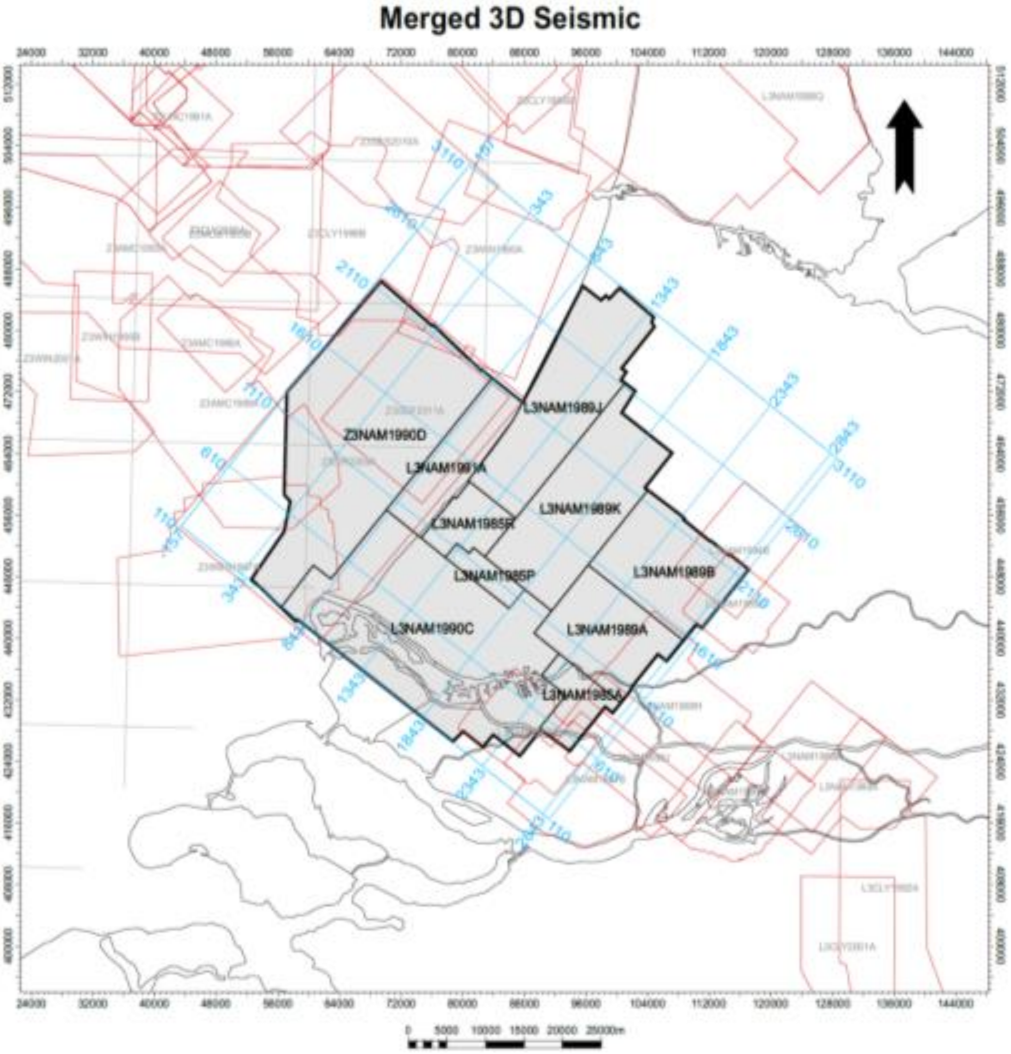

Figure 9-1 Used parts of the seismic cubes for the merged cube.

9.2 Structural grain sections

Six seismic sections showing the interpreted horizons and in the un-flattened section the fault activity is marked by yellow bars.

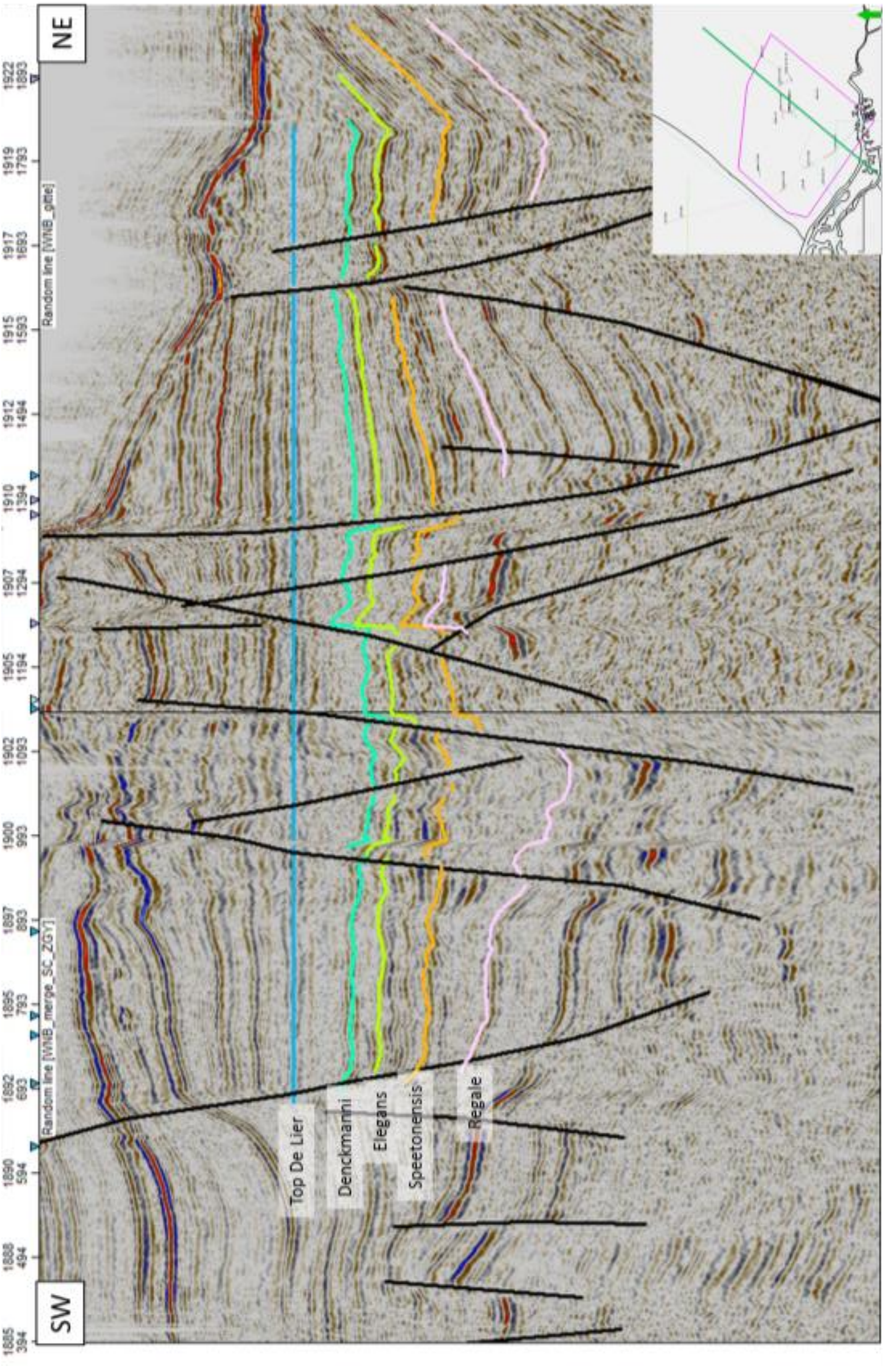

NE
SW
Top De Lier
Denckmanni
Elegans
Speetonensis
Regale
Random line [WNB_merge_SC_ZGY]

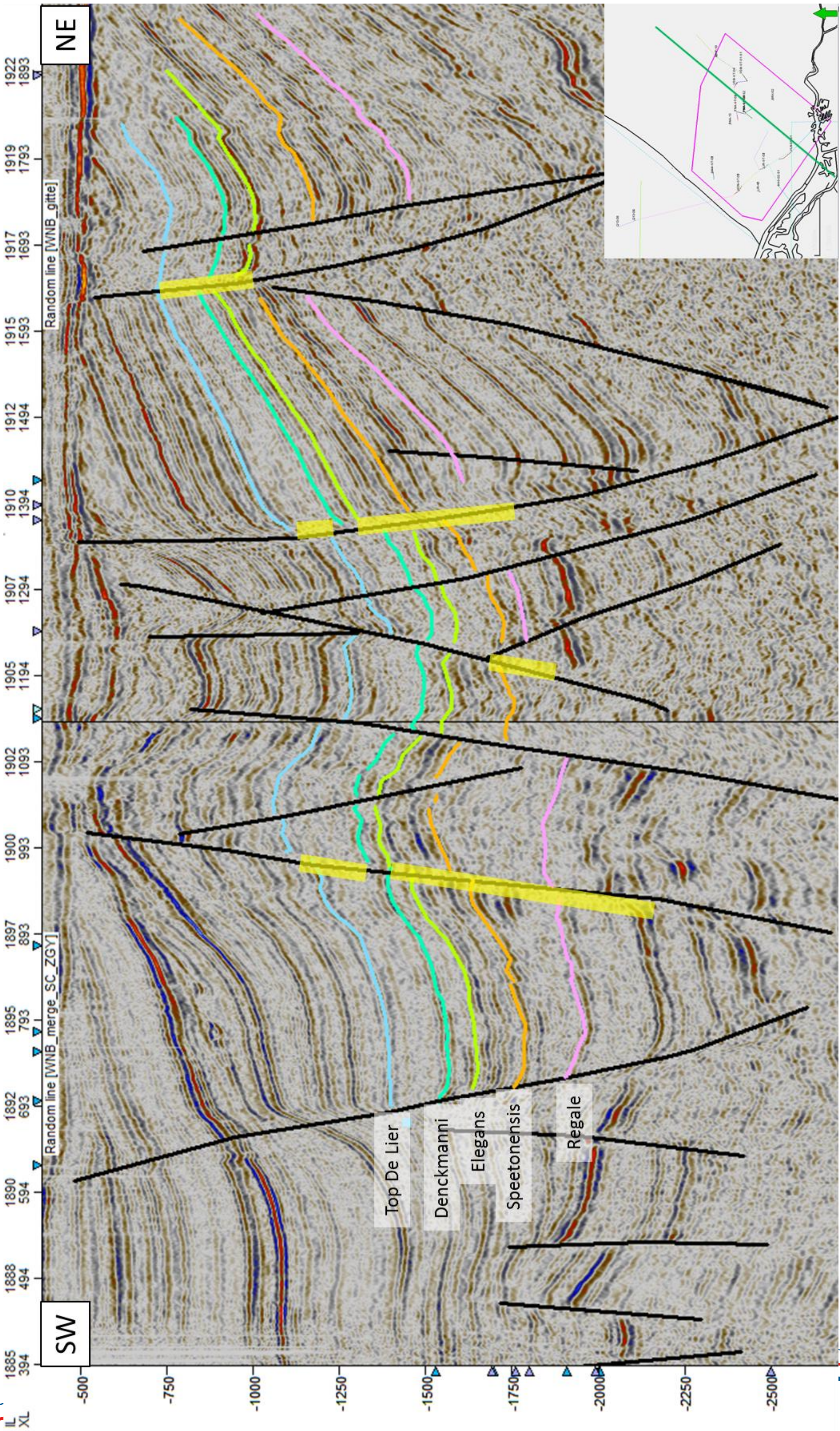
NE
SW
Random line [WNB_gitte]
Random line [WNB_merge_SC_ZGY]
Top De Lier
Denckmanni
Elegans
Speetonensis
Regale
IL
XL

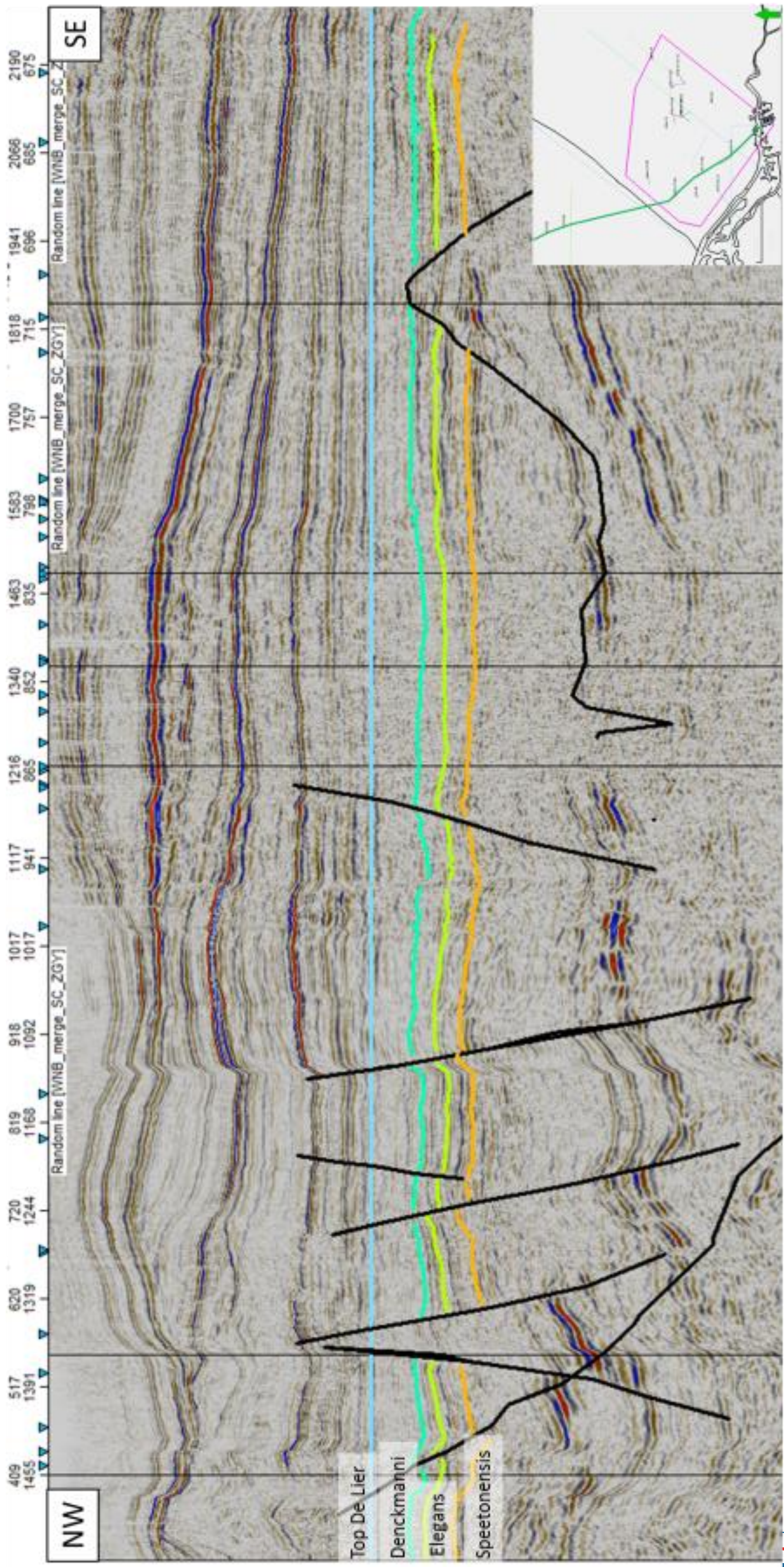
SE
NW
Top De Lier
Denckmanni
Elegans
Speetonensis
Random line [WNB_merge_SC_ZGY]
IL
XL

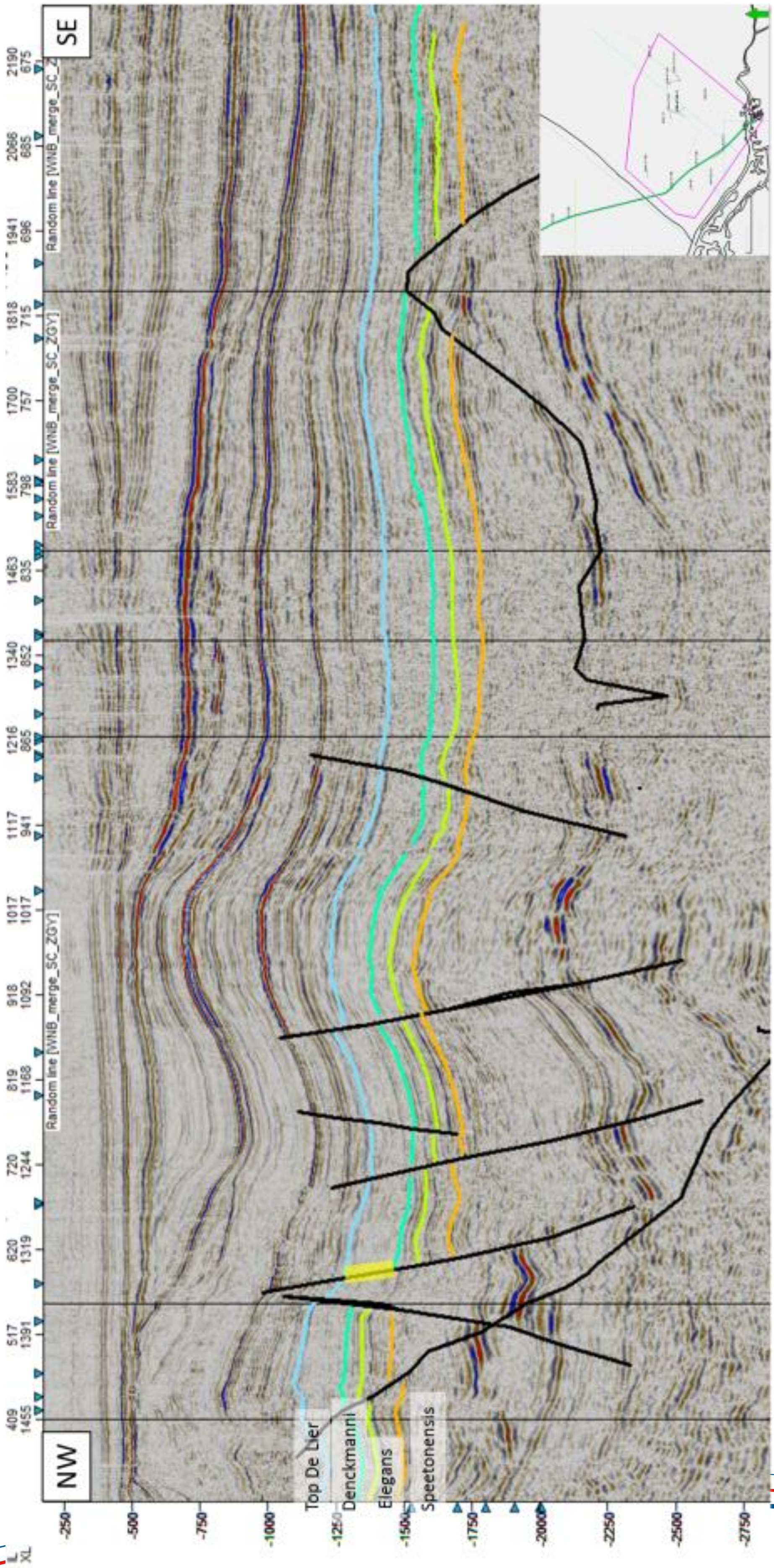
NW
SE
Random line [WNB_merge_SC_ZGY]
Top De Lier
Denckmanni
Elegans
Speetonensis

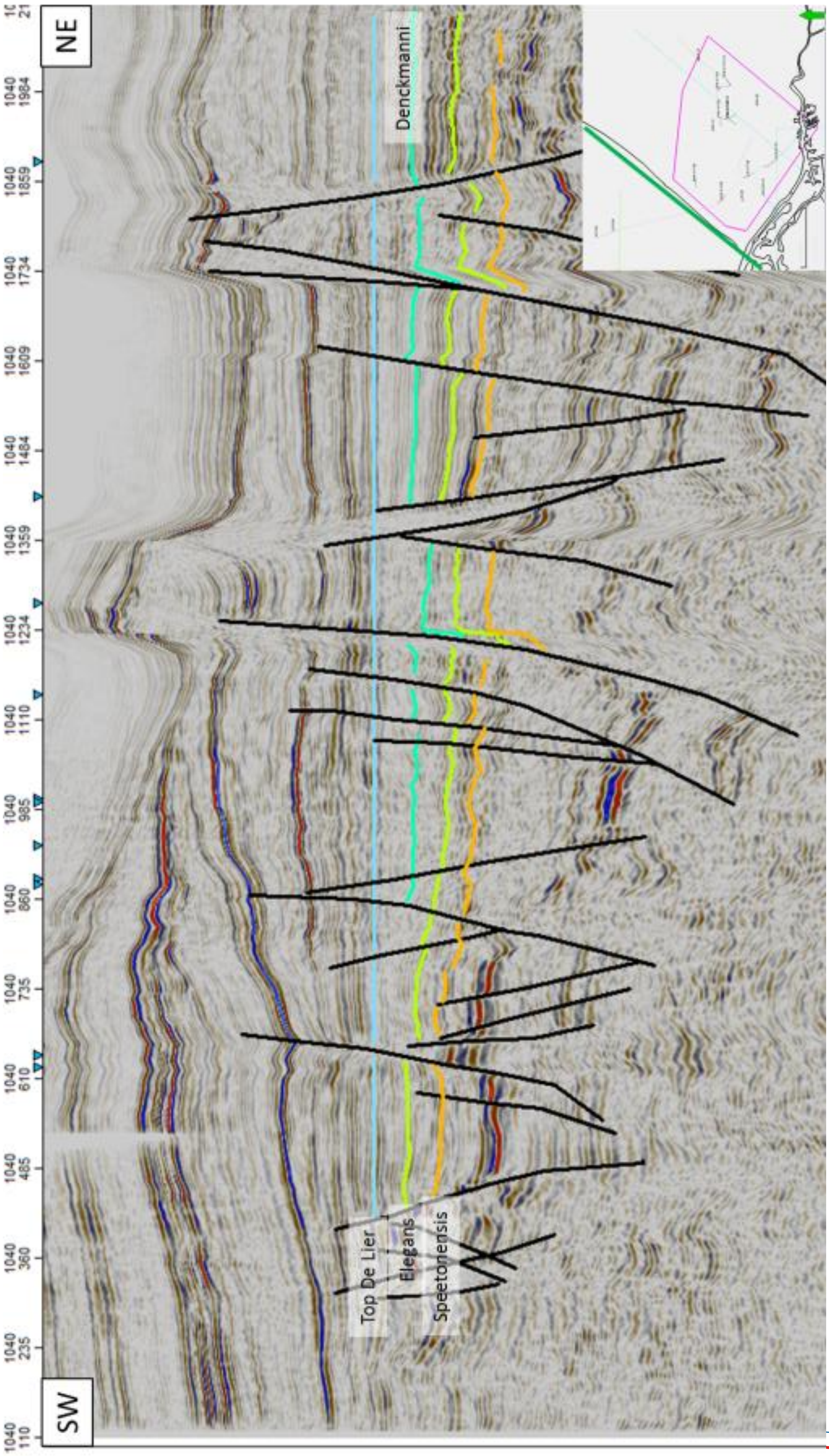
NE
SW
Denckmanni
Top De Lier
Elegans
Speetonensis
IL
XL

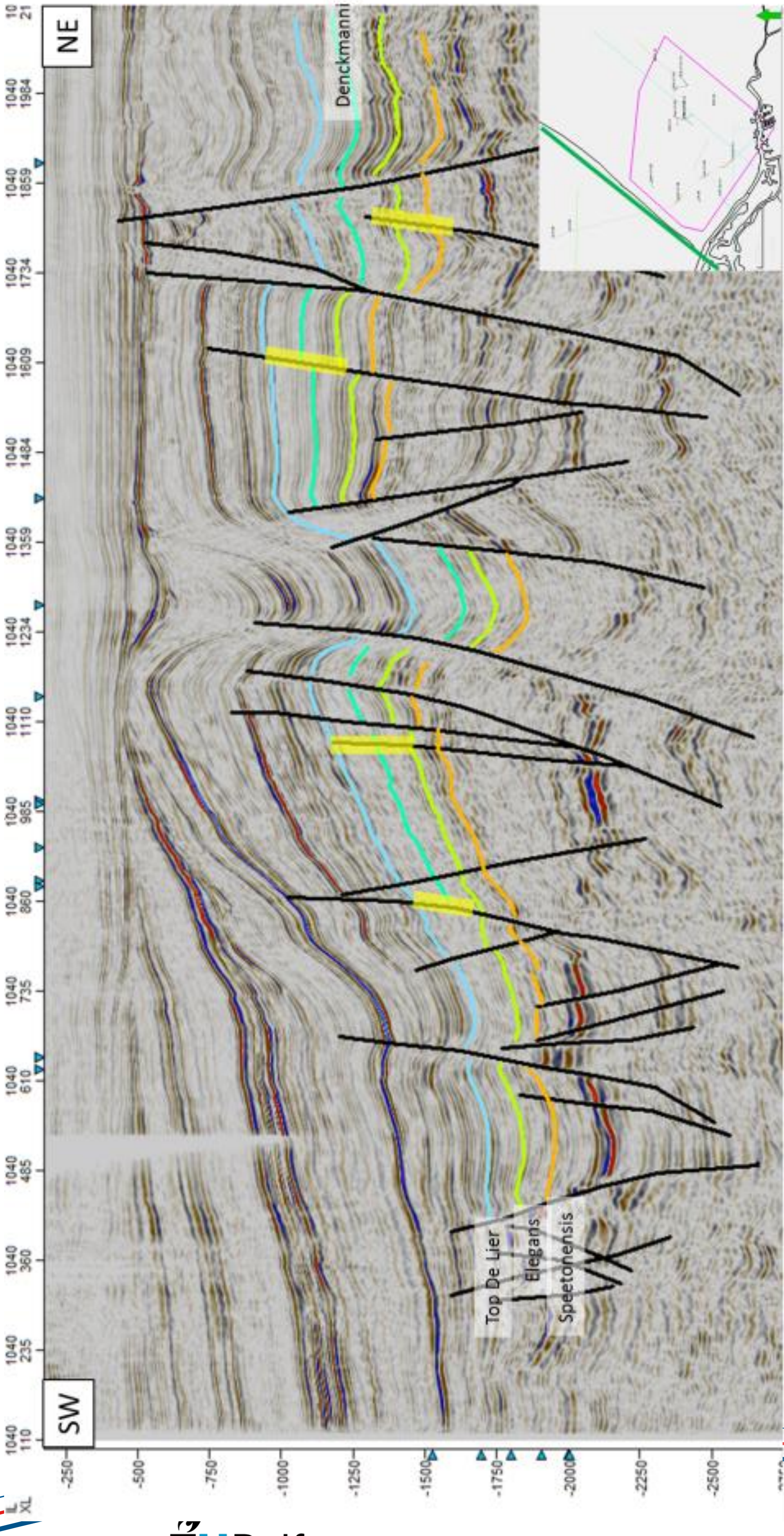
NE
SW
Denckmanni
Top De Lier
Elegans
Speetonensis

9.3 Biostratigaphic studies reports

9.4 INPEFA correlations

Below a well panel showing per well: the GR, the global INPEFA curve and INPEFA curve covering smaller intervals. In blue the interpreted Paratolia marker is indicated in black another marker is shown, this marker is close to the top of Sand 2. The depth is in TVD in m.

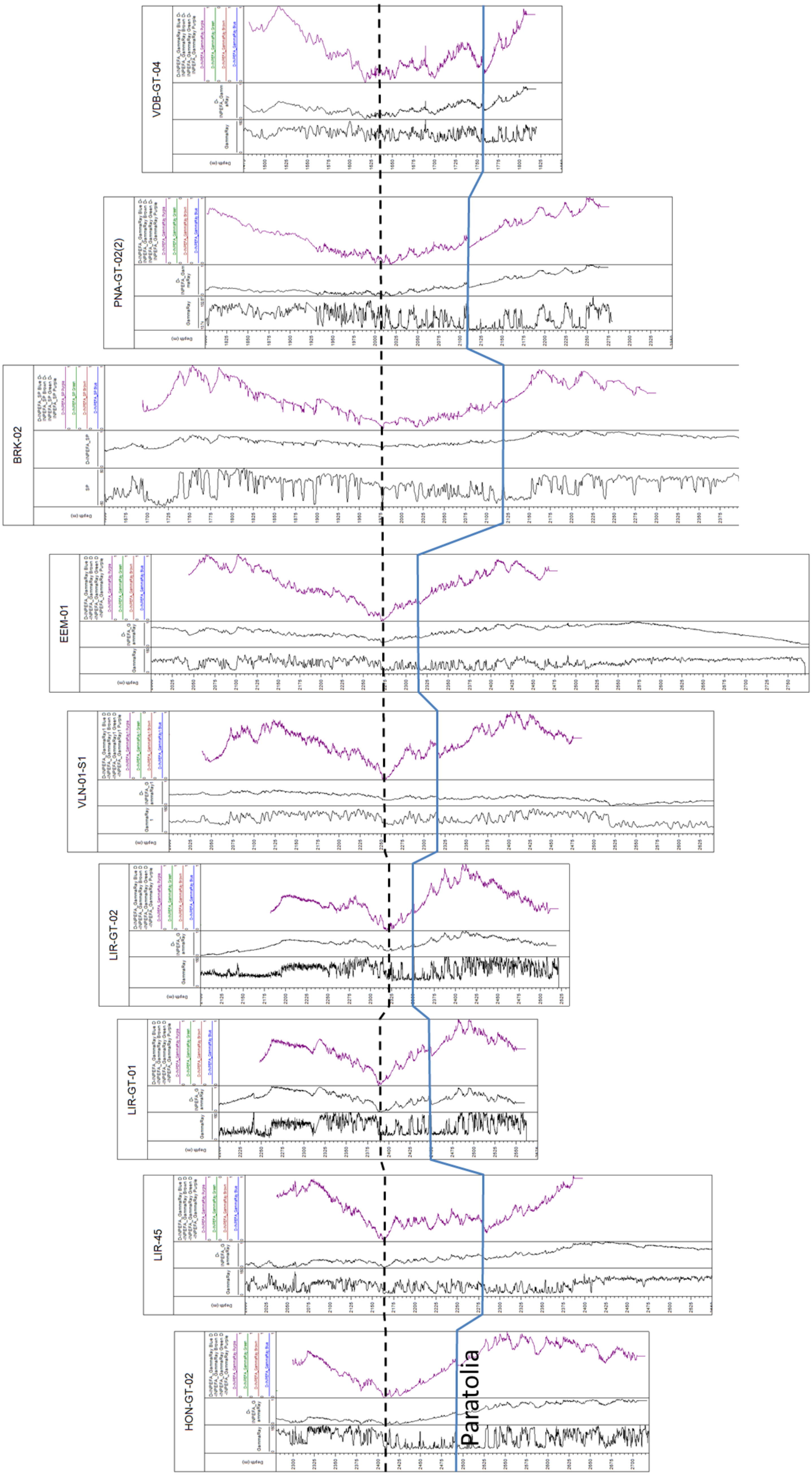

.

9.5 Well correlation panels

The following figures show the well correlations between the different wells, the wells are scaled on TVD. The panels are flattened on the top of De Lier (yellow marker).

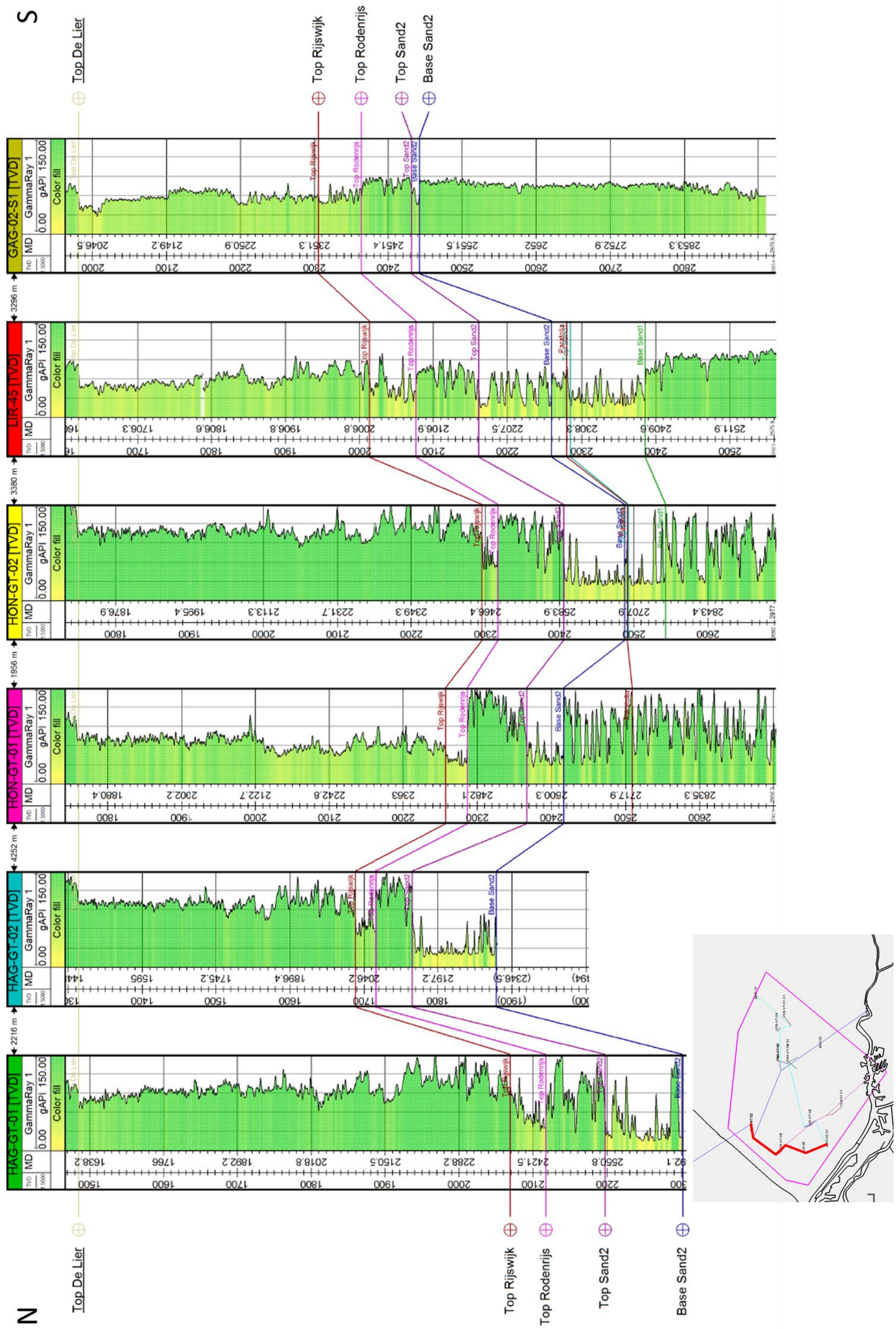

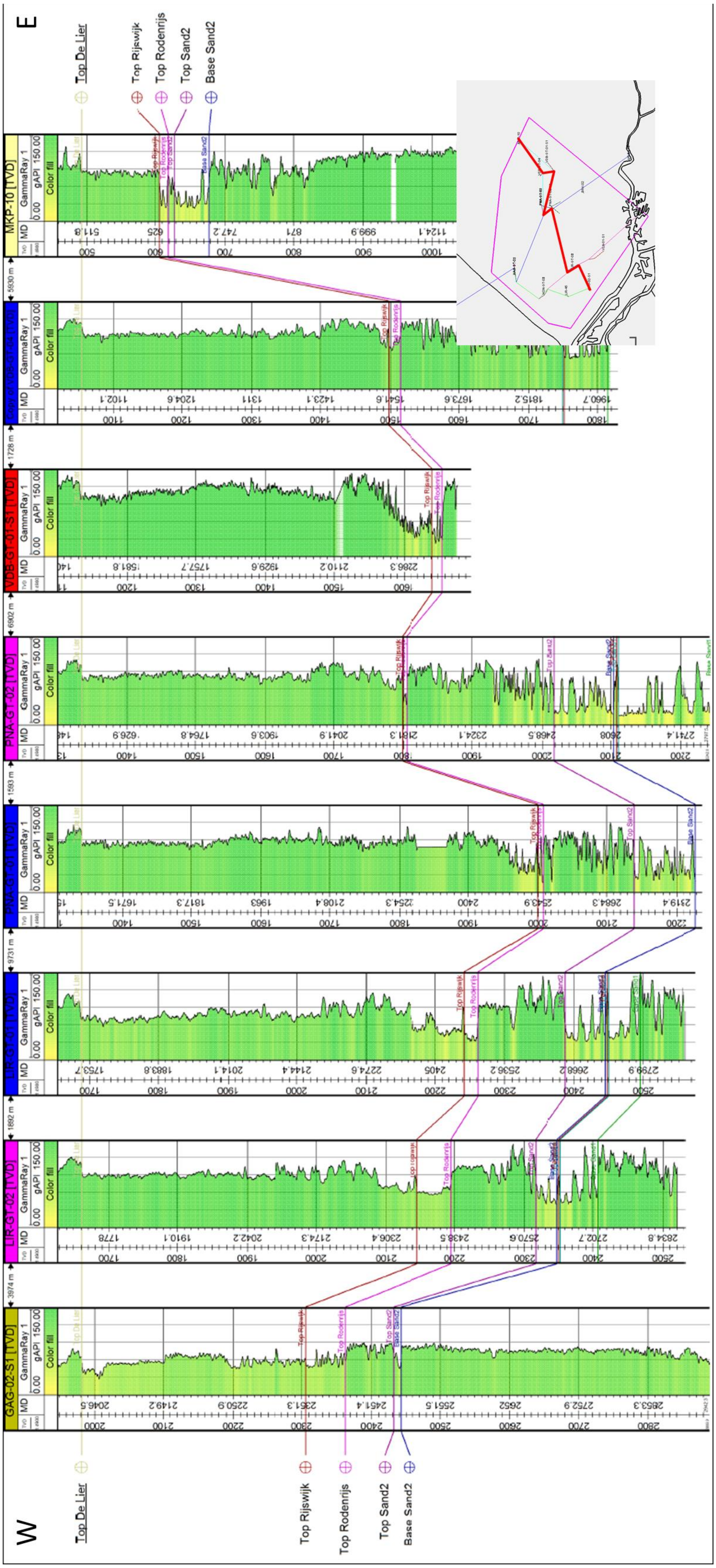
W
E
Top De Lier
Top Rijswijk
Top Rodenrijs
Top Sand2
Base Sand2
GAG-02-S1 [TVD]
LIR-GT-02 [TVD]
LIR-GT-01 [TVD]
PNA-GT-01 [TVD]
PNA-GT-02 [TVD]
VDB-GT-01-S1 [TVD]
MKP-10 [TVD]
GammaRay 1
0.00 gAPI 150.00
Color fill
TVD
MD
3974 m
1892 m
9731 m
1593 m
6902 m
1728 m
5930 m


W
E
Top De Lier
Top Rodenrijs
Top Sand2
Base Sand2
Q13-09 [TVD]
Q13-08 [TVD]
HAG-GT-01 [TVD]
HAG-GT-02 [TVD]
PNA-GT-01 [TVD]
PNA-GT-02 [TVD]
PNA-GT-03-S2 [TVD]
PNA-GT-04 [TVD]
IJS-64-S2 [TVD]
GammaRay 1
gAPI
Color fill
MD

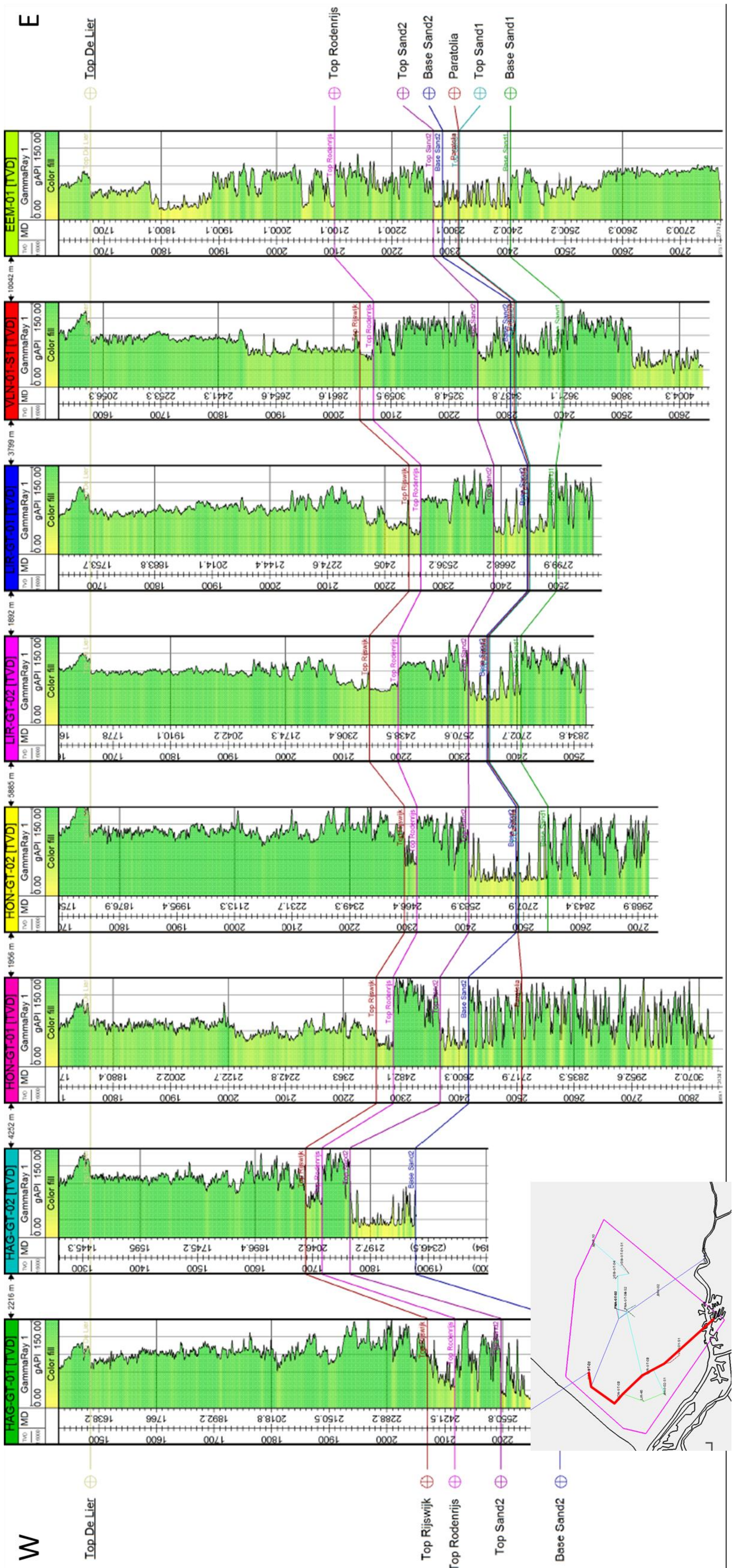
E
W
Top De Lier
Top Rodenrijs
Top Sand2
Base Sand2
Paratolia
Top Sand1
Base Sand1
Top Rijswijk
EEM-01 [TVD]
VLN-01-S1 [TVD]
LIR-GT-01 [TVD]
LIR-GT-02 [TVD]
HON-GT-02 [TVD]
HON-GT-01 [TVD]
HAG-GT-02 [TVD]
HAG-GT-01 [TVD]
GammaRay 1
gAPI
Color fill
MD
TVD

9.6 Well to seismic ties

For the time-depth conversion not all of the selected wells are useful, some were highly deviated (e.g. VLN-01-S1), others were crossing faults (e.g. PNA-13). However, since there is limited check shot data available all wells (nine wells) containing this information have been used.

9.6.1 **Synthetics**

Synthetics were created for wells with T-Z data and a sonic log over a long enough interval, containing proper markers (e.g. base North Sea Group). The T-Z data was a calibrated sonic, the original VSP data or check shot data.

For wells containing a calibrated sonic logs a number of T-Z pairs were taken from these logs, then a synthetic trace was created and if needed a bulk shifts was applied, using clear markers.
For the wells containing check shot data, the sonic was calibrated. This was carried out by creating so-called drift curves (comparing the integrated sonic with the check shot data). The resulting time depth relation was imported into petrel and used as a starting point for the preparation of synthetics.

The wells listed below contained T-Z data:

- CAP-01
- GAG-02-S1
- IJS-64-S2
- LIR-45
- MKP-10
- PNA-13
- Q13-08
- Q13-09
- VLN-01-S1

The following is a listing of applied shifts and methodologies for to the wells with T-Z data.

CAP-01
T-Z pairs from calibrated sonic log were taken and a bulk shift of -50ms applied to obtain a visual match with the base of the North Sea Group and the top De Lier.

In GAG-02-S1 the seismogram was bulk shifted with -25 ms to obtain a visual match with the base of the North Sea Group. GAG-02-S1 is a deviated well, and it crosses a fault close to the top of the Rijnland Group. This results in difficulties to have a nice well tie.

IJS-64-S2
T-Z pairs from calibrated sonic log were taken and a bulk shift of -45ms applied to obtain a visual match with the base of the North Sea Group.

In LIR-45 the seismogram needed a bulk shift of -82 ms to obtain a visual match with the base of the North Sea Group.

In MKP-10 a bulk shift of -30 ms was applied.

For PNA-13 the integrated sonic was used in combination with check shots (where no sonic log data is available). PNA-13 is deviated and is crossing a number of faults, also this well is located in a separate fault block and thus not easily correlatable in the seismic to neighbouring wells.
This resulted in a large uncertainty of the T-Z conversion in this well.

Q13-08
T-Z pairs from calibrated sonic log were taken and a bulk shift of 15ms applied to obtain a visual match with the base of the North Sea Group and the top of the Middle Holland Claystone Member.

Q13-09

T-Z pairs from calibrated sonic log were taken and a bulk shift of 7ms applied to obtain a visual match with the top of the Middle Holland Claystone Member.

For the VLN-01-S1 well, the raw (uncorrected) check shot data was used to calibrate the integrated sonic log, over the part available in digital format. The well path does not fit very well in the seismic, even after bulk shifting. This may be due to the fact that the well is strongly deviated and crossing a major fault.
Eventually the Velmod2 approach (see next paragraph) was used for this well. Using the Velmod2 T-Z data the synthetics were plotted on the seismic and a bulk shift of -20ms was applied to match the top De Lier marker. The part in the well that contains a sonic log is in the deviated section, therefore the well was matched on a random line constructed over the well path.

After creating the synthetics and applying bulk shifts a Time - Depth relation was achieved for these wells. The next step was a stretch and squeeze exercise, in order to obtain a better fit between the synthetics and the seismic this was done for wells Q13-08, Q13-09, LIR-45, GAG-02-S1 and EEM-01. This results in a second Time Depth relation. Images of all the synthetics are shown in Figure 9-2 - Figure 9-21.

Velmod2
For the other geothermal wells, EEM-01 and VLN-01-S1 wells, the Velmod2 approach was used (V0*k, where the k is a constant and the V0 was derived from the map (Van Dalfsen, et al., 2007). For each velocity layer the middle of that interval in the well was selected on the V0 map and thus the V0 was derived per well, per velocity layer.

In well EEM-01 a sonic log is available and synthetics were created, after which a bulk shift was applied of -35ms, to obtain a visual match with the base of the North Sea Group.

In well HON-GT-01 a sonic log is available, however, the interval is too small and not covering any clear markers to use the generated synthetics to be able to tie the well to the seismic.

For each well the generated synthetic is displayed below.

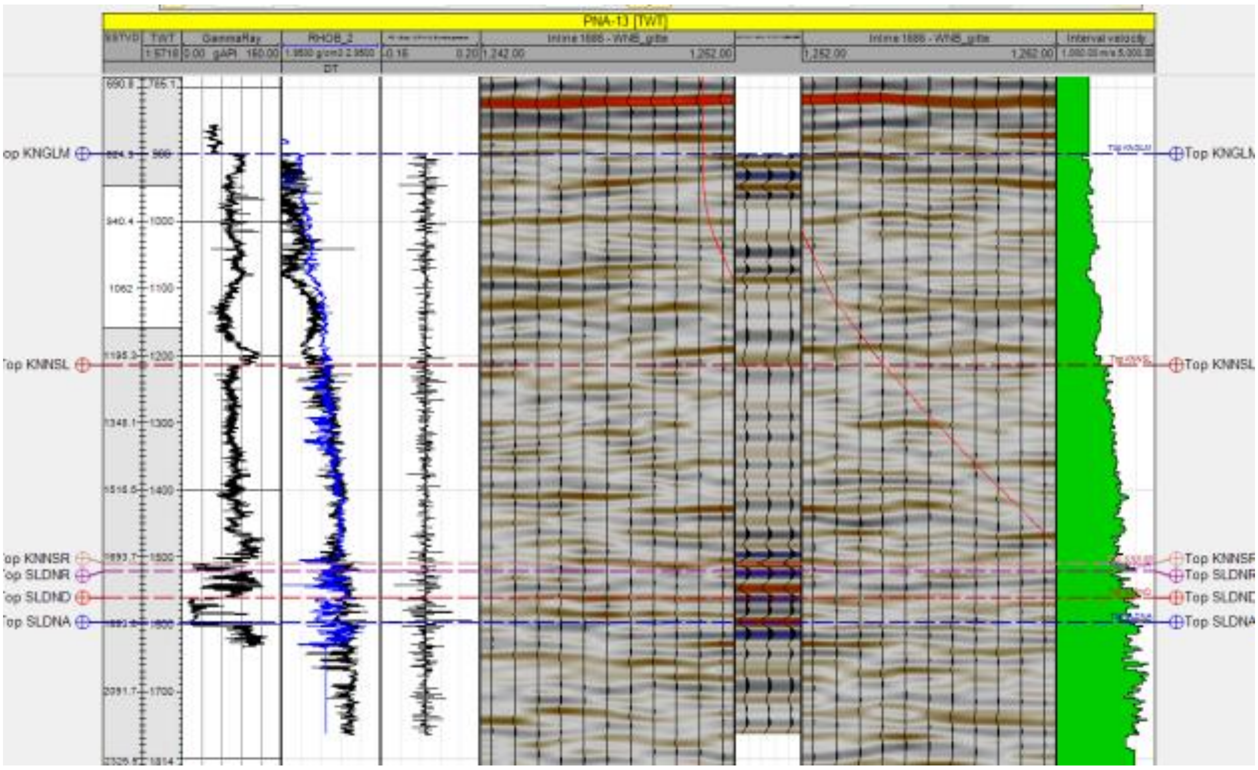

Figure 9-2 PNA-13 not despiked (also calibration not despiked)

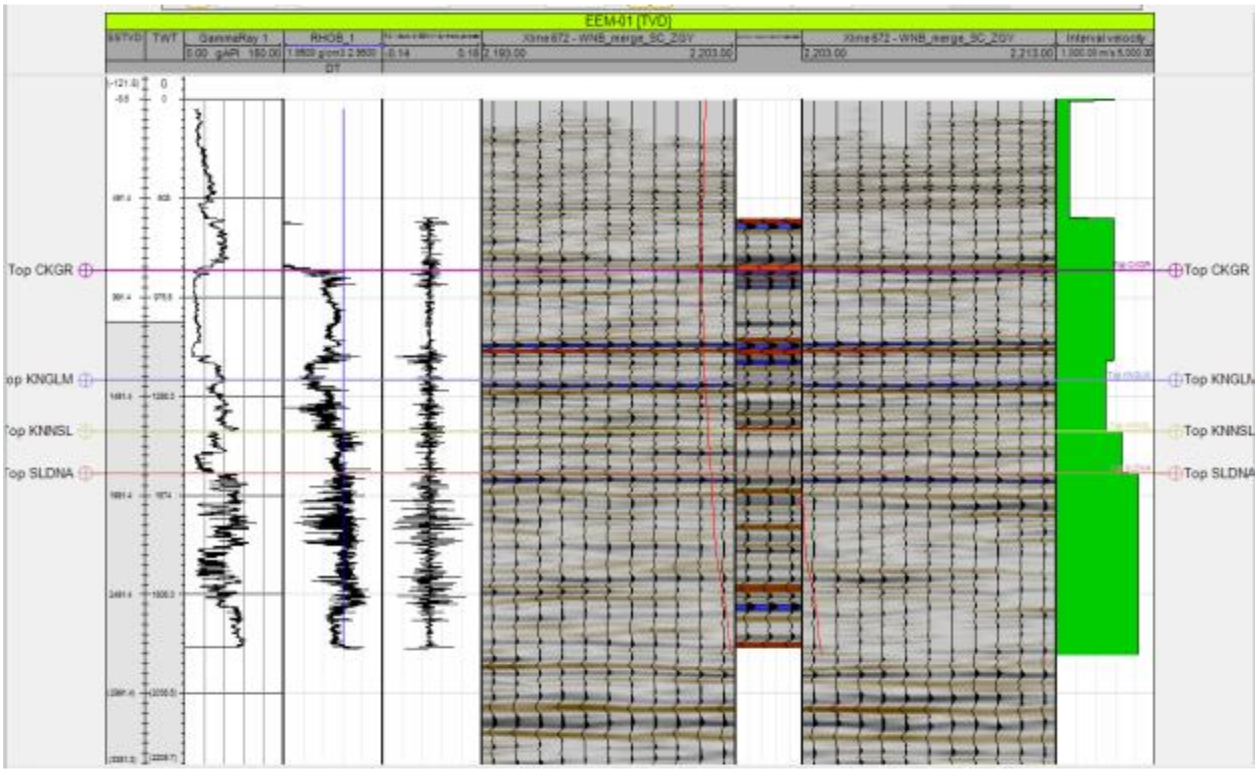

Figure 9-3 EEM-01 bulk shift -35ms, (no despiking done), input TZ from VelMod data.

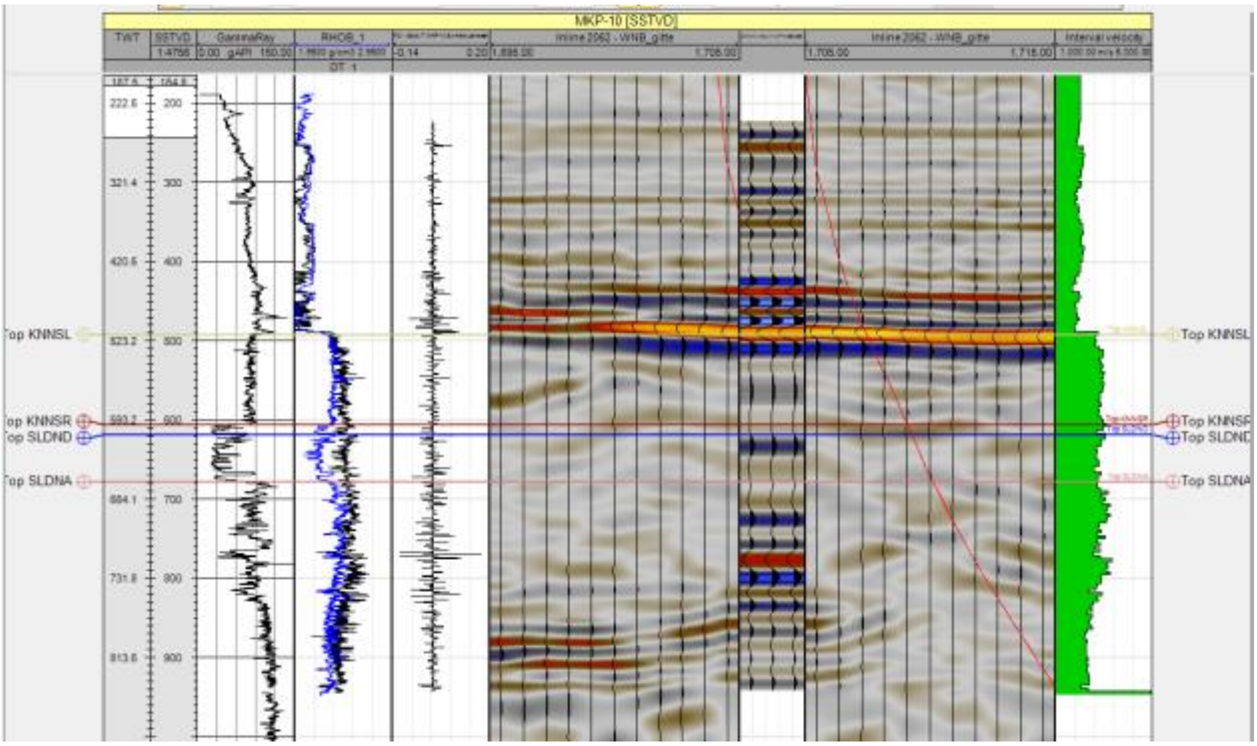

Figure 9-4 MKP-10 bulk shift -30ms, (no despiking done)

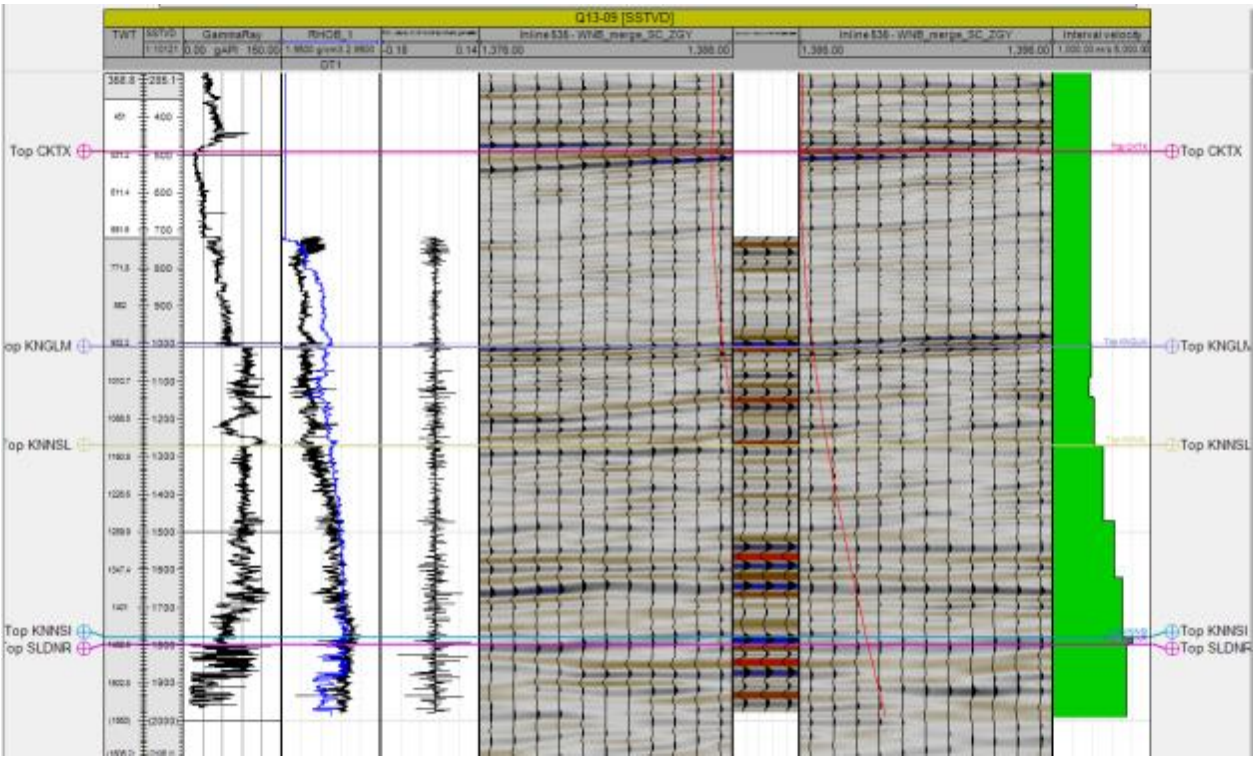

Figure 9-5 Q13-09 not despiked (also calibration not despiked), from calibrated sonic log bulk shift of 7ms applied

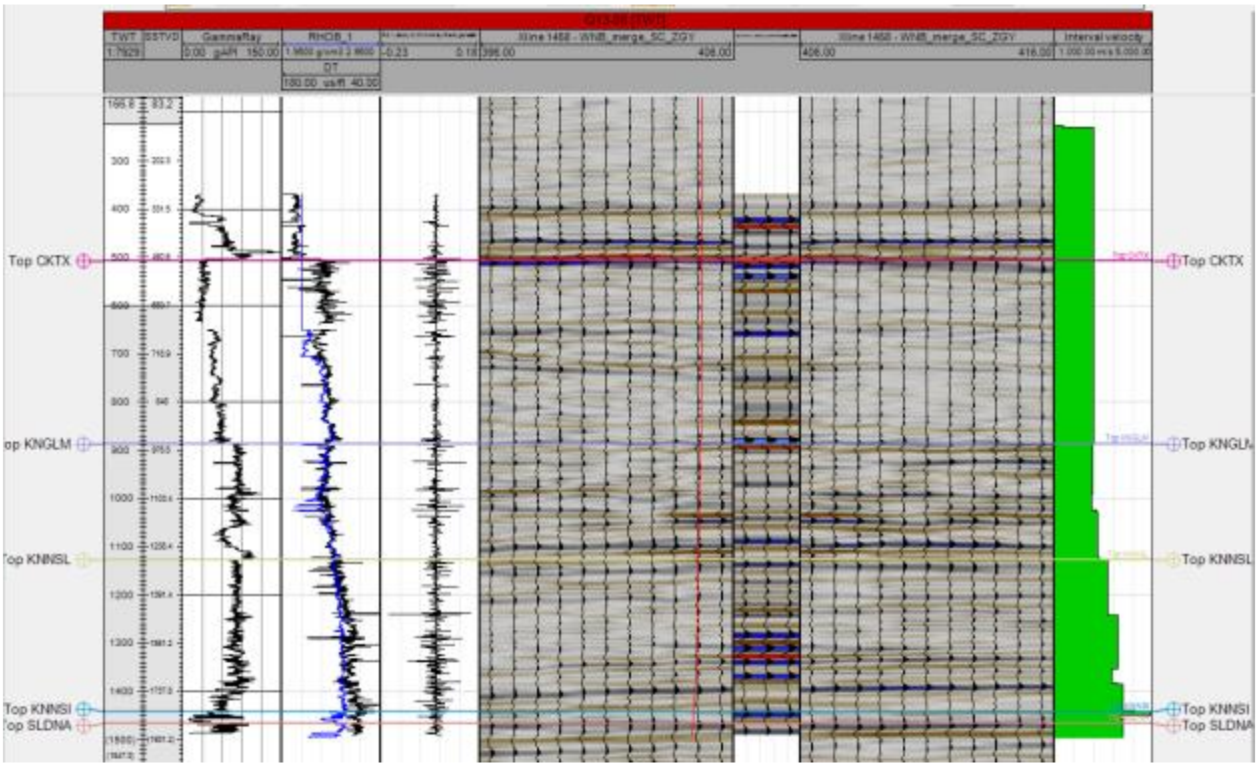

Figure 9-6 Q13-08 not despiked, from calibrated sonic log bulk shift of -15ms applied

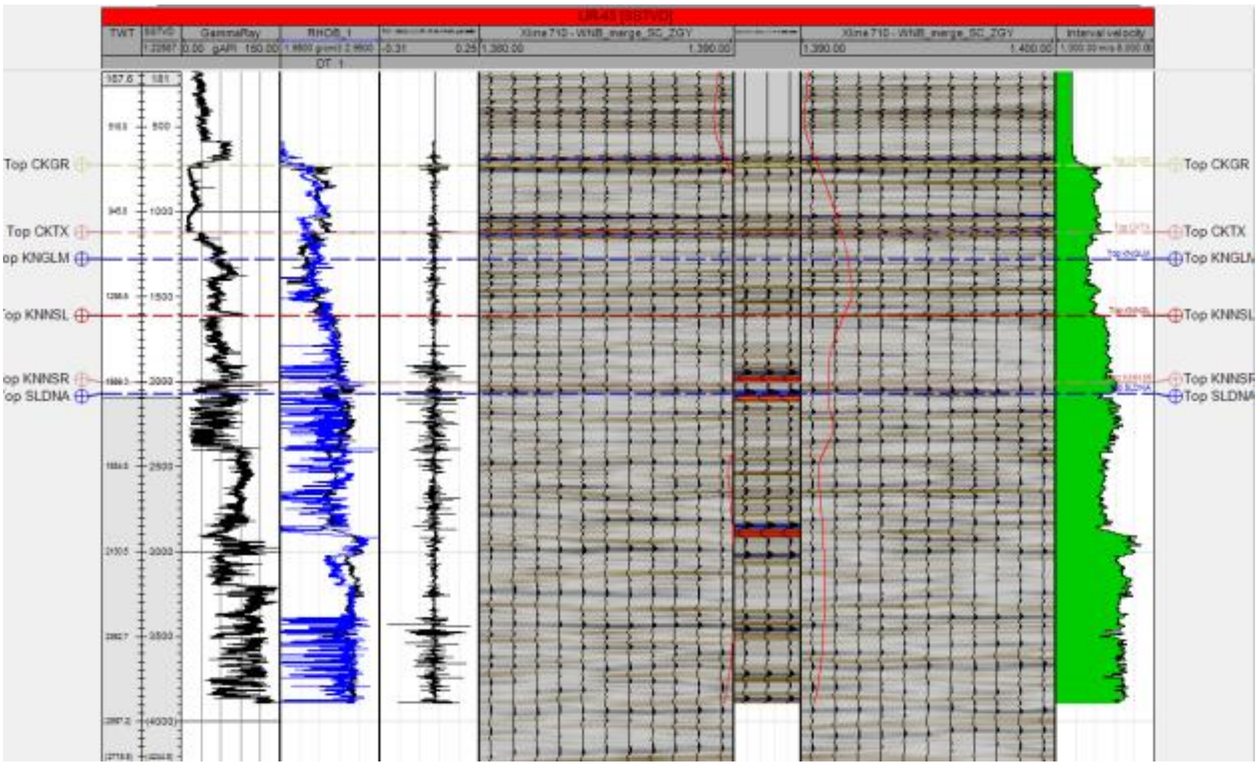

Figure 9-7 LIR-45 bulk shift of -82ms, not despiked (also calibration not despiked)

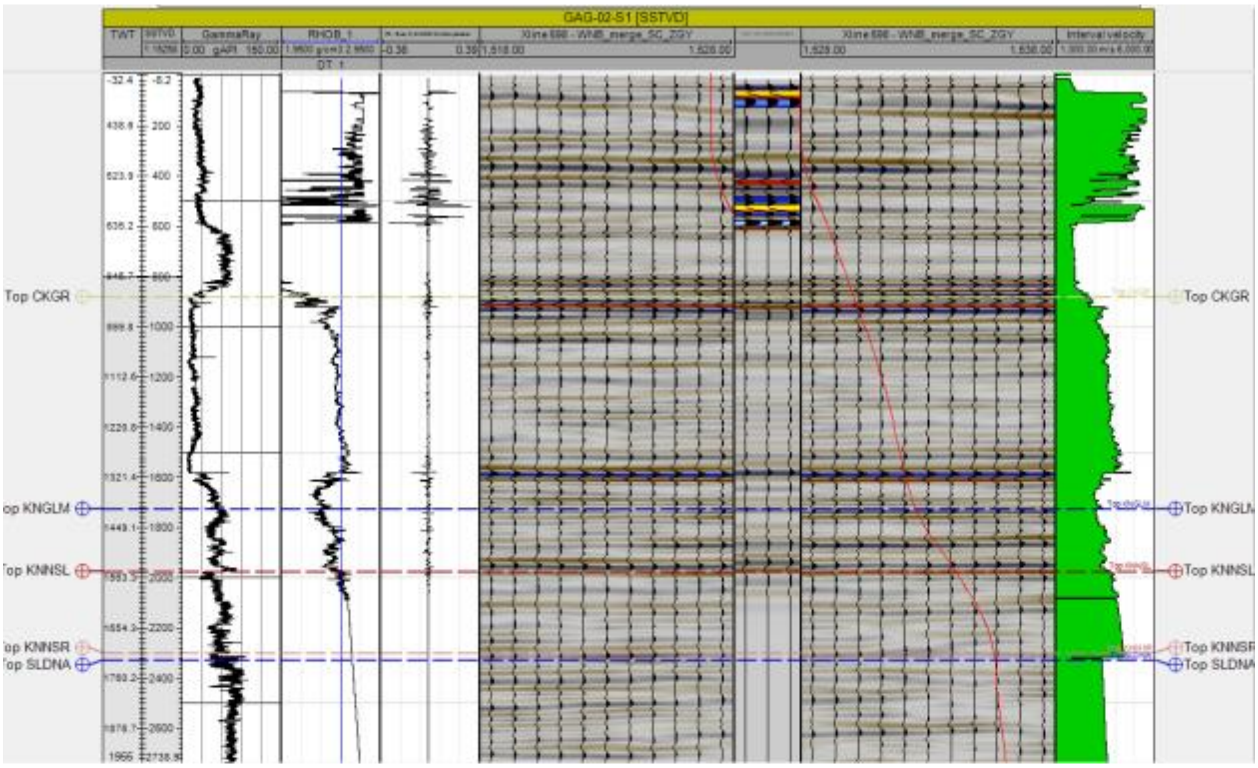

Figure 9-8 GAG-02-S1 bulk shift of -25ms, no clipping/despiking also used in calibrated sonic

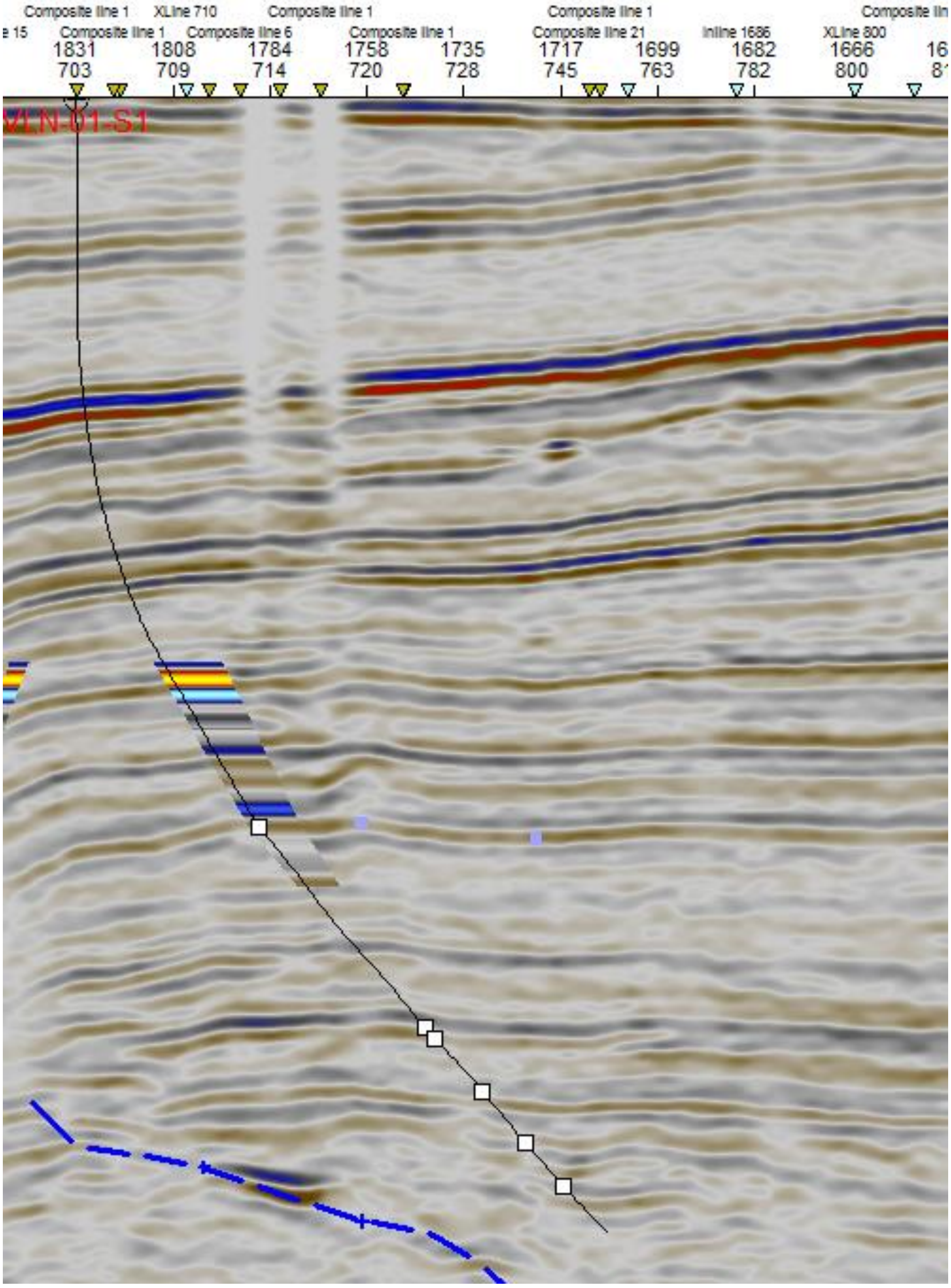

Figure 9-9 VLN-01-S1 Velmod2 input, bulk shift of -20ms was applied. The section with sonic log is deviated, therefore a random line across the well was generated. De Lier was used as a reference marker (purple dots).

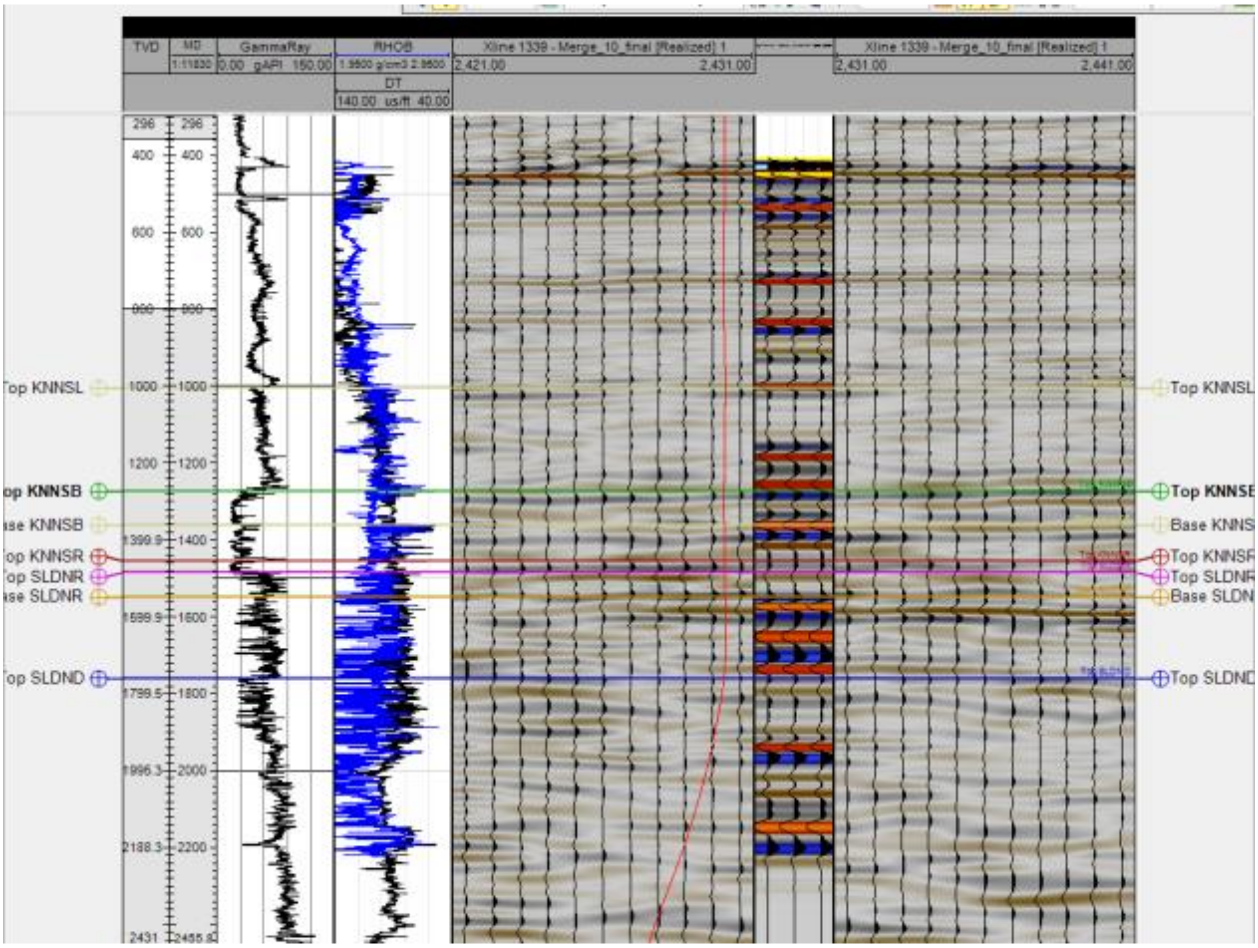

Figure 9-10 CAP-01 Input data from calibrated sonic log, a bulk shift of -50ms was applied.

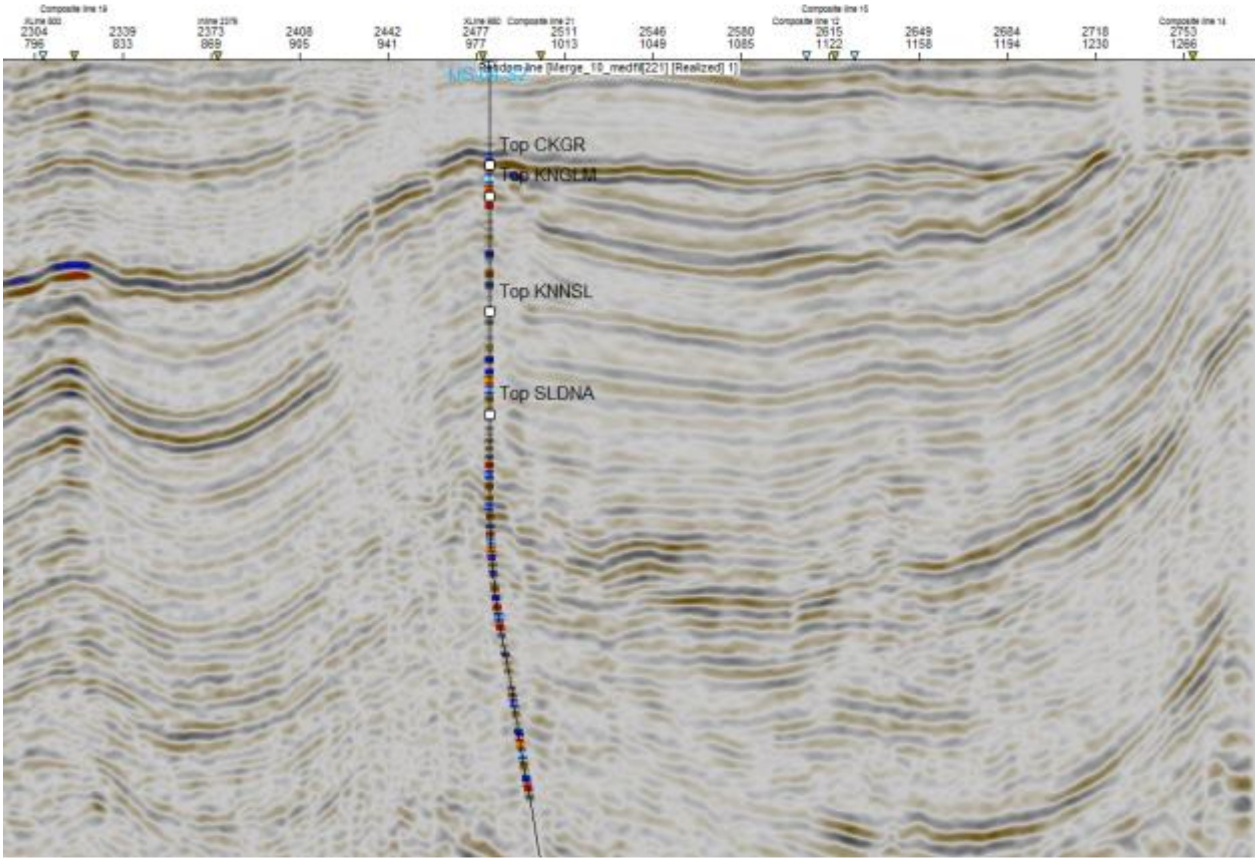

Figure 9-11 Synthectics along IJS-64-S2. The section of interest with sonic log is deviated, therefore a random line across the well was generated. Input data from calibrated sonic log, a bulk shift of -45ms was applied.

9.6.2 Synthetics adjusted

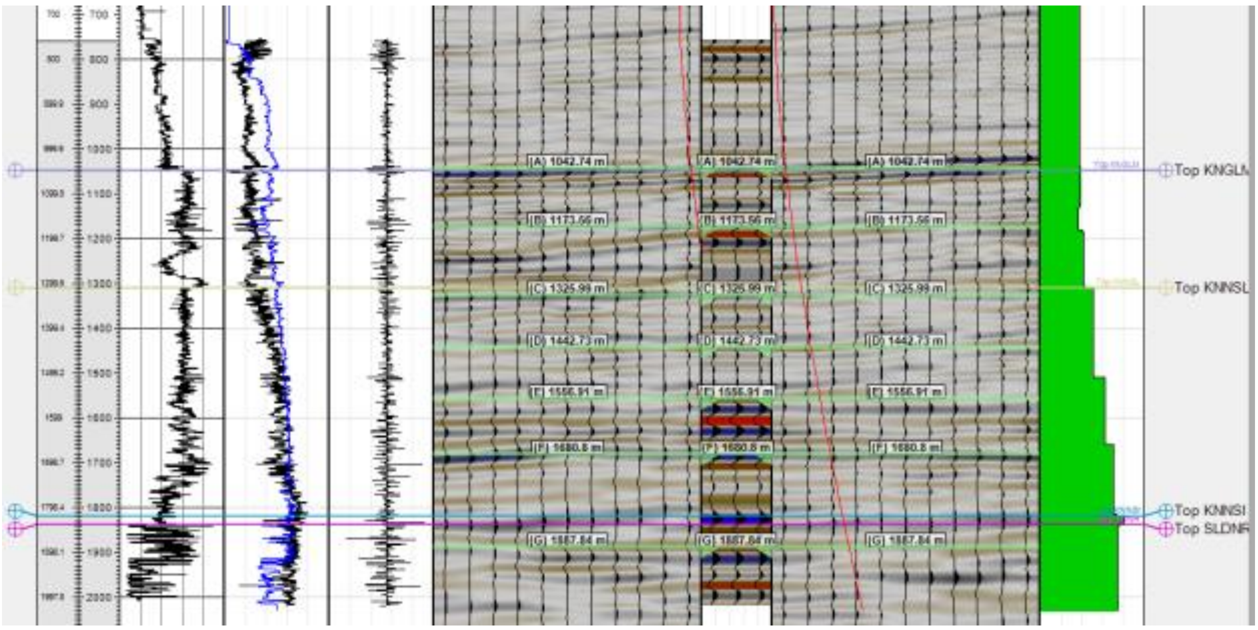

Figure 9-12 Q13-09 alignment points

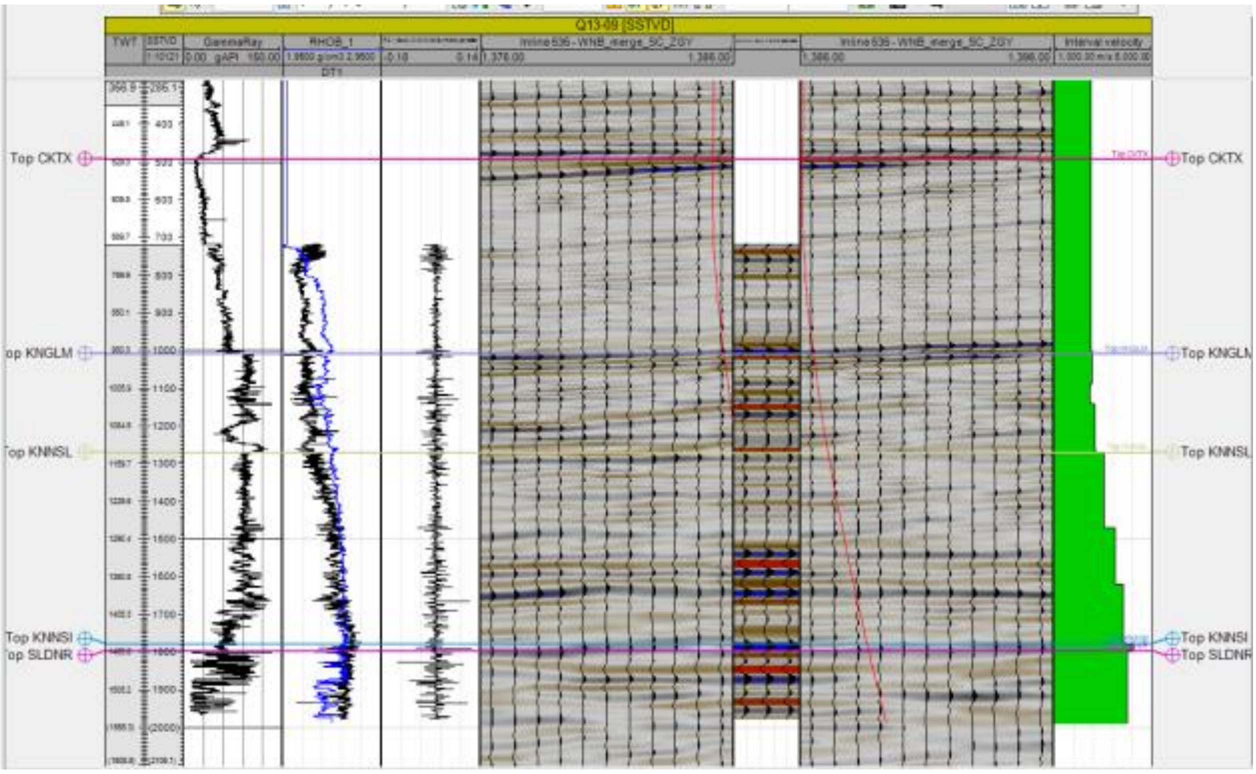

Figure 9-13 Q13-09 aligned synthetic.

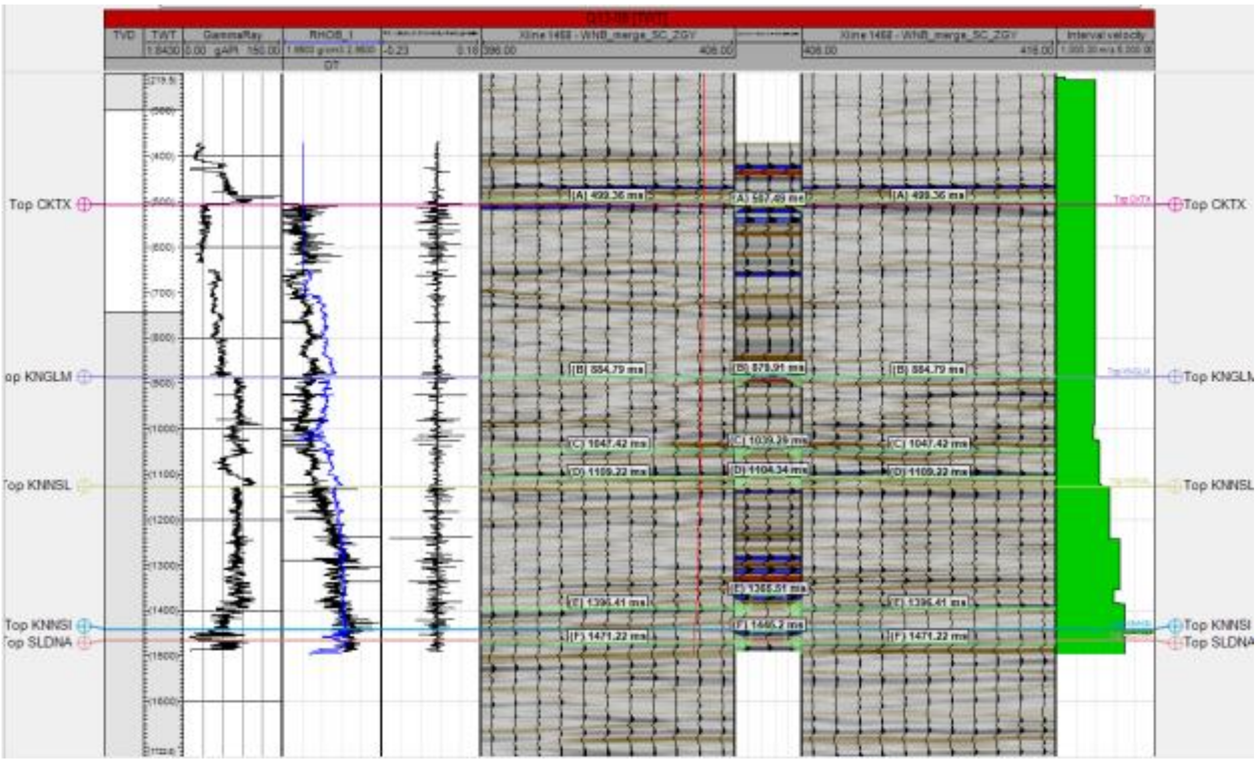

Figure 9-14 Q13-08 alignment points.

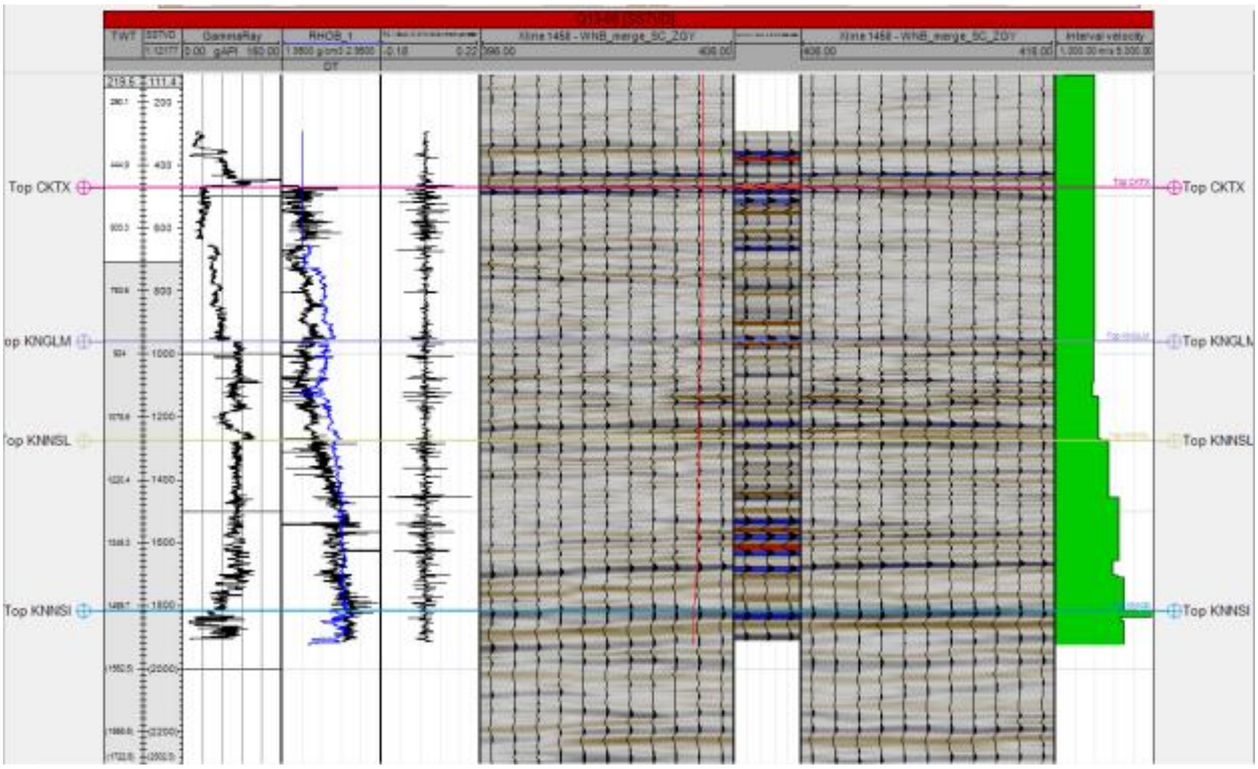

Figure 9-15 Q13-08 aligned synthetic.

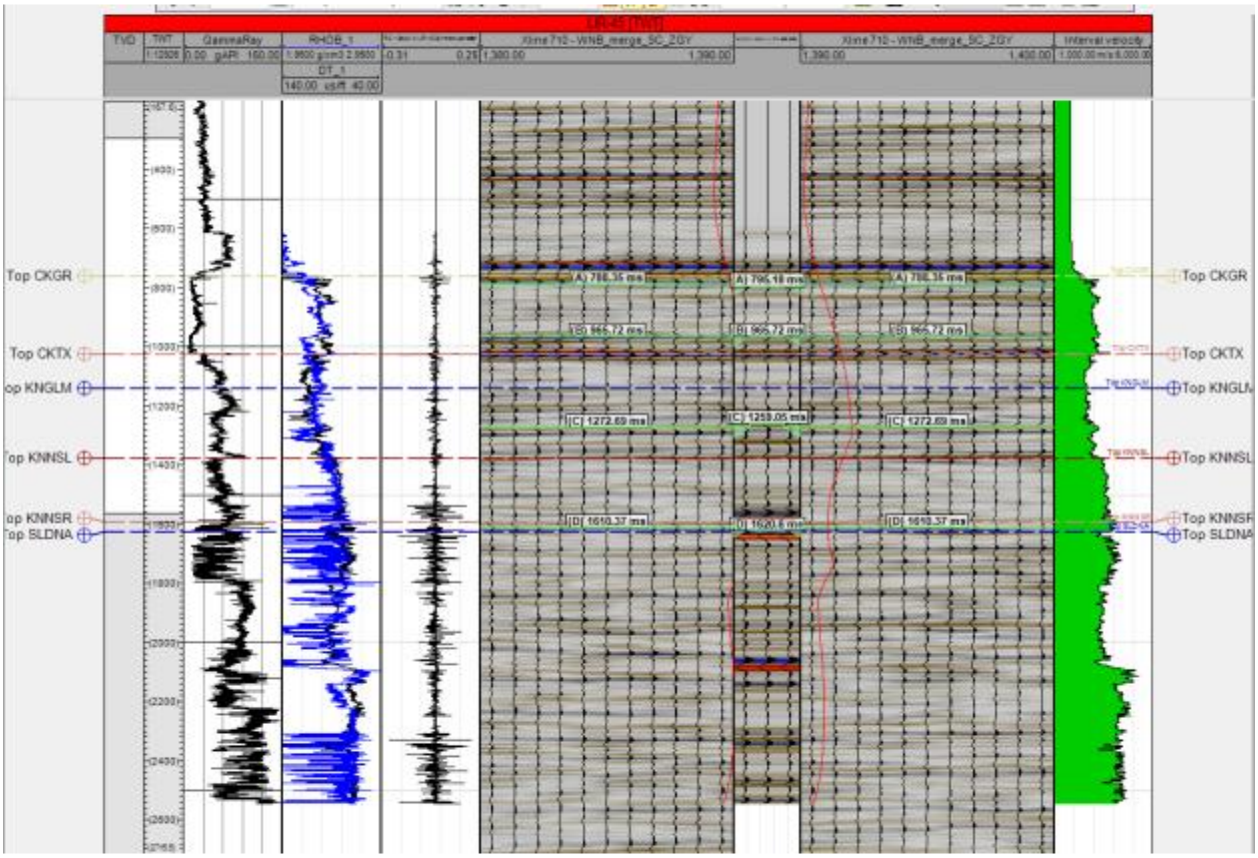

Figure 9-16 LIR-45 alignment points

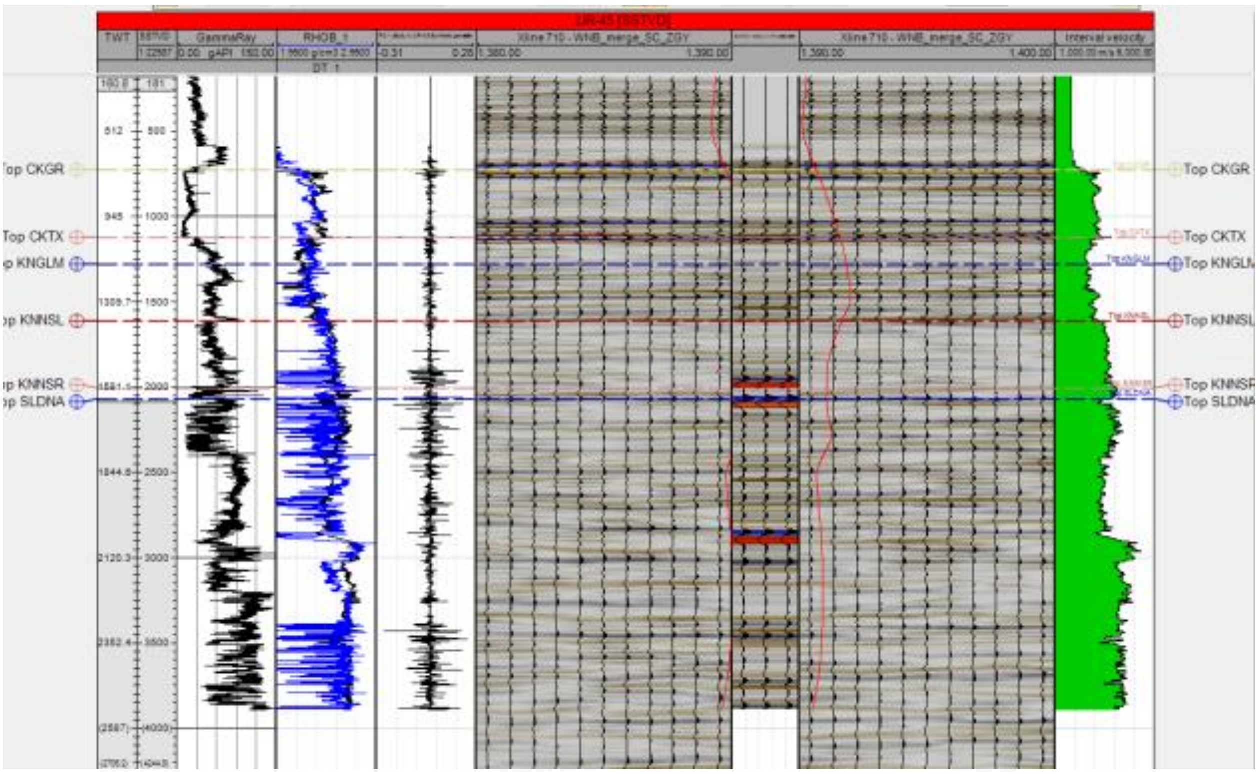

Figure 9-17 LIR-45 aligned synthetic.

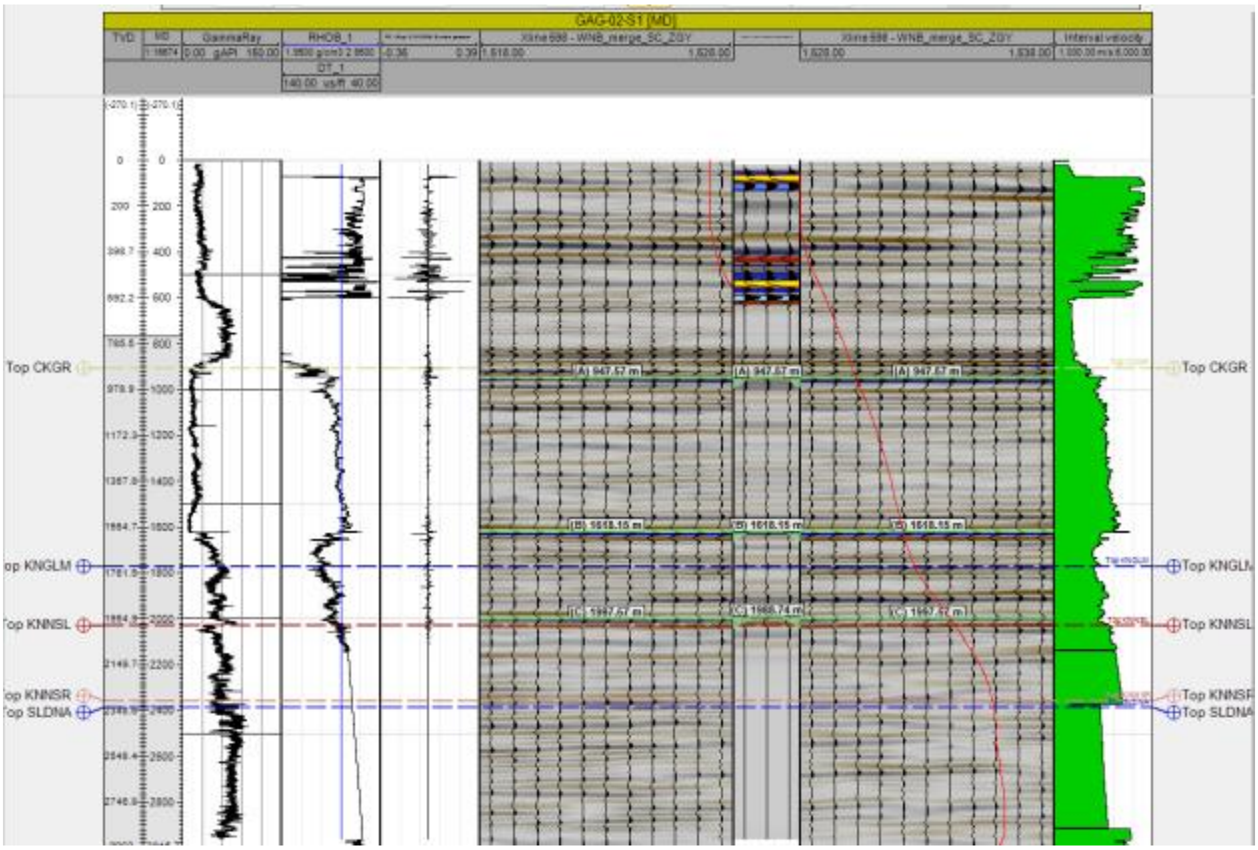

Figure 9-18 GAG-02-S1 alignment points

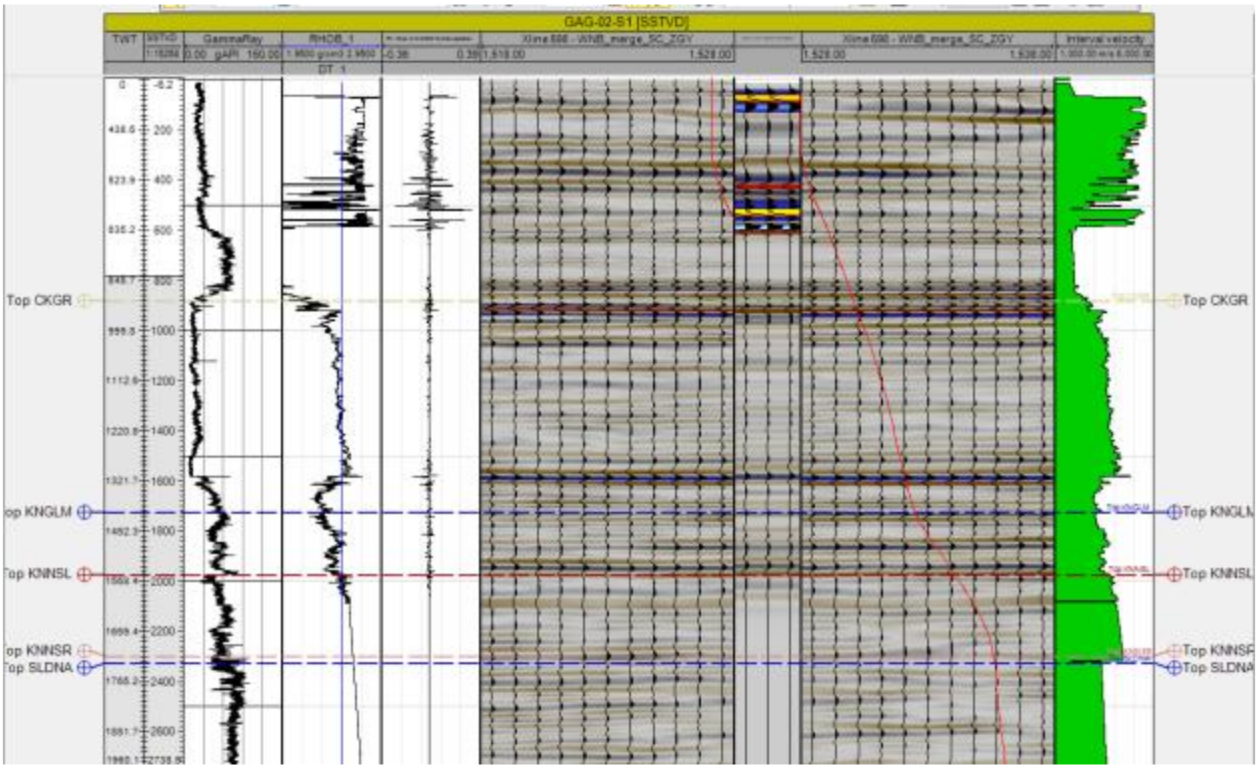

Figure 9-19 GAG-02-S1 aligned synthetic.

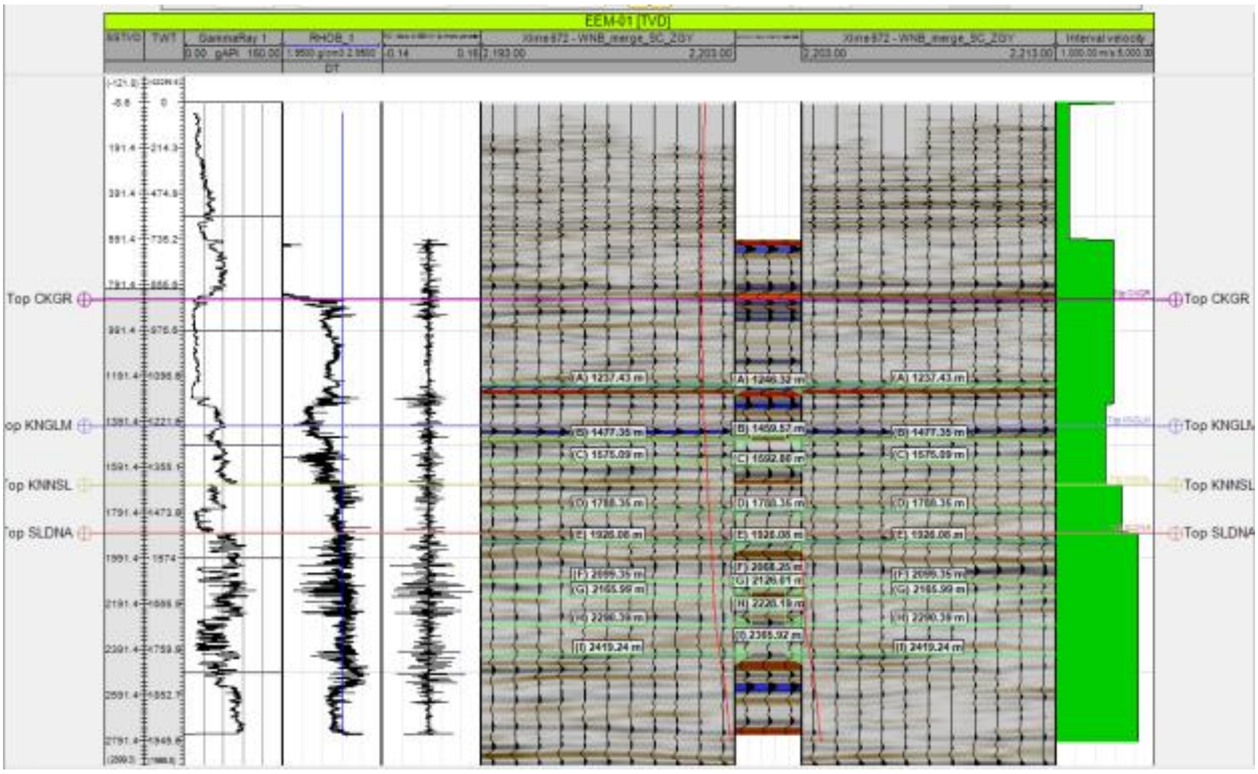

Figure 9-20 EEM-01 alignment points.

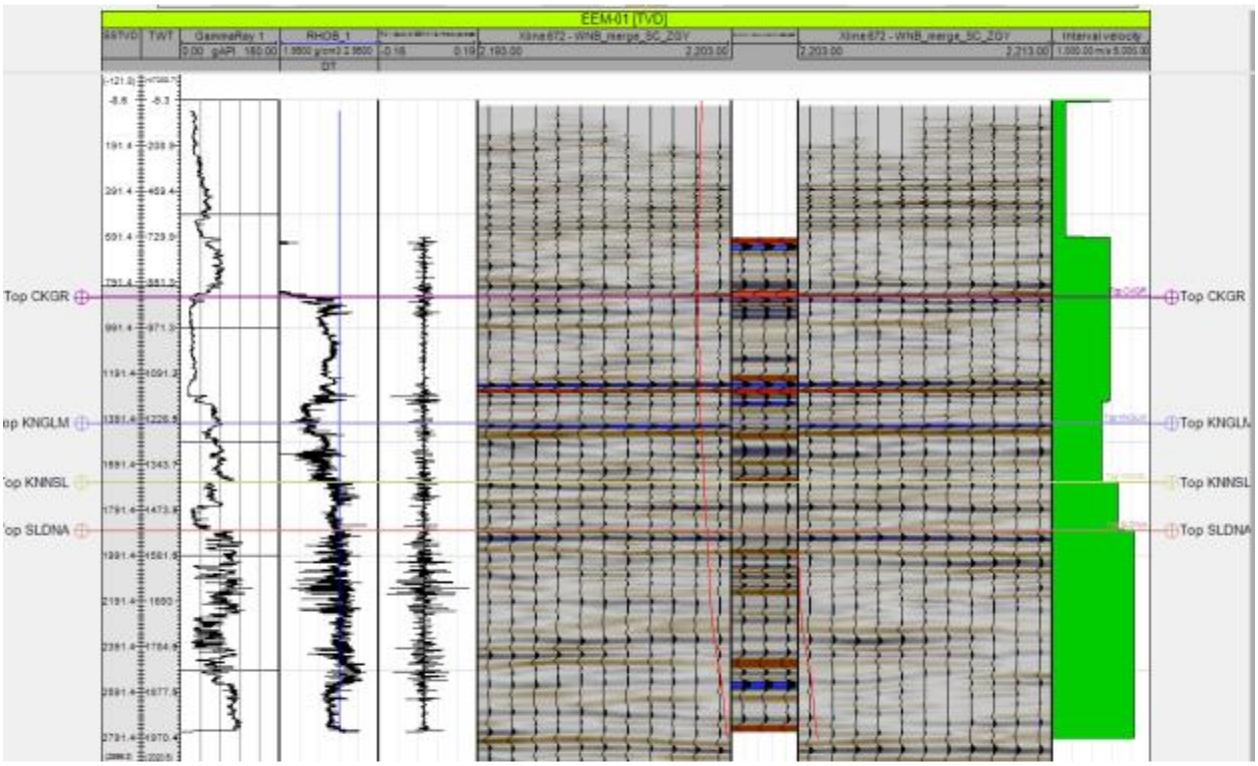

Figure 9-21 EEM-01 aligned synthetic.

9.7 Wells – seismic

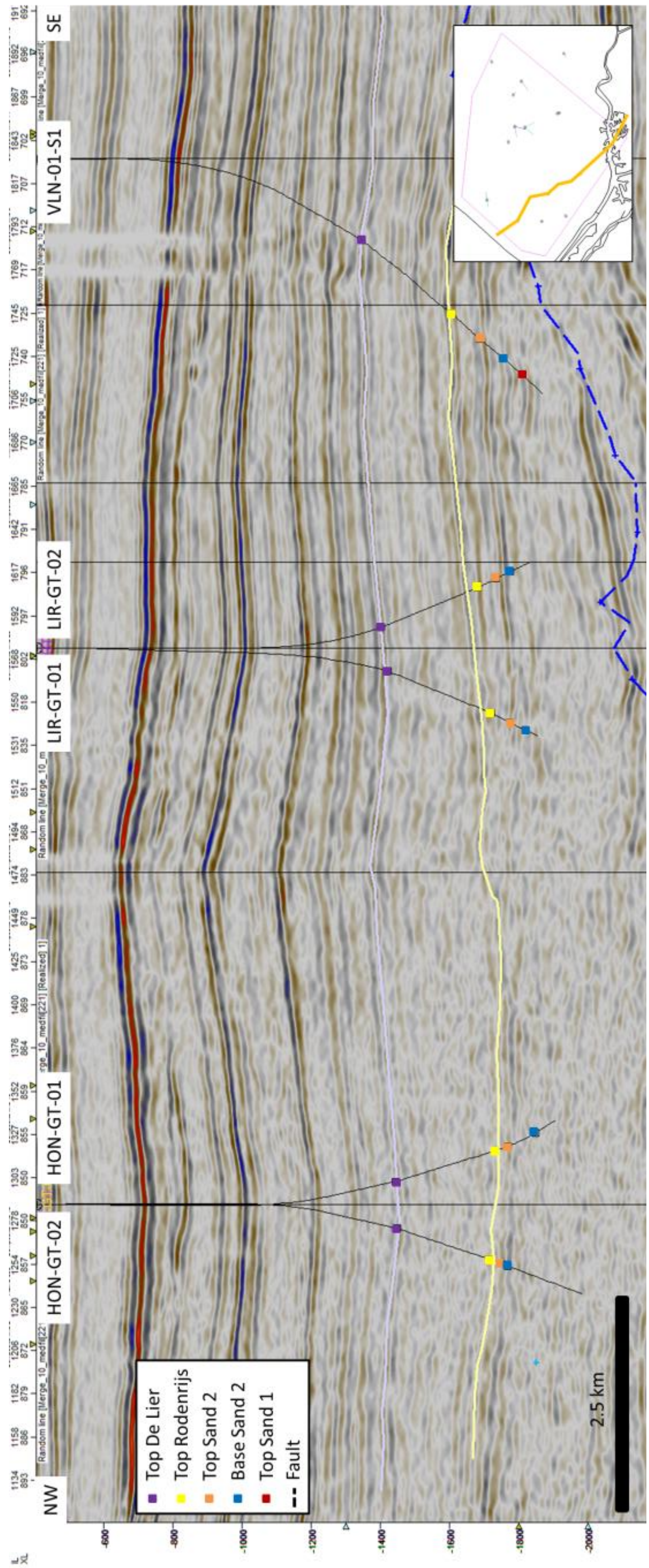

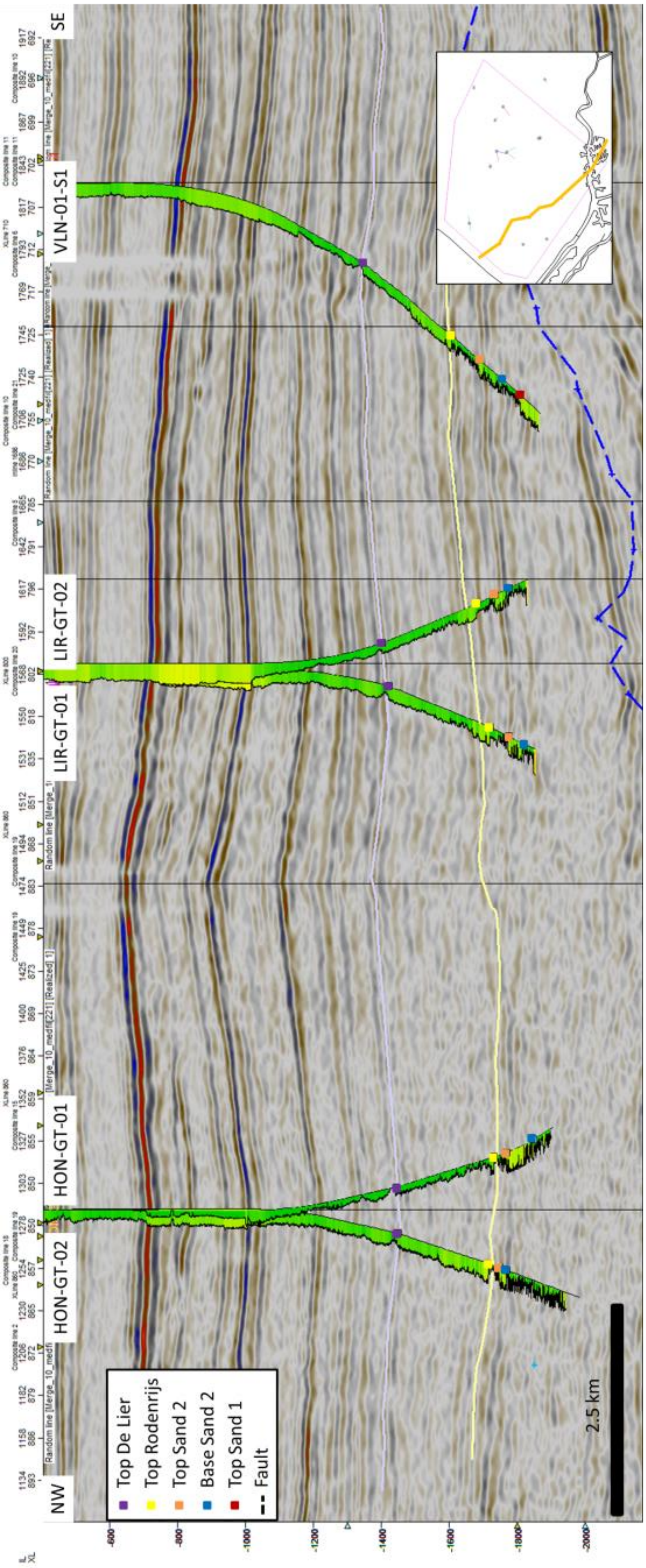
NW
SE
HON-GT-02
HON-GT-01
LIR-GT-01
LIR-GT-02
VLN-01-S1
Top De Lier
Top Rodenrijs
Top Sand 2
Base Sand 2
Top Sand 1
Fault
2.5 km
-600
-800
-1000
-1200
-1400
-1600
-1800
-2000

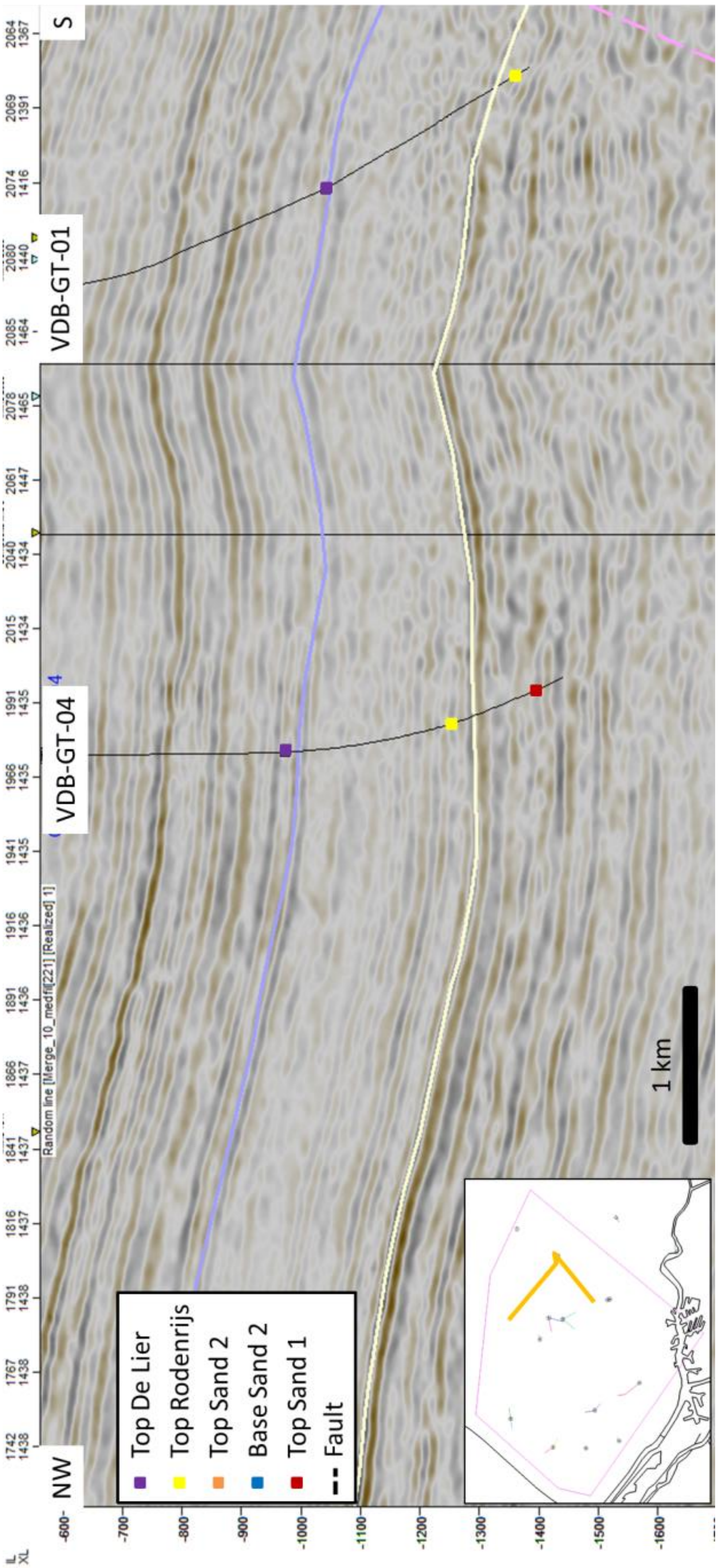

NW
S
VDB-GT-04
VDB-GT-01
Random line [Merge_10_medfil[221] [Realized] 1]
Top De Lier
Top Rodenrijs
Top Sand 2
Base Sand 2
Top Sand 1
Fault
1 km

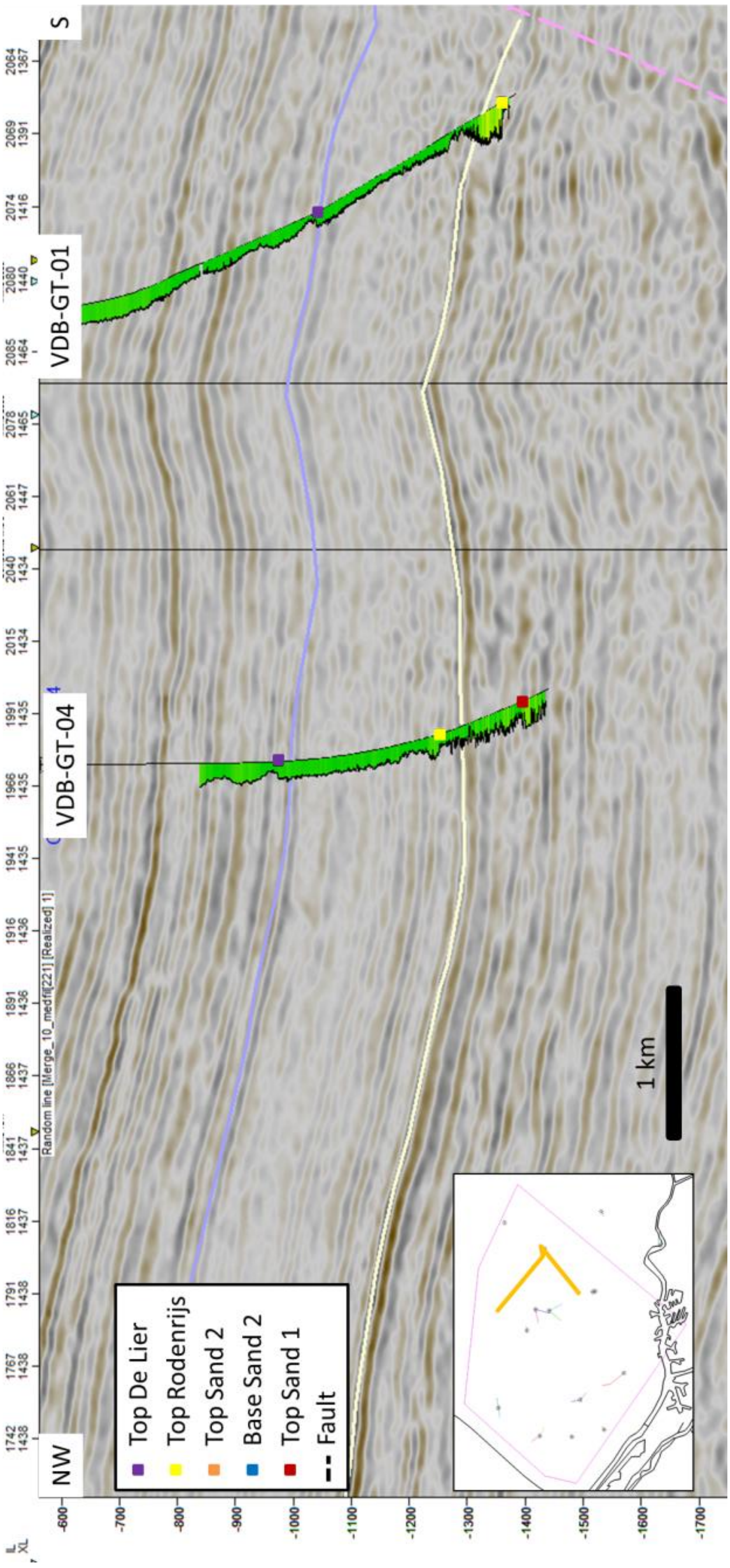
NW
S
VDB-GT-01
VDB-GT-04
Top De Lier
Top Rodenrijs
Top Sand 2
Base Sand 2
Top Sand 1
Fault
1 km
Random line [Merge_10_medfilt[221]] [Realized] 1
IL
XL
-600
-700
-800
-900
-1000
-1100
-1200
-1300
-1400
-1500
-1600
-1700

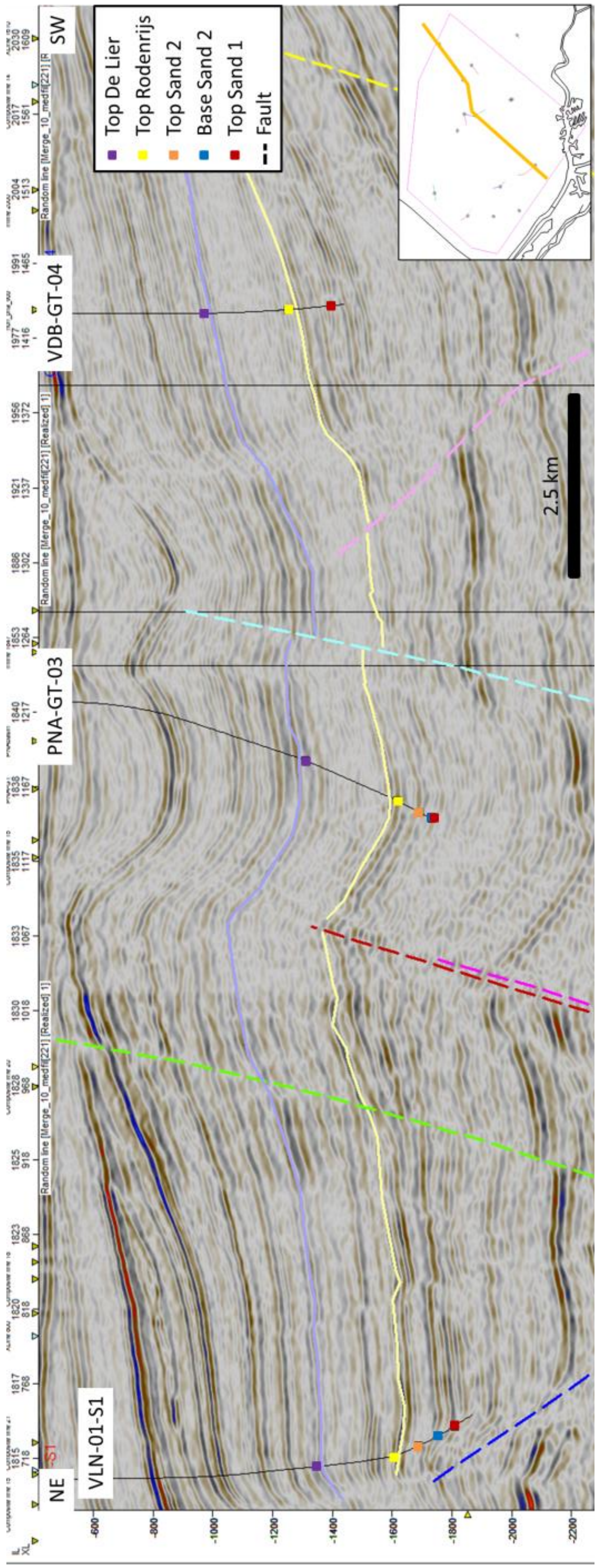
SW
NE
Top De Lier
Top Rodenrijs
Top Sand 2
Base Sand 2
Top Sand 1
Fault
VDB-GT-04
PNA-GT-03
VLN-01-S1
2.5 km
-600
-800
-1000
-1200
-1400
-1600
-1800
-2000
-2200

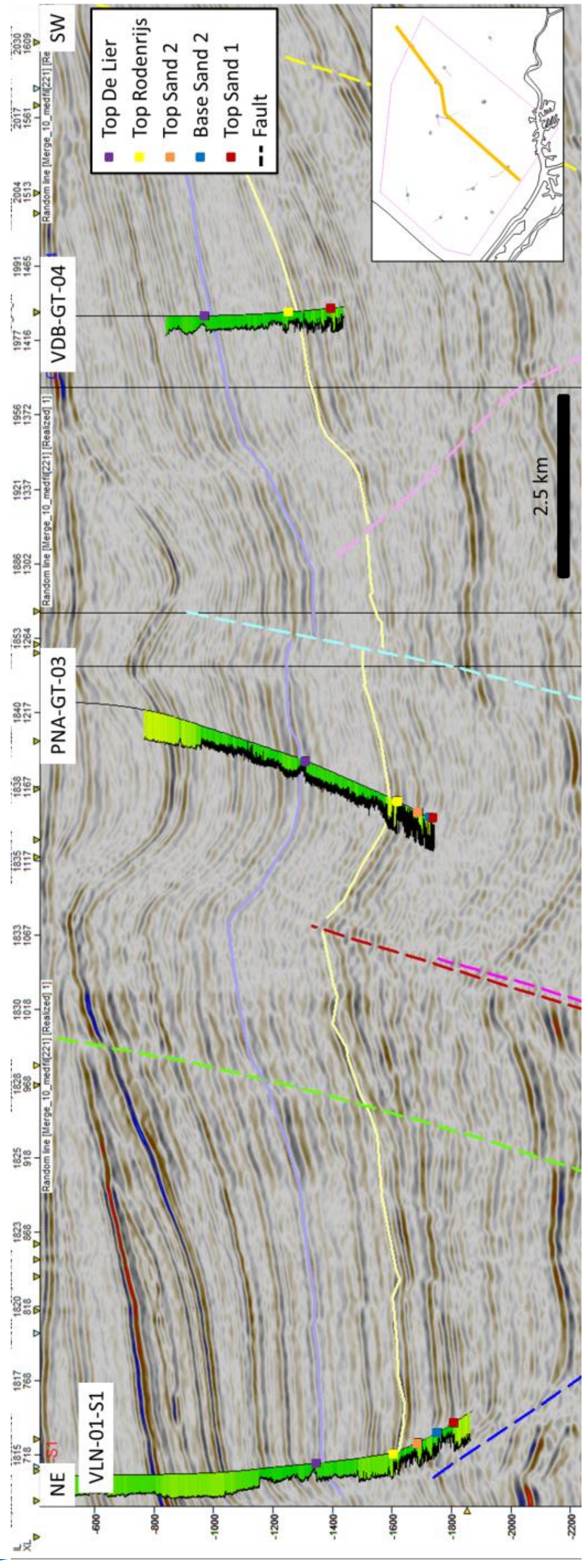
NE
SW
VLN-01-S1
PNA-GT-03
VDB-GT-04
Top De Lier
Top Rodenrijs
Top Sand 2
Base Sand 2
Top Sand 1
Fault
2.5 km
-600
-800
-1000
-1200
-1400
-1600
-1800
-2000
-2200

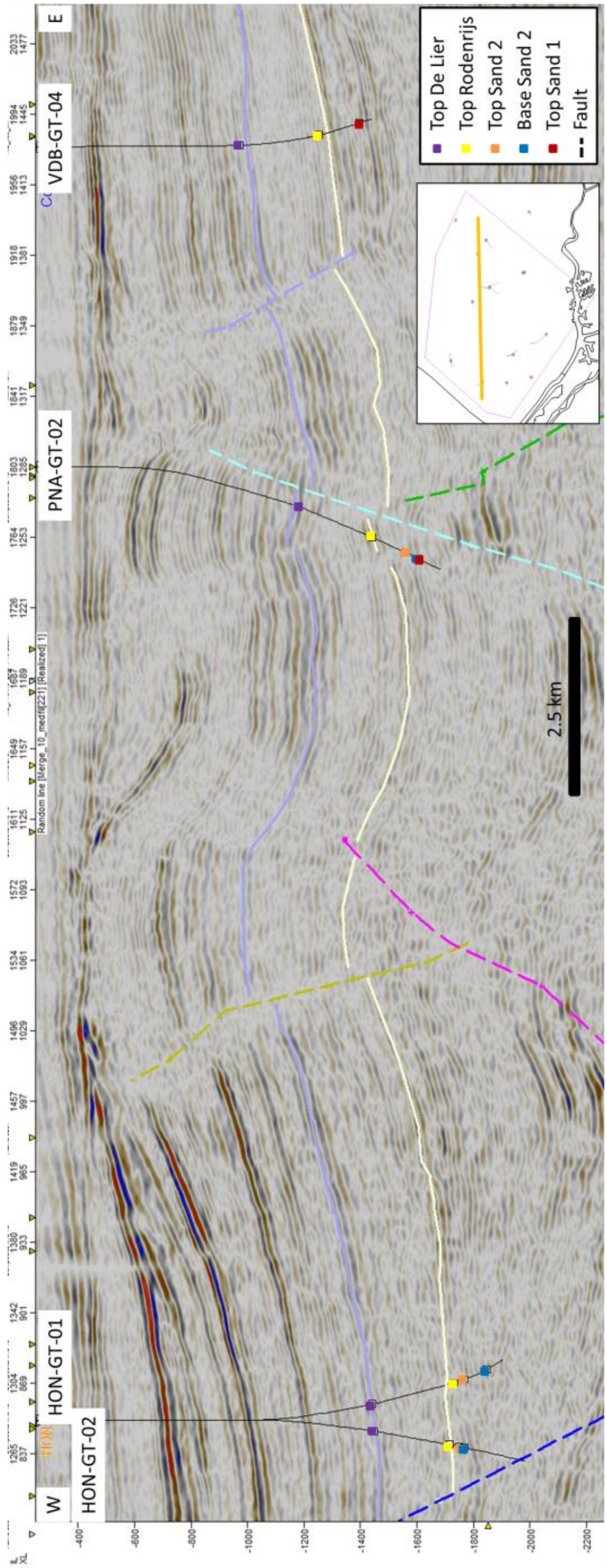
W
E
HON-GT-02
HON-GT-01
PNA-GT-02
VDB-GT-04
Top De Lier
Top Rodenrijs
Top Sand 2
Base Sand 2
Top Sand 1
Fault
2.5 km

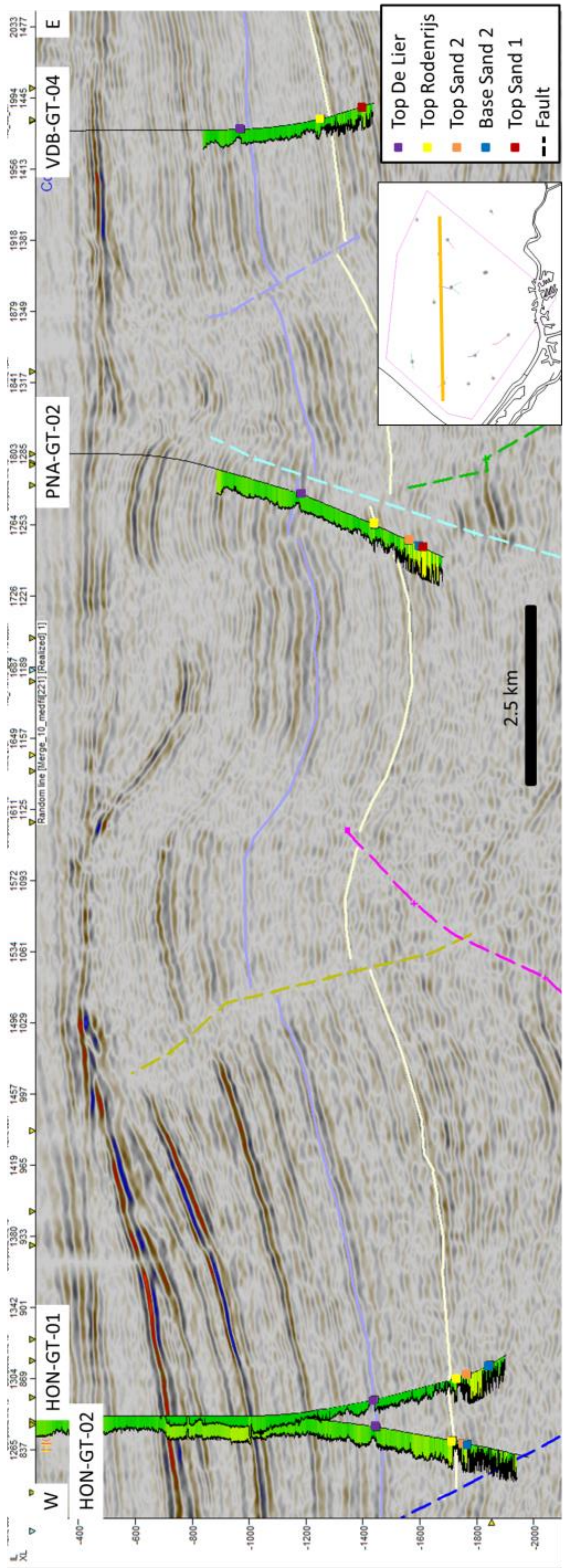

W
E
HON-GT-02
HON-GT-01
PNA-GT-02
VDB-GT-04
Top De Lier
Top Rodenrijs
Top Sand 2
Base Sand 2
Top Sand 1
Fault
2.5 km

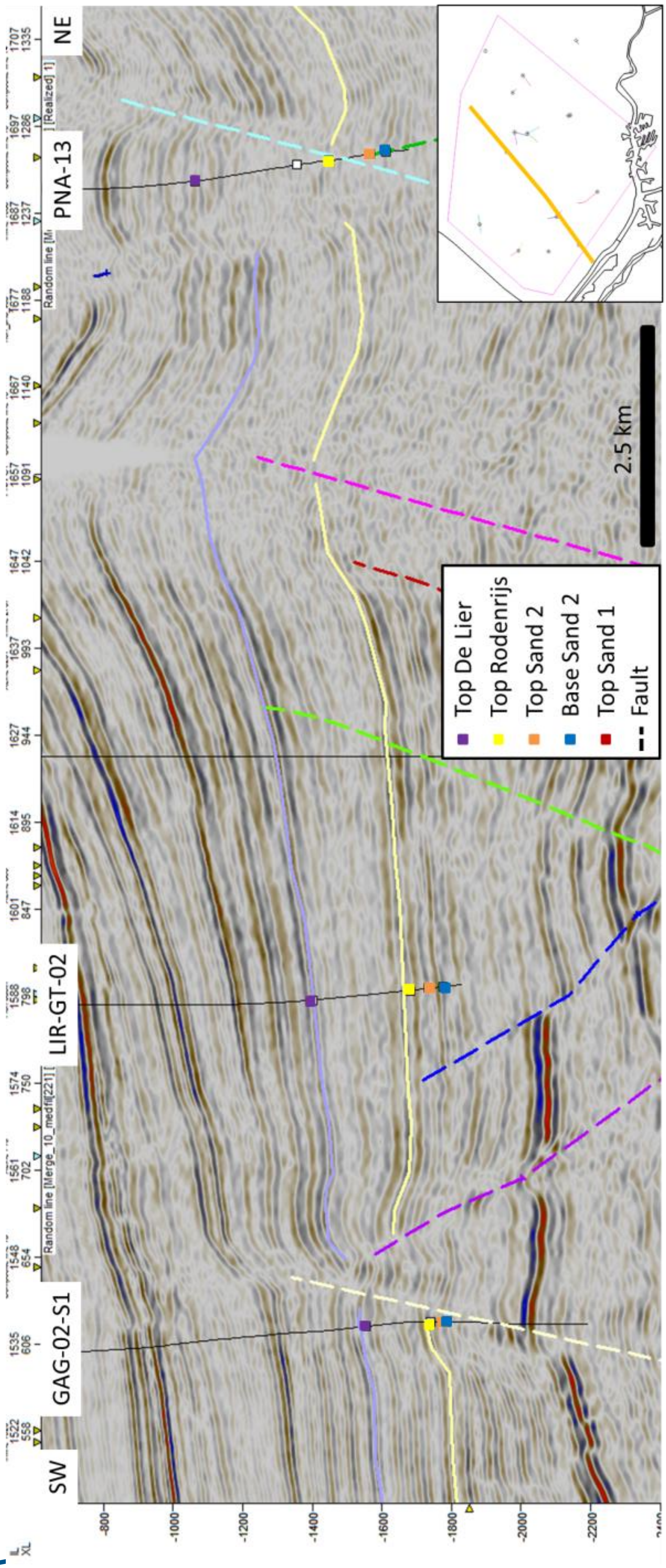
SW
NE
GAG-02-S1
LIR-GT-02
PNA-13
Top De Lier
Top Rodenrijs
Top Sand 2
Base Sand 2
Top Sand 1
Fault
2.5 km

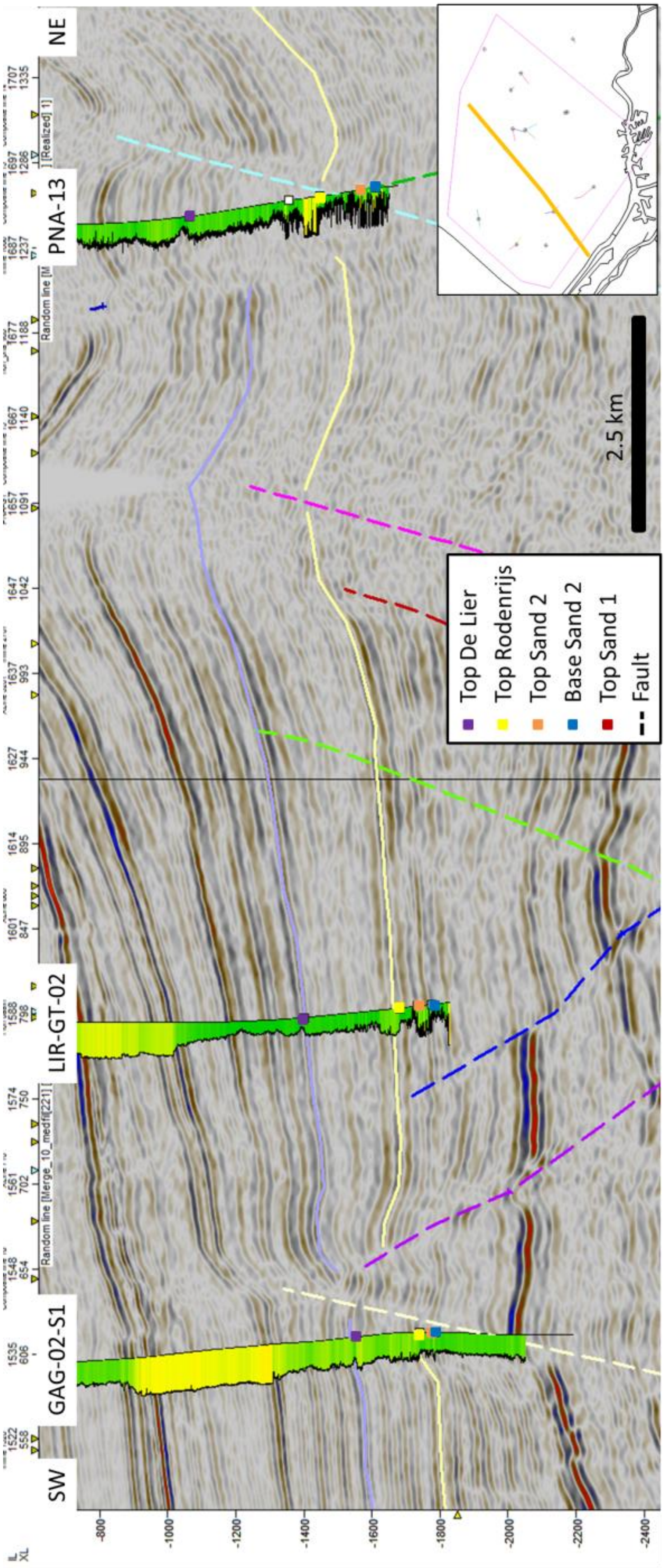

SW
NE
GAG-02-S1
LIR-GT-02
PNA-13
2.5 km
Top De Lier
Top Rodenrijs
Top Sand 2
Base Sand 2
Top Sand 1
Fault

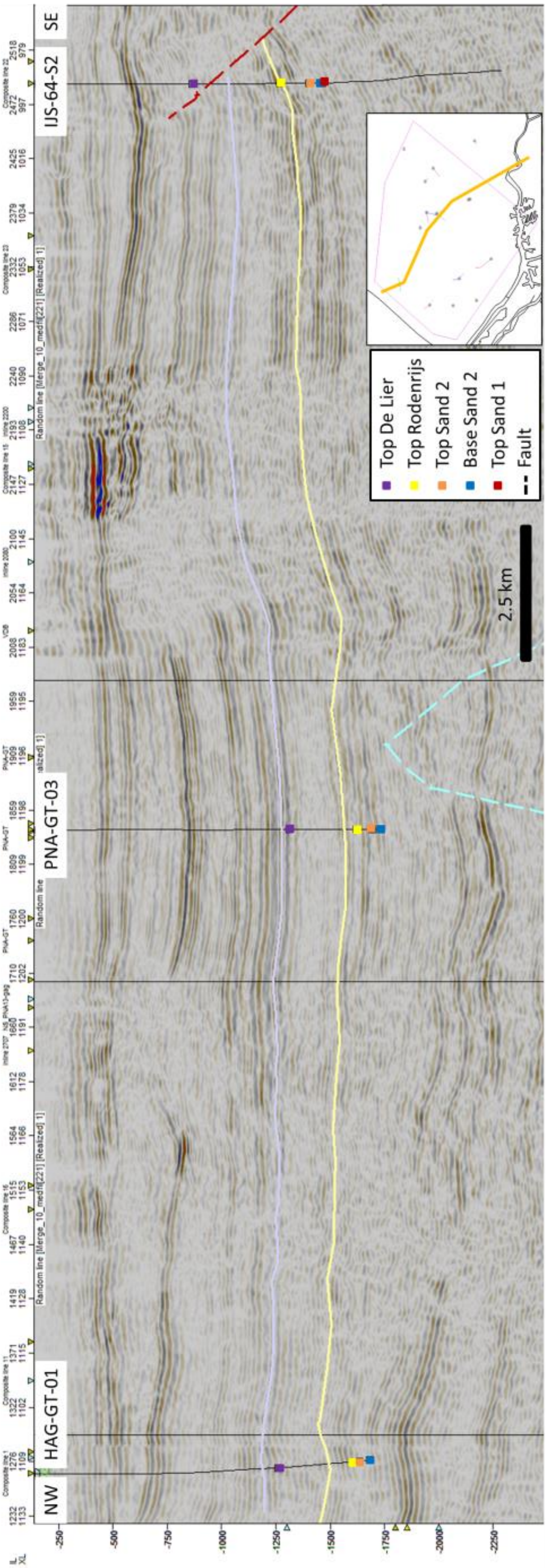
NW
SE
HAG-GT-01
PNA-GT-03
IJS-64-S2
Top De Lier
Top Rodenrijs
Top Sand 2
Base Sand 2
Top Sand 1
Fault
2.5 km

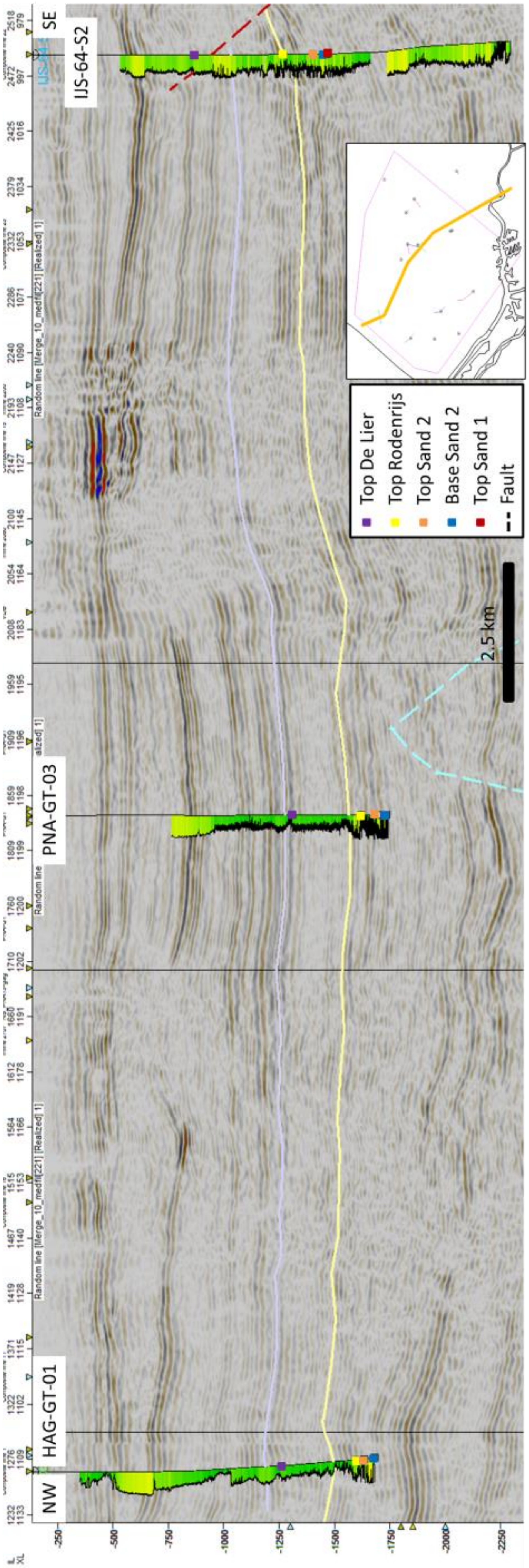

SE
IJS-64-S2
PNA-GT-03
HAG-GT-01
NW
Top De Lier
Top Rodenrijs
Top Sand 2
Base Sand 2
Top Sand 1
Fault
2.5 km

9.8 Maps

The two conceptual gross thickness maps are shown below with the depth of the top of the respective sand in the wells indicated in m TVD.

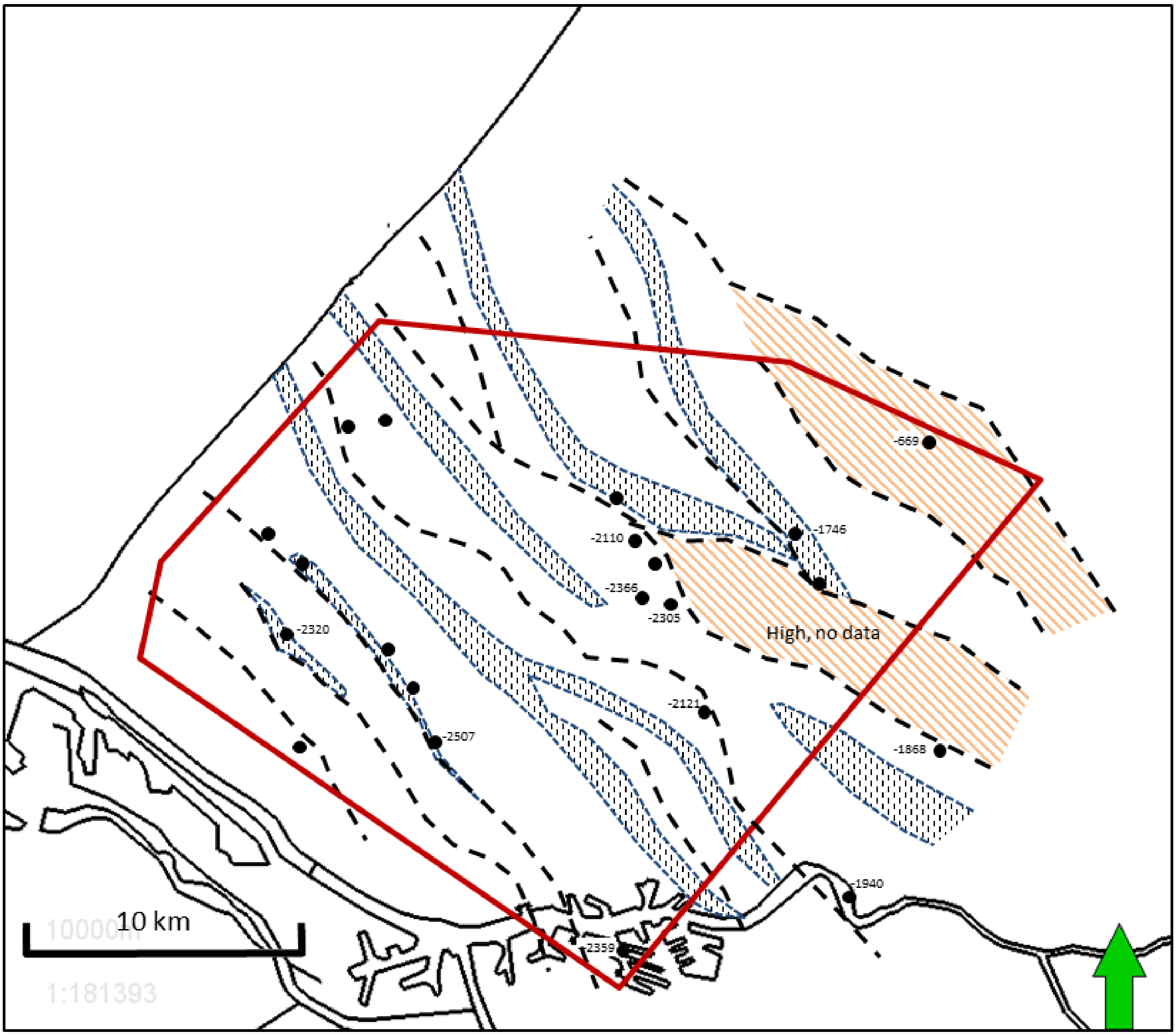

Figure 9-22 Conceptual thickness map of Sand 1, with TVD for each well.

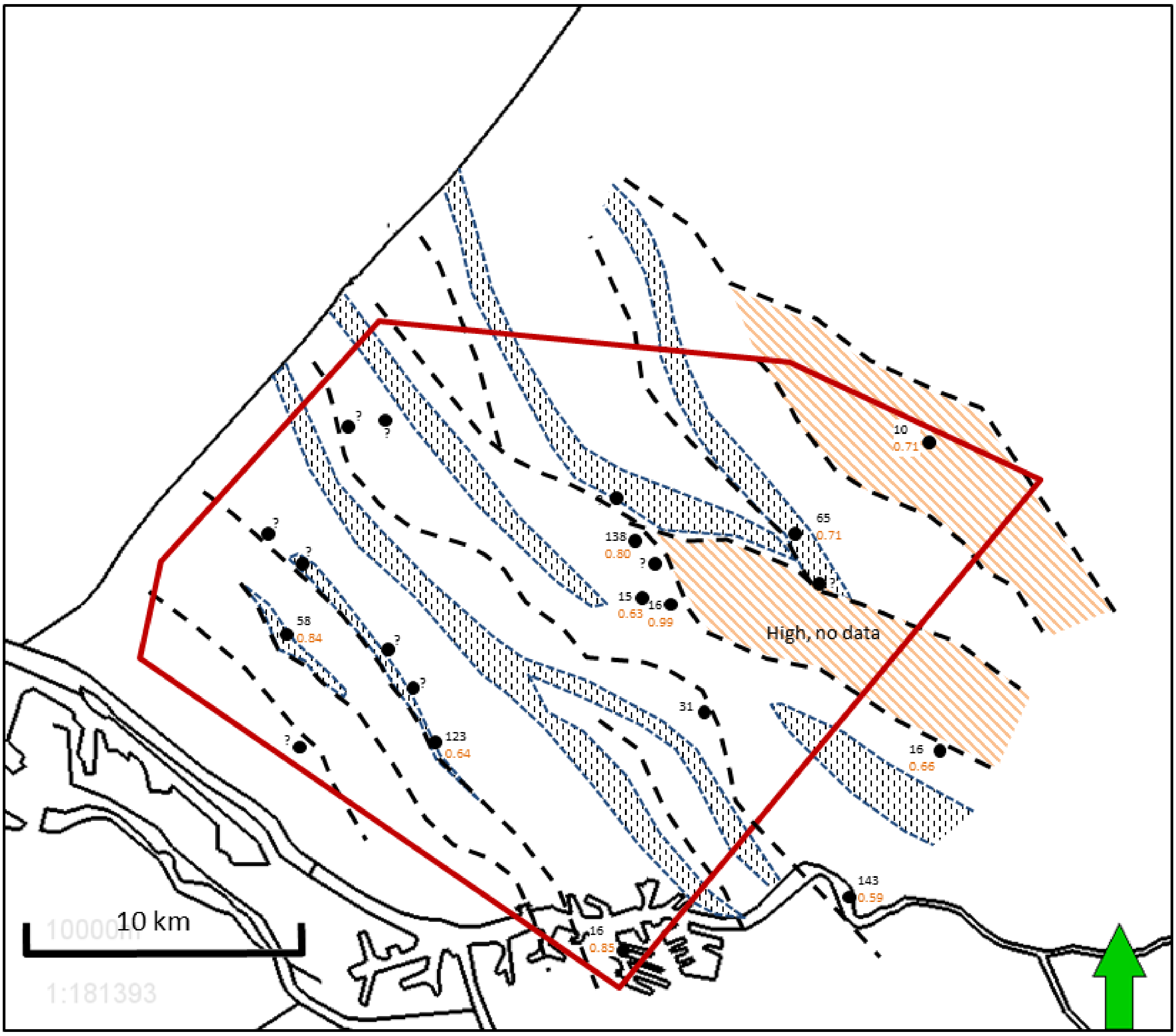

Figure 9-23 Conceptual thickness map of Sand 1. The map shows the depocenters in blue (where the Nieuwerkerk Formation is the thickest), and the highs in orange. There is too little data to create conceptual contour lines for Sand 1. Next to the wells the vertical thickness and the N/G is listed.

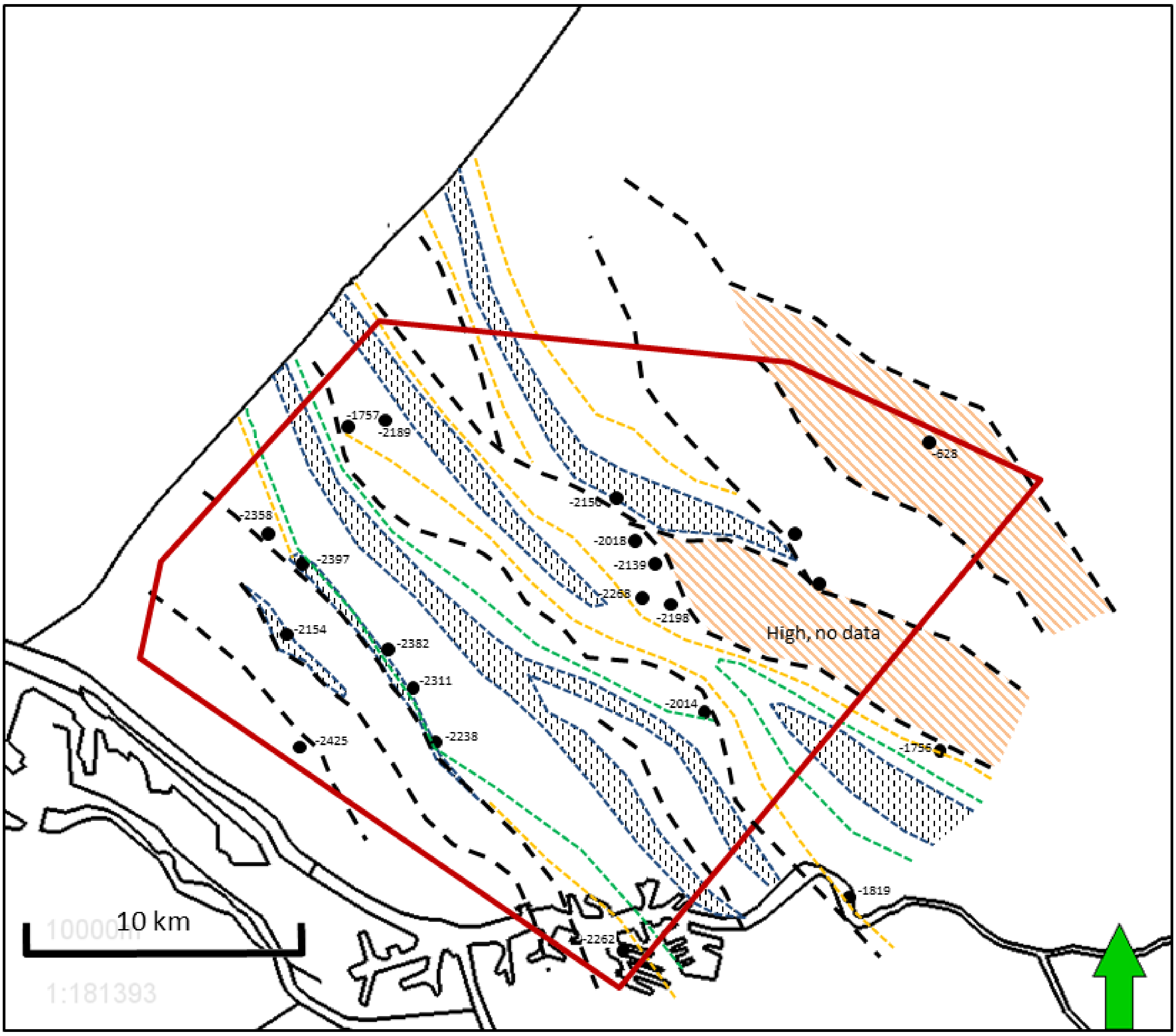

Figure 9-24 Conceptual thickness map of Sand 2, with TVD for each well.

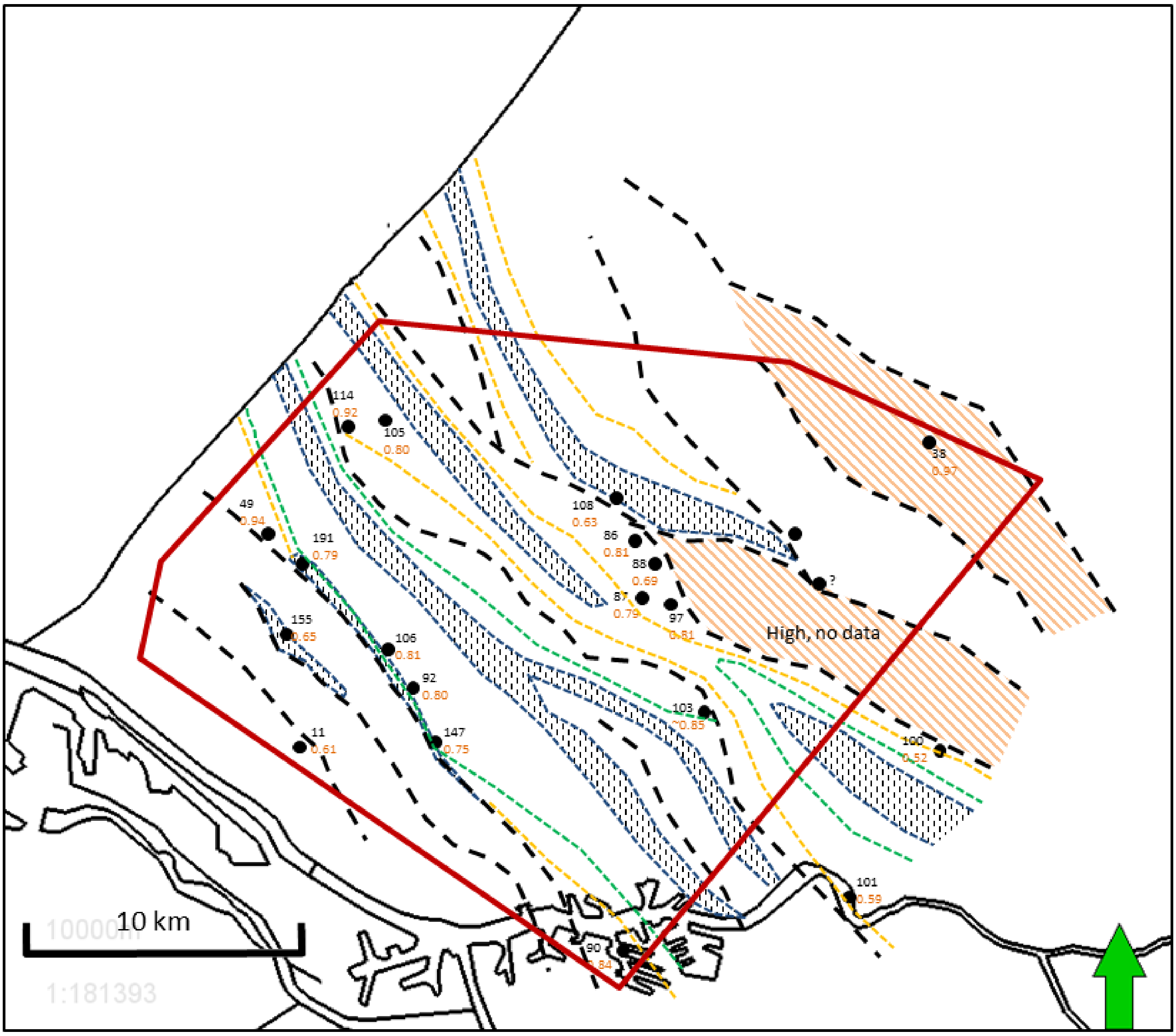

Figure 9-25 Conceptual thickness map of Sand 2. The map shows the proposed thickness variations throughout the study area, in blue the depocenters (where the Nieuwerkerk Formation is the thickest), in green intermediate thickness and in yellow the thinnest contour. Next to the wells the vertical thickness and the N/G is listed.